

**Primary Study on Ureolysis-Based Microbially-
Induced Calcium Carbonate Precipitation Technique
for Geotechnical Applications**

Hamed Khodadadi Tirkolaei

Submitted to the
Institute of Graduate Studies and Research
in partial fulfillment of the requirements for the degree of

Doctor of Philosophy
in
Civil Engineering

Eastern Mediterranean University
February 2016
Gazimağusa, North Cyprus

Approval of the Institute of Graduate Studies and Research

Prof. Dr. Cem Tanova
Acting Director

I certify that this thesis satisfies the requirements as a thesis for the degree of Doctor of Philosophy in Civil Engineering.

Prof. Dr. Özgür Eren
Chair, Department of Civil Engineering

We certify that we have read this thesis and that in our opinion it is fully adequate in scope and quality as a thesis for the degree of Doctor of Philosophy in Civil Engineering.

Assoc. Prof. Dr. Huriye Bilsel
Supervisor

Examining Committee

1. Prof. Dr. Erol Güler

2. Assoc. Prof. Dr. Huriye Bilsel

3. Assoc. Prof. Dr. Hanifi Çanakcı

4. Assoc. Prof. Dr. Zalihe Sezai

5. Asst. Prof. Dr. Eriş Uygur

ABSTRACT

Environmental concerns and application limitations of the conventional techniques for geotechnical engineering problems persuaded the geotechnical engineers to look for alternative solutions. In this regard, biogeotechnics which deals with bio-mediated and bio-inspired solutions to the challenges that vex geotechnical systems has been recently introduced. Within only around one decade of emerging this topic, it has received many attentions by researchers as it offers the promise of cost-effective, sustainable and non-disruptive solutions for a diversity of geotechnical applications. Microbially induced CaCO_3 precipitation (MICP) is one the biological solutions, through which calcium carbonate is precipitated as binding agent between grains and/or filling materials within soil pores, by mediation of microorganisms. Successful development and implementation of the MICP technique for ground improvement would have wide application to many important geotechnical problems, such as increasing stiffness and shear strength to mitigate liquefaction potential; to enhance bearing capacity of soil beneath foundation and reduce associated settlements; to stabilize slopes; to facilitate excavation, boreholing and tunneling; to control erosion; and reducing permeability to reduce seepage of dikes and cut-off walls. Application of this technique may be especially useful underneath or near existing structures, where the application of conventional soil improvement techniques is restricted due to high cost or ground deformation associated with available technologies.

There are several mechanisms for MICP. Ureolysis mechanism is the most concentrated one in the literature, in which ureolytic microorganisms are employed

as biological mediators. Since introducing the ureolysis-based MICP into geotechnical engineering, many researches has been carried out on development and application of this technique into soil at laboratory scale. Although much success and progress have been attained by these studies, it was found that there is still lack of some geotechnical insights in biology-oriented side and some biological insights in geotechnics-oriented sides; for instance, no cheap, fast and geotechnical engineer-friendly method for estimation of precipitation progress was presented; and few attention has been also paid to the mineralogy of the precipitated calcium carbonate as it can influence mechanical properties of the treated soil and durability.

In the present study, a hybrid of conductometry and precipitation mass measurement method in treatment solution (Biogrout) has been developed for monitoring the precipitation progress, which facilitates controlling over precipitation pattern, i.e. estimation on type, time, amount and place of precipitation within soil. It was found that the precipitation pattern in every treatment solution follows a logistic function, which was herein designated as microbial CaCO_3 precipitation characteristics curve (MCPCC) since it represents three important characteristics (i.e. precipitation rate, precipitation ratio and lag duration). Effect of some significant influencing factors on these characteristics was investigated. Statistical models for precipitation rate and ratio were also presented. Potential type and morphology of the precipitates at different environmental conditions have been also assessed. It was observed that calcite as the most stable type of calcium carbonate does not always occur. Formation of non-stable phases can cause change in mechanical properties of treated soil as change in type and morphology of the precipitates during time was demonstrated in this study. Treatment of soil samples by using soaking and injection methods at high and low rate of precipitation were also separately evaluated.

Different soil treatment methods were found to influence the mineralogy, shear wave velocity and unconfined compressive strength.

Keywords: Biogeotechnics; Microbially-induced calcium carbonate precipitation; Biogrout; Ground improvement; Ureolysis

ÖZ

Çevre farkındalığının artışı ve konvansiyonel metodların limitasyonlarından dolayı geoteknik mühendisliği problemlerinin çözümü için alternatif yaklaşım arayışına girilmiştir. Bu çerçevede son yıllarda biyogeoteknik alanı, biyolojik veya biyolojiden esinlenen yaklaşımlarla geoteknik mühendisliği alanındaki sorunlara çözüm önermektedir. Son on yıl içerisinde oluşan ve gelişen bu yeni alan, çok yönlü geoteknik sorunların önlenmesinde ekonomik, sürdürülebilir ve çevre dostu çözümler sunmasından dolayı araştırmacılar tarafından, ilgi görmektedir. Mikrobiyolojik yöntemle mikro-organizmanın tetiklenmesi (indüksiyon) ile oluşan CaCO_3 presipitasyonunun (MICP) tanecikleri bağlayıcı veya araları dolduran bir etkin madde olarak kullanılabilirliği çalışılmaktadır. Bu yöntemin başarılı bir şekilde geliştirilmesi ve zemin iyileştirmesinde uygulanabilir hale getirilmesi, zemin sıklığının ve kayma mukavemetinin artırılması, sıvılaşma potansiyelinin iyileştirilmesi, zeminlerin taşıma gücünün artırılması, oturmaların azaltılması, şev stabilitesinin artırılması, kazı işlerinin kolaylaştırılması, tünel kazısının, erozyon kontrolünün yapılabilmesi, hidrolik iletkenliğin azaltılması gibi önemli geoteknik problemlerin çözümünde yararlı olacaktır. Özellikle konvansiyonel metodlarla iyileştirmeleri mümkün olmayan, pahalı veya deformasyonlara neden olabileceğinden, var olan binaların altında veya yanındaki zeminlerin iyileştirilmelerinde bu teknik çok kullanışlı olabilecektir.

MICP'nin bir kaç yönteminden biri olan ve literatürde en yoğun çalışılan üreoliz yöntemi mikro organizmanın biyolojik bir aracı gibi çalıştırılmasıdır. Üreoliz kaynaklı MICP tekniğinin geoteknik mühendisliğinde uygulanabilirliği irdelenmeye

başlandıđından beri yöntemin geliştirilmesi ve zemine uygulanabilmesi için laboratuvar ölçeğinde çok sayıda araştırma yapılmıştır ve halen yapılmaktadır. Bu çalışmalarda belirli bir başarı elde edilmesine rağmen halen biyoloji kanadında geoteknik bilgisinin, geoteknik kanadında ise biyolojinin derinlemesine anlaşılamadığı gözlemlenmiştir. Dolayısıyla ucuz, süratli, ve kolay presipitasyon oluşumunun takip yöntemi geliştirilememiştir. Biyolojik yöntemle iyileştirilen zeminin mekanik davranış ve dayanıklılıđını etkileyen kalsiyum karbonatın minerolojisi de yeterli çalışılmamıştır.

Bu çalışma iyileştirme solüsyonu (Biogrout) içerisinde kondaktometri ve kütle presipitasyon ölçümü yöntemleri kullanılarak hibrid bir yöntemle, zemin içerisinde presipitasyon oluşumunu, gelişimini monitor ederek, zaman, miktar ve presipitasyon lokasyonlarının tesbitini içerir. Presipitasyon oluşumu ve dağılımının bir lojistik fonksiyon olan mikrobiyal CaCO_3 karakteristik eğrisi (MCPCC) ile ifade edilebildiđi ve üç önemli karakteristiđi içerdiđi izlenmiştir: presipitasyon hızı, presipitasyon oranı ve gecikme süresi. Bu çalışmada bazı önemli faktörlerin bu karakteristik unsurlara etkisi de araştırılmıştır. Presipitasyon hızı ve oranını ifade eden statistiki modeller sunulurak, presipitasyonun potansiyel türü ve morfolojisi farklı çevresel faktörlerin etkisi altında değerlendirilmiştir. Sonuç olarak, en stabil kalsiyum karbonat türü olan kalsitin her zaman oluşmayabildiđi gözlemlenmiştir. Ayrıca presipitasyonun türü ve morfolijisinde zaman içerisinde oluşan deđişimin, iyileştirilmiş zeminin mekanik davranışında deđişimlere neden olduđu da bu araştırma kapsamında irdelenmiştir. Sonuç olarak, en stabil kalsiyum karbonat türü olan kalsitin her zaman oluşmayabildiđi gözlemlenmiştir. Ayrıca presipitasyonun türü ve morfolijisinde zaman içerisinde oluşan deđişimin, iyileştirilmiş zeminin

mekanik davranışında deęişimlere neden olduęu da bu araştırma kapsamında irdelenmiştir.

Anahtar kelimeler: Biyo-geoteknik; Mikrobiyolojik tetikleme ile kalsiyum karbonat presipitasyonu; Biyo-harç; Zemin iyileştirmesi, Üreoliz.

DEDICATION

To my family
and
especially it is lovingly dedicated to my wife,
Samira Ghayekhloo
for her support, encouragement, and her endless love during my life

ACKNOWLEDGMENT

First and foremost, I would like to thank Dr. Huriye Bilsel for providing the opportunity for me to work on this unique subject. Her vision and feedback has been instrumental in the success of this research. Dr. Bilsel has always been a great supervisor, a mentor, and a close friend. I am always indebted to her countless kind and sincere supports impacted my personal and professional growth significantly since I met her five years ago.

I would like to thank Dr. Zalihe Sezai whose Soil Behavior class opened a new insight to me on soil chemistry and mineralogy, which has been afterward very useful for me throughout this study.

I am grateful to Dr. Heshmat Rahimian from Mazandaran University (Iran) for the opportunity of getting trained on the basic biological experiments in his laboratory with his helpful students. I am thankful to Dr. Bahar Taneri, chairlady of the Department of Biological Science in EMU, for providing me the access of using their laboratory.

I am also honored to acknowledge Dr. Edward Kavazanjian, director of Center for Bio-mediated and Bio-inspired Geotechnics (Arizona State University, US), for admitting me into his fantastic group as a visiting scholar. It was really a great experience for me to work with the people working at the highest level in this subject.

Most importantly, I must thank my wonderful wife and best friend Samira Ghayekhloo, for putting up with me over the seven years. She has always been incredibly supportive and a source of unending happiness. Her aid, quiet patience, exhortation and endless love were certainly the most important reasons that I am in this place.

Last, but never least, I would like to express my deepest appreciation and love to my parents for their always encouragement, endless patience and spiritual supports throughout my study and my life in general.

TABLE OF CONTENTS

ABSTRACT.....	iii
ÖZ	vi
DEDICATION	ix
ACKNOWLEDGMENT.....	x
LIST OF TABLES	xvi
LIST OF FIGURES	xviii
LIST OF ABBREVIATIONS	xxiii
1 INTRODUCTION	1
1.1 General.....	1
1.1.1 Evolution of Geotechnical Engineering.....	1
1.1.2 Biogeotechnics	3
1.2 Scope and Organization	6
2 UREOLYSIS-BASED MICROBIALLY INDUCED CALCIUM CARBONATE PRECIPITATION.....	8
2.1 Introduction.....	8
2.2 Mechanisms for Biologically Mediated CaCO ₃ Precipitation.....	9
2.2.1 Ureolysis Mechanism.....	10
2.2.2 Denitrification Mechanism.....	13
2.3 Comparison between Microbial Ureolysis, Enzymatic Ureolysis and Microbial Denitrification Mechanisms.....	14
2.4 Previous Efforts on Evaluation and Development of Microbially Induced Calcium Carbonate Precipitation Technique for Geotechnical Engineering Applications	16

2.5 Conclusion	21
3 ESTIMATION ON UREOLYSIS-BASED MICROBIALLY INDUCED CALCIUM CARBONATE PRECIPITATION PROGRESS	23
3.1 Introduction	23
3.2 Materials and Methods	25
3.2.1 Bacterial Growth Condition	25
3.2.2 Treatment (Cementation) Solution.....	26
3.2.3 Electrical Conductometry of the Calcium Free Treatment Solution.....	26
3.2.4 CaCO ₃ Precipitation Mass Measurement.....	27
3.2.5 Measuring the Bacterial Cell Concentration	28
3.2.6 Design of Experiments, Analysis of Variance, Regression Analysis	28
3.3 Results and Discussions	31
3.3.1 Pattern of Change in Electrical Conductivity of the Treatment Solution in the Absence of Calcium	31
3.3.2 Calcium Carbonate Precipitation Progress in Treatment Solution	33
3.3.3 Comparison between Precipitation Progress and Conductivity Changes in a Treatment Solution at Different Test Conditions	33
3.3.4 Microbial CaCO ₃ Precipitation Characteristic Curve (MCPCC).....	38
3.3.5 Variations in Microbial CaCO ₃ Precipitation Characteristics.....	39
3.4 Conclusion	42
4 EFFECT OF SELECTED ENVIRONMENTAL FACTORS ON MICROBIAL CaCO ₃ PRECIPITATION CHARACTERISTICS	45
4.1 Introduction	45
4.2 Materials and Methods	46
4.2.1 Bacterial Growth Condition	46

4.2.2 Treatment Solution.....	46
4.2.3 Monitoring the Microbial CaCO ₃ Precipitation Characteristics	47
4.3 Results and Discussions	48
4.3.1 Effect of Initial Cell Concentration, CaCl ₂ /urea Concentration and Temperature on Microbial CaCO ₃ Precipitation Characteristics	48
4.3.2 Effect of the Presence of Seawater on Precipitation Ratio	63
4.3.3 Effect of Various Concentration of Nutrient Broth on Microbial CaCO ₃ Precipitation Characteristics.....	64
4.3.4 Effect of Lack of Air on Precipitation Ratio.....	67
4.4 Conclusion	68
5 POTENTIAL MORPHOLOGY AND TYPE OF <i>S.PASTEURII</i> -INDUCED CALCIUM CARBONATE PRECIPITATION IN TREATMENT SOLUTION.....	71
5.1 Introduction	71
5.2 Materials and Methods	75
5.2.1 Bacterial Culture	75
5.2.2 Harvested Calcium Carbonate Precipitates	75
5.2.3 Precipitation Rate Measurement	78
5.2.4 Micro-scale Identification Methods	78
5.3 Results and Discussions	79
5.3.1 In Urea-NB-NH ₄ Cl Solution.....	79
5.3.2 In Urea-NH ₄ Cl Solution.....	90
5.3.3 In SW-Urea-NB-NH ₄ Cl Solution.....	90
5.3.4 Effect of Aging.....	95
5.4 Conclusion	99

6 MICP-TREATMENT OF SAND THROUGH INJECTION AND SOAKING METHODS AT THE LOWEST AND HIGHEST RATE OF PRECIPITATION ..	101
6.1 Introduction	101
6.2 Materials and Methods	103
6.2.1 Soil Properties	103
6.2.2 Injection Treatment Method.....	103
6.2.3 Development of Soaking Treatment Method.....	107
6.2.4 Shear Wave Velocity Measurement and Compressive Strength Test.....	110
6.2.5 Acid Washing of Treated Samples.....	112
6.3 Results and Discussions	112
6.3.1 Treatment Using Injection Method at the Highest Rate.....	112
6.3.2 Treatment Using Injection Method at the Lowest Rate	116
6.3.3 Treatment Using Soaking Method at the Highest Rate.....	119
6.3.4 Treatment Using Soaking Method at the Lowest Rate	123
6.4 Conclusion	128
7 CONCLUSION	130
7.1 Summary	130
7.2 Future Research.....	135
REFERENCES.....	137
APPENDICES	152
Appendix A: Choosing the best regression line by comparing the AICc statistics of the applied models.....	153
Appendix B: Model statistics for precipitation rate	155

LIST OF TABLES

Table 3.1. Factors and their experimental range of amount and level.	29
Table 3.2. Matrix design of experimental runs and their corresponding results of bacterial growth change (Δ (OD ₆₀₀) [*]).	31
Table 4.1. Three-level full factorial experiments and their corresponding response [*]	49
Table 4.2. Summary statistics of different models applied to the precipitation rate data.	52
Table 4.3. Table of ANOVA for 2FI model applied to the precipitation rate data.	52
Table 4.4. Comparison between actual values from verification tests and predicted values by presented model for precipitation rate.	56
Table 4.5. Summary statistics of different models applied to the precipitation ratio data.	58
Table 4.6. Table of ANOVA which represents the significance level of each factor and their second order interactions on precipitation ratio.	58
Table 4.7. Set of experiments performed for finding the precipitation ratio at different CaCl ₂ , urea and initial cell concentrations.	59
Table 4.8. Significance of parameters of the response surface model fitted to the electrical conductivity data points.	61
Table 4.9. Fit statistics of the electrical conductivity model resulted from the least square method analysis.	61
Table 4.10. Comparison between actual values from verification tests and predicted values by presented models for electrical conductivity and precipitation ratio.	62
Table 4.11. Precipitation ratio below the minimum EC _{critical} at 10 ⁴ and 10 ⁵ cell/ml initial cell concentration.	62

Table 4.12. Effect of 50% seawater (by volume) on precipitation ratio; temperature was kept constant at 35°C within the tests.	64
Table 4.13. Effect of lack of nutrient broth on microbial CaCO ₃ precipitation characteristics.	66
Table 4.14. Effect of various concentrations of nutrient broth on precipitation ratio; temperature was kept constant at 35°C during the tests.	67
Table 4.15. Effect of lack of air on precipitation ratio.	68
Table 5.1. Full factorial design of the experiments for examining the effect of three variables at two levels on micro-scale properties of the precipitates harvested from NB-urea-NH ₄ Cl solution.	77
Table 5.2. Composition of seawater used in this study (the ion concentrations are in mg/l).	77
Table 6.1. Specifications of ASTM 20-30 Ottawa Sand.	103
Table 6.2. Specifications of polypropylene mesh.	108
Table 6.3. Summary of the treatment of the samples through injection method at the highest rate of precipitation.	114
Table 6.4. Summary of the treatment of the samples through injection method at the lowest rate of precipitation.	114
Table 6.5. Summary of the treatment of the samples through injection method at the highest rate of precipitation.	127
Table 6.6. Summary of the treatment of the samples through injection method at the lowest rate of precipitation.	127

LIST OF FIGURES

Figure 3.1. Electrical conductivity (EC) of treatment solution containing 0.1M urea (left) and 1M urea (right) versus temperature.	27
Figure 3.2. Change in conductivity of a calcium exclusive treatment solution versus time.....	32
Figure 3.3. Normalized conductivity (●) and precipitation (Δ) data points and their best fitting regression lines at initial cell concentration of 10^6 cell/ml, urea concentration of 1 M, and 20°C.	34
Figure 3.4. Normalized conductivity (●) and precipitation (Δ) data points and their best fitting regression lines at initial cell concentration of 10^8 cell/ml, urea concentration of 0.1 M, and 20°C.	35
Figure 3.5. Normalized conductivity (●) and precipitation (Δ) data points and their best fitting regression lines at initial cell concentration of 10^8 cell/ml, urea concentration of 0.1 M, and 50°C.	35
Figure 3.6. Normalized conductivity (●) and precipitation (Δ) data points and their best fitting regression lines at initial cell concentration of 10^6 cell/ml, urea concentration of 0.1 M, and 20°C.	36
Figure 3.7. Normalized conductivity (●) and precipitation (Δ) data points and their best fitting regression lines at initial cell concentration of 10^7 cell/ml, urea concentration of 0.55 M, and 35°C.	36
Figure 3.8. Normalized conductivity (●) and precipitation (Δ) data points and their best fitting regression lines at initial cell concentration of 10^8 cell/ml, urea concentration of 1 M, and 50°C.	37

Figure 3.9. Normalized conductivity (●) and precipitation (Δ) data points and their best fitting regression lines at initial cell concentration of 10^8 cell/ml, urea concentration of 1 M, and 20°C.	37
Figure 3.10. Calculating the rate and lag time for each experiment by finding the tangent line on the log phase and its time-intercept (in the legends, Bact., Urea and Temp. represent initial bacterial cell concentration, initial Ca^{2+} /urea concentration and temperature).....	40
Figure 4.1. Response surface (3D and counter plots) of the precipitation rate at the (a) lowest, (b) mid and (c) highest level of urea concentration.	53
Figure 4.2. Trend line for precipitation ratio versus electrical conductivity of the treatment solution at different initial cell concentrations.....	60
Figure 5.1. FTIR spectra of the precipitates harvested from urea-NB-NH ₄ Cl solutions at the rates of 0.05 min ⁻¹ (a), 0.47 min ⁻¹ (b) and 0.17 min ⁻¹ (c); and from SW-urea-NB-NH ₄ Cl solutions with [CaCl ₂] = 0.1 M (d) and 0.23 M (e).	82
Figure 5.2. XRD spectra of the precipitates harvested from urea-NB-NH ₄ Cl solutions at the rates of 0.05 min ⁻¹ (a), 0.47 min ⁻¹ (b) and 0.17 min ⁻¹ (c); and from SW-urea-NB-NH ₄ Cl solutions with [CaCl ₂] = 0.1 M (d) and 0.23 M (e); (A: aragonite; C: calcite; M: monohydrocalcite; V: vaterite).	83
Figure 5.3. Visual appearance of the precipitates under naked eyes: granular particles obtained at the rates of 0.05 and ~0.17 min ⁻¹ (a) and thread-like particles acquired at the 0.47 min ⁻¹ rate (b).....	85
Figure 5.4. Light (a and b) and electron (c-e) micrographs of the precipitates obtained at the precipitation rate of 0.05 min ⁻¹	86
Figure 5.5. Light (a-c) and electron (d-f) micrographs of the precipitates obtained at the precipitation rate of ~0.17 min ⁻¹	87

Figure 5.6. Light (a-e) and electron (f-l) micrographs of the precipitates obtained at the precipitation rate of 0.47 min^{-1} . The solid arrows in (b) and (c) point out the degenerated spherules. The dashed arrows in (b) indicate the collinear arrangement of the spherules. The arrows in (d) and (h) signalize the presence of hollow in the spherules. Existence of redundancies, linkage between rod-shaped crystals by the spherules, and trace of degenerated spherule on crystal surface were respectively marked in (j), (k) and (l).....	88
Figure 5.7. Light (a and b) and electron (c-g) micrographs of the precipitates acquired from SW-urea-NB-NH ₄ Cl solution containing 0.1 M CaCl ₂	92
Figure 5.8. Electron micrographs of the precipitates acquired from SW-urea-NB-NH ₄ Cl solution containing 0.23 M CaCl ₂	94
Figure 5.9. XRD spectra of the precipitates harvested from urea-NB-NH ₄ Cl solutions at the rate of 0.47 min^{-1} (a) and from SW-urea-NB-NH ₄ Cl solutions with [CaCl ₂] = 0.1 M (b) and 0.23 M (c) after one year; (A: aragonite; C: calcite; V: vaterite).....	96
Figure 5.10. Electron micrograph of the precipitates obtained at the precipitation rate of 0.47 min^{-1} after one year on keeping at room condition.....	97
Figure 5.11. Electron micrographs of the precipitates acquired from SW-urea-NB-NH ₄ Cl solution containing 0.1 M CaCl ₂ after one year.....	97
Figure 5.12. Electron micrographs of the precipitates acquired from SW-urea-NB-NH ₄ Cl solution containing 0.23 M CaCl ₂ after one year.....	98
Figure 6.1. The columns used for injection treatment: (top) BE-equipped column, and (bottom) simple treatment column.....	105
Figure 6.2. Mesh columns used for soaking treatment.....	108
Figure 6.3. Schematic view of temperature-controlled treatment bath.....	109
Figure 6.4. Treated sample with BE-equipped platens at top and bottom.....	111

Figure 6.5. Flattening the two end surfaces of the treated sample with putty for unconfined compression test.	111
Figure 6.6. Treated samples by using injection method at the highest rate.	115
Figure 6.7. Change in shear wave velocity versus precipitation mass percent for the samples treated by injection method at the highest rate.	115
Figure 6.8. Calcite precipitation in the soil treated through injection method at the highest rate of precipitation.	116
Figure 6.9. Treated samples by using injection method at the lowest rate.	117
Figure 6.10. Change in shear wave velocity versus precipitation mass percent for the samples treated by injection method at the lowest rate.	118
Figure 6.11. Unconfined compressive strength versus shear wave velocity after treatment for the samples treated by injection method at the lowest rate.	118
Figure 6.12. High concentration of calcite in the soil treated through injection method at the lowest rate of precipitation.	119
Figure 6.13. Change in shear wave velocity versus precipitation mass percent for the samples treated by soaking method at the highest rate.	121
Figure 6.14. Treated samples by using soaking method at the highest rate.	122
Figure 6.15. Soil grain from the sample by soaking method at the highest rate is covered by amorphous calcium carbonate. Spherical vaterite and immature calcite crystals are also observed on the grain surface.	122
Figure 6.16. The sample treated through soaking method at the highest rate was crumbled by soaking into distilled water.	123
Figure 6.17. Change in shear wave velocity versus precipitation mass percent for the samples treated by soaking method at the lowest rate.	125
Figure 6.18. Treated samples by using soaking method at the lowest rate.	125

Figure 6.19. SEM images of the grains from (a) lateral surface and (b) the middle part of sample treated by using soaking method at the lowest rate of precipitation. 126

LIST OF ABBREVIATIONS

$[\text{CaCl}_2]_0$	Initial concentration of calcium chloride
$\Delta (\text{OD}_{600})$	Change in optical density at 600 nm
2FI	Second order full factorial interaction
ANOVA	Analysis of variance
EC	Electrical conductivity
FTIR	Fourier transform infrared spectroscopy
MCPC	Microbial CaCO_3 precipitation characteristics
MCPCC	Microbial CaCO_3 precipitation characteristic curve
MICP	Microbially-induced CaCO_3 precipitation
NB	Nutrient broth
P_{max}	Maximum precipitation ratio
r	Precipitation rate
SEM	Scanning electron microscopy
SW	Seawater
T_{lag}	Lag duration
XRD	X-ray diffraction analysis

Chapter 1

INTRODUCTION

1.1 General

1.1.1 Evolution of Geotechnical Engineering

The term *engineering* is originated from the Latin words *ingeniare* and *ingenium*, meaning “to contrive or to devise” and “cleverness” respectively. Humans have been always struggling with meeting new challenges within history; the challenges arisen by their endless demands. Therefore, there has been no way but to contrive the challenges by using cleverness; in other words, there has been no way but to engineer the challenges!

Humans have been historically involved in soil related challenges for their primary requirements of survival and habitation. They used soil as a material for irrigation purposes, burial sites, flood control, construction material, and as building foundations. First activities for engineering the soil related challenges were linked to earth dams, dikes, caissons, steep piles of stones and sliding resistant dating back to 2750-2500 BC that were found in ancient Egypt. Efforts on controlling the large settlements and soil reinforcement with woven reed mats were also observed in the structures built at 2100-2300 BC in Mesopotamia (current Iraq). Applying strip footings for concentrated loads, retaining walls and reinforcement of the foundations and walls with more ductile

materials like wooden bars and iron clamps were noticed in the structures of 150-500 BC in ancient Greece. In ancient Rome at the first century BC, technologic solution of soil related challenges started appearing: concrete foundations, building cofferdam for constructing the piers, and paved roads. These advancements were owed to Vitruvius, contemporary Roman architect and military engineer. He had written a ten-volume treatise in which he talked about many technologies such as building materials and different kinds of water pumps. Code for engineering practice has been first introduced by him. Compaction techniques, clayey soil improvement through replacing the undesirable layer with stones, and shallow foundations for bridges were perceived in old China at 500-1000 AD. Medieval time was accompanied by development in wooden pile foundations for bridges and houses in Europe; but still there was a lack of scientific approaches to examining the soils underneath the structures with problematic foundations, like leaning Pisa. It prompted the scientists to think of theories behind the problems. Theoretical study on geotechnical engineering was formally initiated in the Enlightenment Period when Coulomb presented earth pressure and shear strength theory. Before this time, engineering the geotechnical problems was mainly based on empirical knowledges. Following Coulomb's work, development of the theoretical studies by Darcy, Rankine, Mohr and Boussinesq led to the emerging of basic soil mechanics in 19th century. Subsequent to these theoretical progress, Terzaghi's theories on principle of effective stress, consolidation, and bearing capacity of foundations opened the modern soil mechanics around 1925. The fundamental theories presented by Atterberg, Casagrande, Hvorslev and Roscoe within the first half of the 20th century complemented the modern soil mechanics. In 1960s, it was found that the classical theories cannot explain the problems of unsaturated soils as they had been mainly developed for dry and

saturated conditions. Hence, the basic theories of unsaturated soil mechanics have been brought up. Fredlund was the first geotechnical engineer who has introduced the classical soil mechanics for unsaturated soils. Geotechnical engineering problems and consequently the theories developed to describe specific soil behaviors have been getting more and more complicated. Therefore, within last decades of previous century, efforts have been focused on development of advanced numerical methods for solving the problems. Around early years of the current century, together with escalation of world's environmental and energy concerns, geotechnical engineers noticed that they have to be much more cautious in finding solutions for geotechnical problems. They have even seriously started investigating the geotechnical issues for habitation on the moon as an alternative planet for living (lunar geotechnical engineering). Biogeotechnics and energy geotechnics, as the new disciplines with environmental-friendly and energy-saving solutions, have been recently introduced regarding the environmental and energy concerns. They promise to be further transformative practices in Geotechnics.

1.1.2 Biogeotechnics

Rachel Armstrong (2009), applied scientist and innovator:

“All buildings today have something in common. They are made using Victorian technologies. This involves blueprints, industrial manufacturing and construction using teams of workers. All of this effort results in an inert object. And that means that there is a one-way transfer of energy from our environment into our homes and cities. This is not sustainable. I believe that the only way that it is possible for us to construct genuinely sustainable homes and cities is by connecting them to nature, not insulating them from it”.

Environmental concerns (e.g. soil and ground water contamination, atmospheric carbon sequestration, etc.) in geotechnical engineering applications have become more acute by increasing the number of soil improvement projects within the last decade. There are

variety of mechanical and grouting techniques which are applied for soil improvement practice (e.g. dynamic compaction, soil mixing, jet grouting, chemical grouting, permeation grouting, etc.). Mechanical techniques are energy-consuming, costly, noisy, and air polluting. On the other hand, grouting techniques introduce some synthetic man-made materials into soil to clog the pores and/or bind the particles together. The materials used for this purpose can disturb soil and groundwater ecosystem and create health and occupational risks. Micro-fine cement, phenoplasts, epoxy, silicates, acrylamide and polyurethane are the common-used materials for grouting. There are several reports on environmental and human health hazards caused by application of these materials (Karol 2003). Using these materials has increasingly come under the public scrutiny during last years. Recent initiatives in some countries propose to ban all grout components. In Japan, nearly all kinds of the synthetic grout materials have been banned. US federal regulations have also forced the withdrawal of most chemical grouts on the market. Besides the environmental and human health concerns, all prevalent grouting approaches are not able to create the same improvement conditions as specified in the primary design in-situ (DeJong et al. 2010). They can just treat the soil within 1-2 m depth from injection point. Injection pressure and volume are the only factors for controlling the treatment process. The actual changes in the treated subsurface cannot be measured along time. These lack of adequate control on the grouting process forces a conservative design to overconsumption of grouts, and consequently increase in costs and environmental concerns.

All these environmental concerns and application limitations persuaded geotechnical engineers to search for alternative techniques for soil improvement. In this regard,

potential application of microorganisms into geotechnical engineering has been introduced for the first time by Mitchel and Santamarina in 2005. Since that time, many studies have been conducted, investigating the applications of various biological techniques for different geotechnical problems. Application of biological techniques was previously limited to a few specific cases of using plants for erosion mitigation and slope stabilization and applying microorganisms for soil contamination remediation. Development of biological techniques in the last decade caused emerging a new field of study in geotechnical engineering called biogeotechnics, which deals with biologically-based solutions to the challenges that vex geotechnical systems. These solutions can be generally divided into two categories:

- Bio-mediated solutions: using living organisms (e.g. bacteria, ants, worms, plants, etc.) for engineering purposes
- Bio-inspired solutions: mimicking beneficial biological processes without living organisms (e.g. using urease enzymes, xanthan gum, etc.)

Recently, the center for bio-mediated and bio-inspired geotechnics (CBBG; www.biogeotechnics.org) at Arizona state university (US) in collaboration with Georgia Institute of Technology, University of California (Davis), New Mexico State University and other outstanding international collaborators such Cambridge University (UK), Delft University (Netherlands) and Joseph Fourier University (France) has been established. It has received funding of around \$20,000,000 by US National Research Foundation (NSF) towards the implementation of the biological techniques into geotechnical applications and educating the first generation of biogeotechnical engineers by 2020. This is one of

the biggest projects in geotechnical engineering. All these events indicate the importance of the subject and the world tendency for finding the environmental friendly solutions for geotechnical problems.

1.2 Scope and Organization

Current research includes conducting bench-scale experiments to better understand the ureolysis-based microbially induced calcium carbonate precipitation process at different conditions, ultimately resulting in prevailing over some current challenges restricting applications of the technique to geotechnical engineering problems. The scope of this study is investigation of the main factors influencing the time, type, amount and place of precipitation within soil pores. It is limited to those factors which can be only controlled by changing the properties of treatment solution as the most controllable component of a soil treatment matrix. The goals of this research presented herein are to:

- i. Summarize previous efforts from literature and identify the research gaps, *Chapter 2*;
- ii. Establish a reliable, cheap, fast and easy-to-use method for monitoring the precipitation progress, *Chapter 3*;
- iii. Identify the characteristics illustrating the precipitation progress, *Chapter 3*;
- iv. Investigate the effect of initial cell concentration, CaCl_2 /urea concentration and temperature on precipitation characteristics, *Chapters 3 and 4*;
- v. Evaluate the effect of concentration of nutrient broth, different proportions of CaCl_2 and urea, and presence of seawater on precipitation characteristics, *Chapter 4*;

- vi. Identify the potential type and morphology of the calcium carbonate precipitates in different conditions, *Chapter 5*;
- vii. Comparison between injection and soaking treatment methods on treatment quality, *Chapter 6*;
- viii. Monitoring the change in compressive strength and shear wave velocity of the MICP-treated sand at varied amounts of precipitation, *Chapter 6*;
- ix. Determine future areas of research on applications of the ureolysis-based MICP technique to geotechnical problems, *Chapter 7*.

Chapter 2

UREOLYSIS-BASED MICROBIALLY INDUCED CALCIUM CARBONATE PRECIPITATION

2.1 Introduction

Although microbiological involvement in calcium carbonate precipitation has been identified at early 20th century (Drew 1914), potential application of microbial processes for geotechnical engineering problems was first explicitly discussed in the past decade (Mitchel and Santamarina 2005; US National Research Council 2006). Further studies have demonstrated the potential of microbial subsurface processes for soil improvement. One of the processes is biocementation as a promising technique for modification of mechanical properties in granular soils, through which minerals precipitate as binding agent between grains and/or fine materials within the soil pores. Applying this process into soils has been appropriately named as biogrouting (Harkes et al. 2010; van Paassen et al. 2010), in which treatment solution (or cementation solution) composed of bacterial cells, nutrients for bacterial growth, and substrate (e.g. CaCl_2 and urea in ureolysis mechanism) are prepared ex-situ and then injected into soil as biogrout. Bacterial cells may be excluded from treatment solution when stimulating the indigenous soil bacteria is aimed (Burbank et al. 2011 and 2012). Bacterial cells may be also replaced with another kind of bio-agent like pure enzyme (Karatat 2008; Hamdan et al. 2013; Neupane et al. 2013; Hamdan 2015). Successful development and implementation of the

biogrouting technique would have various applications to a wide range of geotechnical problems, such as slope stabilization; erosion control; seepage control; increasing the bearing capacity of soil; facilitating bore-holing and tunneling in granular soils; mitigating the potential for liquefaction and dynamic settlement (Whiffin 2004; DeJong et al. 2006 and 2010; Karatas 2008; Kavazanjian and Karatas 2008; van Paassen et al. 2009 and 2010). Biogrouting technique may be applied for soil improvement underneath or near existing structures, where application of the conventional techniques is more difficult, costly and risky.

2.2 Mechanisms for Biologically Mediated CaCO₃ Precipitation

Microbially (or enzyme) induced CaCO₃ precipitation is a particular kind of biocementation process through which calcium carbonate as one of the most common natural minerals is produced. In the nature, any biotic or abiotic action which causes a decrease in solubility or an increase in concentration of carbonate or calcium ions in calcium-rich solutions can lead to precipitation of calcium carbonate. Natural precipitation of calcium carbonate is mostly due to biotic actions (Castanier et al. 2000). Biologically mediated processes of calcium carbonate precipitation are also faster than those produced by abiotic changes (Stocks-Fischer et al. 1999). The biological activities in calcium-rich solution can increase the pH and carbonate content to the supersaturation point corresponding to calcium carbonate precipitation. There are several biological mechanisms which can induce calcium carbonate precipitation by producing alkalinity in the subsurface, such as urea hydrolysis (or ureolysis), denitrification, sulfate reduction and iron reduction. Ureolysis and denitrification has been more extensively focused in geotechnical studies.

2.2.1 Ureolysis Mechanism

Ureolysis is the mechanism within which urea is hydrolyzed to ammonia and carbamate (Equation 2.1). Carbamate spontaneously breaks down to another ammonia and carbonic acid (Equation 2.2).



Afterwards, carbonic acid and ammonium molecules equilibrate in water with their protonated and deprotonated form, leading to pH raise (Equations 2.3 & 2.4).



The pH increase shifts the bicarbonate equilibrium reaction toward carbonate ions production (Equation 2.5).



Lastly, in the presence of calcium ions, the produced carbonate ions precipitate as calcium carbonate (Equation 2.6).



Presence of urease enzyme in the system catalyzes the urea hydrolysis reaction (Equation 2.1). It can make the reaction around 10^{14} times faster than the uncatalyzed one (Upadhyay, 2012). Urease is composed of active sites in its structure, which only bind to urea or hydroxyurea. Urease activity depends on the presence of urea and

hydroxyurea substrates, temperature and other factors like cation exchange capacity and organic matter. The enzyme instantly catalyzes the degradation of urea into ammonium and carbamate ions as soon as it comes in exposure of the substrate. Temperature raise leads to increase in urease activity. Urease activity can be inhibited in presence of some organic or inorganic matters (i.e. enzyme inactivation). The inactivation can be reversible or irreversible. The enzyme activity can be totally or partially retrieved by removal of inhibiting agent, i.e. enzyme reactivation (Olech et al. 2014).

Two processes for ureolysis-based biologically induced calcium carbonate precipitation has been identified based on the type of bioagents catalyzing the mechanism: microbial and enzymatic. In microbial process, microbes are applied for intercellular urease enzyme generation while in enzymatic process pure urease enzyme is utilized.

Urease is found in plants (e.g. soybeans, jack beans, water melon seed, and pea seeds), soils, animals, and microorganisms with various chemical compositions and properties. It can be extracted and purified from these resources. It has been the first isolated enzyme in history (Sumner, 1926). The enzyme is around 12 nm in size (Blakely and Zerner 1984). Jack bean-extracted enzyme is used in most geotechnical studies (Karatas 2008; Hamdan et al. 2013; Neupane et al. 2013; Hamdan 2015).

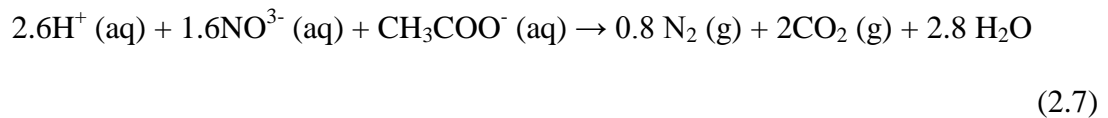
There are different species of bacteria which can produce urease. Urease active microorganisms are abundantly found in most soils. *Sporosarcina pasteurii* is a facultative aerobe, alkalophilic, rod-shaped, non-pathogen, gram-positive, and highly urease active soil bacterium which have been used in most studies. Its activity is

dependent on various factors like pH, temperature and oxygen; and it is not repressed in presence of high concentration of ammonium (Whiffin 2004). When this bacteria, like other alkalophiles, is in an alkaline medium (low H^+), it diffuses proton (H^+) from inside the cells to outside due to concentration gradient between cytoplasm and microenvironment outside; but alkalophiles require the protons to produce adenosine triphosphate (ATP) which is a consumable form of energy for cells to derive other reactions which need energy. Therefore, the bacteria develop two mechanisms to return the protons back into their cells: first, reducing the pH difference (H^+ concentrations) between inside and outside the cells in order to prevent the protons diffusion. For this purpose, in presence of urea as a source of energy, it imports urea into its cell cytoplasm. Hydrolysis of urea (NH_4^+) in presence of intercellular urease enzyme results in a raise in cytoplasmic alkalinity close to outside pH; second, increasing membrane potential to diffuse the ammonium ions outward and driving back the protons into the cell. By increasing the ammonium concentration and reduction in proton concentration inside the cell due to intercellular hydrolysis and ATP synthesis, respectively, potential membrane increases. Increasing the potential membrane means the ions diffusion from high concentration to lower concentration across the cell membrane. So, ammoniums diffuse outward and protons diffuse inward within the second mechanism. This ammonium production causes an increase in pH of the environment around bacteria. This mechanism has been discussed by Whiffin (2004). Al-Thawadi (2008) also explained autotrophic and heterotrophic metabolic pathways for microbial carbonate formation. Within the autotrophic pathway, carbonate ions are depleted in the bacterial environment as a result of consumption of carbon dioxide as an inorganic carbon source by bacteria. In heterotrophic pathway, organic carbon sources are used for carbonate ions formation.

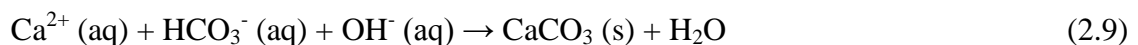
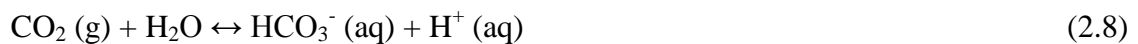
Higher concentration of carbonate ions around each cell in a calcium contained solution creates a localized supersaturation condition for calcium carbonate precipitation (at pH around 8.3). In addition, the negatively charged surface of the bacteria can absorb calcium cations from the medium to deposit on the cell surface. Therefore, bacteria act as nucleation sites for calcium carbonate crystallization. The bacteria are then embedded in successive layers of precipitation.

2.2.2 Denitrification Mechanism

Calcium carbonate precipitation through bacterial denitrification involves an initial step at which the bacteria consume available organic carbon source (as energy) in oxygen deficient environment (heterotrophic metabolism) to reduce nitrate (NO_3^-), as nitrogen source (electron acceptor), to nitrogen gas (N_2). This microbial process is called dissimilatory reduction. It leads to alkalinity (consumes H^+ from aqueous medium) and carbon dioxide (CO_2) production (Equation 2.7).



Afterwards, as described in Equations 2.8 and 2.9, the produced carbon dioxide and alkalinity facilitate calcium carbonate precipitation in a similar way as described above for ureolysis mechanism:



There are many kinds of denitrifying organisms. *Pseudomonas denitrificans* is a gram-negative facultative anaerobe bacteria, which is commonly used for microbially induced

calcium carbonate precipitation through denitrification (Ehrlich 2002; Karatas 2008; van Paassen et al. 2010). The bacteria play a catalyzing role in nitrate reduction process which includes different intermediate steps. They synthesize enzyme corresponding to each intermediate step. Generation of these enzymes is a function of various parameters, such as oxygen content, pH, and temperature (Hamdan 2013).

2.3 Comparison between Microbial Ureolysis, Enzymatic Ureolysis and Microbial Denitrification Mechanisms

Microbial urea hydrolysis is the first and the most common mechanism in the studies investigating biologically mediated calcium carbonate precipitation technique for ground improvement. Microbial denitrification mechanism has been later introduced as an alternative mechanism (Karatas 2008; van Paasen 2010a; Hamdan 2013; Kavazanjian et al. 2015) due to two main disadvantages of the common microbial ureolysis mechanism:

- First, ammonium as an undesirable by-product, which causes soil and groundwater contamination. van Paassen et al. (2011) used pumping water to wash off the produced ammonium within treatment process. Kavazanjian's team (personal communication) in Arizona State University are working on a technique for encapsulation of the ammonium by-product; and
- Second, aerobicity of the common utilized urease-active bacteria, which restricts its application in low oxygen environment like deep soil and under water table. Of course, there is some evidence demonstrating the bacterial growth and urease activity of *S.pasteurii*, as facultative aerobe not obligate aerobe, under anoxic conditions (Achal et al. 2010; Montoya 2012).

Hamdan (2013) suggested the microbial denitrification as an alternative mechanism for urea hydrolysis because of readily occurring in the absence of oxygen, being more thermodynamically favorable, no toxic by-product, higher carbonate yield, full consumption of electron donors, and no need for providing exogenous organic material. However, it should be noted that the commonly used denitrifying bacteria in the literature are gram negative. The gram negative bacteria are barely resistant against potential physical disruption during soil treatment process (e.g. injection pressure, high confining pressure, etc.) due to having thinner cell wall in comparison with gram positive bacteria. Soil treatment through denitrification under confining pressure has not been found in the literature. Besides, denitrification mechanism is releasing unconsumed carbon dioxide into the atmosphere while microbial urea hydrolysis mechanism sequesters carbon dioxide within autotrophic pathway of the bacterial metabolism. Furthermore, the most important issue limiting practical applications of denitrification mechanism is its very slow rate of precipitation. Achieving a desirable amount of calcium carbonate precipitation may take years (Kavazanjian et al. 2015). Hence, denitrification-based techniques may have very limited applications like when ground improvement by desaturation (e.g. liquefaction mitigation), as a result of fast nitrogen gas bubble formation at the first phase of the reactions, is aimed although the durability of the bubbles has not been also evaluated yet.

Enzymatic urea hydrolysis is another alternative mechanism which has been received attention by some researchers (Karatas 2008; Hamdan et al. 2013; Neupane et al. 2013; Hamdan 2015). Using free urease enzyme eliminates some restrictions raised by application of urease producing bacteria, for instance there will be no concern about the

oxygen availability for bacterial activity; the enzyme is water soluble and can easily transport within soil pores with smaller size than microbes; there will be no need to provide nutrients for bacterial activity, which can reduce the cost and complexity of the system. However, there is still the concern of releasing ammonium into environment. Moreover, the rate of precipitation by this mechanism is very high so that there is hardly enough time for stable CaCO_3 crystal (i.e. calcite) growth. The lack of nucleation site in the enzymatic mechanism is another reason preventing CaCO_3 crystallization.

2.4 Previous Efforts on Evaluation and Development of Microbially Induced Calcium Carbonate Precipitation Technique for Geotechnical Engineering Applications

Since the last decade, many studies have been carried out to evaluate and develop the microbial techniques for implementation into geotechnical applications. Except two field trials (Fujita et al. 2010; van Paassen 2011), all other studies have been at laboratory scale. The biggest laboratory scale is related to the treatment of sand in a 100 m^3 tank by using ureolytic microbially induced calcium carbonate precipitation technique (van Paassen et al. 2010b). The majority of the studies have been at bench and element laboratory scales (Whiffin et al. 2007; van Paassen 2009; van Paassen et al. 2009; Cheng and Cord-Ruwisch 2012). Generally, the studies in this field can be categorized to evaluative and developmental studies. Evaluative studies are those assessing the success or worth of the technique for geotechnical applications; and developmental studies are those improving the technique for laboratory and field implementations.

Evaluative studies on mechanical properties of the microbially treated sand demonstrate the ability of the technique for modification of shear strength and volumetric behavior, stiffness, compressibility, and permeability. Whiffin (2004) carried out triaxial shear strength tests on microbially treated sand by ureolytic bacteria. She reported an 8-fold increase in shear strength and a 3-fold increase in stiffness without significant change in volume of voids. DeJong et al. (2006) also reported increased shear strength for microbially treated sand (by urease producing bacteria) under undrained monotonic shearing. They observed higher initial shear stiffness and bigger modulus of elasticity compared to untreated loose sand, similar to gypsum-cemented sand. Their results also exhibit a change in volumetric behavior from contractive in untreated loose sand to dilative in treated sand. Montoya (2012) attributed the increase in shear strength and the change in volumetric behavior to the cementation at particles contact points and densification caused by precipitation in the pores. She reported a decrease around 17% in initial pore space after microbial treatment, which results in a significant reduction in void ratio and increase in relative density (i.e. densification). This densification alone, regardless of other benefits of bio-treatment (inter-particle bonds, increased particle angularity, etc.) can increase shear strength, reduce compressibility and permeability, and change the contractive volumetric behavior to dilative. Montoya (2012) also reported an increase in the shear wave velocity of microbially treated sand to more than 1200 m/s, which represents an increase in stiffness during cementation. Precipitates can also fill the pores and reduce the permeability. Whiffin et al. (2007) observed a reduction between 22% - 75% in permeability at different levels of treatment. These observations corroborate the effectiveness of microbially induced calcium carbonate precipitation technique for application in a wide range of geotechnical problems

suffering from high compressibility and permeability, and low shear strength and stiffness.

The developmental studies have been concentrated on prevailing over some key challenges including spatial uniform treatment, managing the ammonium by-product, durability and cost, which have retarded practical implementation of these techniques as an alternative for traditional methods. The solutions presented in these studies are mainly based on enhancing bacterial cell attachment to soil grains, desired distribution of bioagent (bacterial cell or free urease enzyme), sufficient delivery of nutrient and substrate throughout soil body, maximizing the amount of precipitates, minimizing the ammonium by-product, and regulating the rate of precipitation. Some of these solutions are:

- Coating soil grains with cations (Whiffin et al. 2007; Harkes et al. 2010; van Paassen et al. 2010; Chu et al. 2014) – It results in adsorption between coated soil grains and negatively charged surfaces of bacteria, which prevent washing off the injected cells from interest treatment area. Although the soil environment can be inoculated through injecting a huge amount of bacterial cells without previous coating (Montoya 2012), concentration of available cells in the interest area cannot be controlled in this way. It may also increase cost and affect the ecosystem outside the treatment zone.
- Using surfactants (Dawoud et al. 2014) – Washing the highly inoculated zone using surfactant can facilitate detachment of cells from that zone and transfer the cells to the less concentrated zone in the soil.

- Adjustment of injection type and rate (Al Qabany et al. 2011; Montoya 2012; Martinez et al. 2013; DeJong et al. 2014) – Different types of injection (percolation, continuous injection, stop-flow injection, etc.) and different rates of injection may influence the bacterial cell distribution and delivery of nutrients and substrate within the soil pores. Hence, these factors can control the uniformity and precipitation ratio ($[\text{CaCO}_3]/[\text{Ca}^{2+}]_0$). Bigger precipitation ratio leads to more efficient precipitation process and consequently lower cost.
- Applying free urease enzyme (Karatas 2008; Hamdan et al. 2013; Neupane et al. 2013; Hamdan 2015) – Free enzymes are water soluble and can easily move within the small pores. Using free enzymes eliminates the concerns for cell attachment to the soil grains, uniform distribution of cells in the soil and delivery of nutrients. It may also reduce the cost as there is no need for nutrient in treatment solution. The problems with using free enzymes are the highest rate of precipitation and the lack of nucleation site for crystal growth. Both of these two problems favor precipitation of the less stable phases of calcium carbonate. Less stable phases are not durable as they may transform to a more stable phase.
- Stimulating the indigenous organisms (Burbank et al. 2011 and 2012) – Stimulating soil indigenous bacteria does not have the difficulties arisen from injecting exogenous bacteria. The cost of treatment process is also reduced in this method. There will be also more possibility to get uniform treatment. Both denitrifying and ureolytic bacteria are ubiquitous in soils.
- Change in type and concentration of substrates (Ca^{2+} and urea) and other ingredients of treatment solution (Al Thawadi 2008; Li et al. 2011; Mortensen et

al. 2011; Martinez et al. 2013) – Various types and concentrations of calcium salts, nitrogen and carbon sources may influence bacterial growth and their urease activity. Cheaper resources which can cause higher urease activity are desirable. Excluding or minimizing the nutrient broth, as a general food for all kinds of microorganisms, can minimize the effect of other competing microorganisms in the system and create a more selective medium for ureolytic bacteria. Amount and proportion of calcium concentration and urea concentration is another factor controlling the precipitation rate and ratio. Higher concentration of calcium ions and urea in treatment solution results in greater amount of precipitation. Greater amount of precipitation reduces the required number of treatment cycles, which consequently lowers the cost. On the other hand, higher concentration of calcium ions produces higher ionic strength which restricts the bacterial growth. As obtaining one mole calcium carbonate through hydrolysis mechanism requires one mole calcium ion and one mole urea, equimolar concentration is the most desirable proportion provided that all the existing calcium ions or urea are consumed. Presence of unconsumed substrate in the soil pores can make environmental disturbance and increase the treatment cost.

- Choosing the most appropriate type of bacteria (Whiffin 2004; Soon et al. 2014; Venda Oliveira et al. 2014) – The bacteria which are non-pathogen, highly urease active and not repressed by high concentration of ammonium in the medium can be applied. There are some species of bacteria which can shrink when they are starved. They can retrieve their normal size and be activated after

feeding. These bacteria can be utilized in treating the soils with the pore size smaller than the bacteria.

- Pre-treatment and mutating of bacterial cells (Li et al. 2011; Chu et al. 2014) – Washing the bacterial cells with normal saline in order to remove the metabolic waste may increase their urease activity. The urease activity may also be increased through pretreatment of the cells with particular mutating agents.
- Considering the presence of other microorganisms (Gat et al. 2011 and 2014) – Presence of other microorganisms in the environment may influence the activity of the target bacteria. They may compete with the target bacteria on consumption of available nutrient resources. They may also act as nucleation sites for calcium carbonate precipitation.
- Pumping out the ammonium by-product (van Paassen 2011) – Ammonium as an undesirable by-product of the ureolysis process can be pumped out of the soil at the end of the treatment cycles. Some researchers are working on encapsulation and neutralization of the ammonium (Kavazanjian, personal communication).

2.5 Conclusion

In spite of undesirable by-production of ammonium as the main disadvantage of the ureolysis-based microbially induced calcium carbonate precipitation, it is still the most promising microbial technique for geotechnical applications. Although many studies have been carried out to improve the technique for field implementation, some fundamental efforts are still needed to overcome the challenges restricting its implementation. For example, a practical and geotechnical engineering-friendly method for estimation of calcium carbonate precipitation progress has not been developed;

mineralogy of the precipitated calcium carbonate in the literature is only limited to identification of calcite polymorph precipitated at the ideal treatment condition. No study was found investigating the potential of formation of other polymorphs of calcium carbonate within a treatment process.

Chapter 3

ESTIMATION ON UREOLYSIS-BASED MICROBIALLY INDUCED CALCIUM CARBONATE PRECIPITATION PROGRESS

3.1 Introduction

As it was explained in the previous chapter, spatial uniform treatment, managing the ammonium by-product, durability and cost are the main challenges retarding the field application of the ureolysis-based microbial calcium carbonate precipitation techniques. These challenges mainly arise from the lack of enough control on CaCO_3 precipitation pattern, i.e. amount, type, time and place of precipitation within soil. Among soil properties (e.g. mineralogy, pore size, hydraulic conductivity, etc.), environmental conditions (e.g. temperature, pH, oxygen availability, presence of other microorganisms, etc.) and treatment solution (e.g. type and concentration of ingredients and bioagent in solution, viscosity of solution, temperature of solution, etc.) as three components of a treatment matrix, treatment solution as a biological grout (biogrout) is the most controllable and the basic component for controlling the precipitation pattern. Monitoring the precipitation progress in treatment solution provides useful information on precipitation pattern prior to injection into soil although a real pattern is never predictable due to many unknowns and complexities in soil systems.

More accurate and close-to-reality precipitation pattern can be estimated from treatment solution by taking into consideration of more number of soil properties and environmental conditions:

- 1- Effect of some soil properties and environmental conditions can be somewhat harnessed by designing an appropriate treatment solution. For instance, treatment solution can contain a water soluble bioagent like pure urease for application into the soils with pores smaller than bacteria (Hamdan et al. 2013; Kavazanjian and Hamdan 2015); or a more selective medium can be considered for minimizing the effect of competing microorganisms in the soil environment (Mortensen et al. 2011); or the solution temperature can be adjusted for getting desirable temperature in the pores.
- 2- Effect of some factors can also be partly simulated in treatment solution. For example, treatment solution can be inoculated with the same type and concentration of the existing indigenous microbes in soil in order to simulate the interactions between the exogenous and indigenous microorganisms in situ.
- 3- The effect of those factors which can be neither harnessed nor simulated in treatment solution can be discretely investigated with respect to precipitation pattern. For instance, effect of soil mineralogy can be explained as a function (or coefficient) acting precipitation pattern acquired from treatment solution.

Anyway, precipitation progress in treatment solution can be an index of precipitation pattern within soil.

In this chapter, it was aimed to develop a simple, cheap, fast and non-expert friendly technique for monitoring the ureolysis-based MICP progress in a treatment solution. For this purpose, an extended time-domain electrical conductometry of calcium free treatment solution was assessed. In order to check the reliability of the method, the change in electrical conductivity of the treatment solution as a result of urea hydrolysis (NH_4^+) was compared with real precipitation progress. The real precipitation progress was monitored through precipitation mass measurement in the same treatment solution containing calcium ions at different time intervals. Finally, a hybrid of conductometry and precipitation mass measurement tests was proposed. A general characteristic pattern was described for precipitation progress. Effect of different initial cell concentrations, Ca^{2+} /urea concentrations and temperatures on precipitation pattern was also investigated.

3.2 Materials and Methods

3.2.1 Bacterial Growth Condition

The urease producing bacteria used throughout the study was *S.pasteurii* (DSM33) grown in Yeast extract-Ammonium-Tris liquid medium. The medium was prepared by dissolving 20 g/l yeast extract and 10 g/l ammonium sulfate into 0.13M Tris buffer solution (Trizma base, pH 9) separately. The solutions were then autoclaved at 121°C for 20 minutes and mixed afterward. 200 ml of the mixture was inoculated with the bacteria and incubated in a 1000 ml flask (i.e. 1 to 5 aeration ratio) for around 70 hours at 30°C and 200 rpm shaking speed to reach the desired cell concentration ($\text{OD}_{600} = 1.4$ equal to 1.2×10^9 cell/ml). It was stored at 4°C for further usage, not more than a week. The same but abiotic (without microbe) medium was also incubated in parallel to control the contamination.

3.2.2 Treatment (Cementation) Solution

The treatment solution was consisted of 3 g nutrient broth (NB), 10 g ammonium chloride, 2.12 g sodium bicarbonate, and varied amounts of urea and calcium chloride ($[\text{Ca}^{2+}]/[\text{Urea}]=2/3$) per liter of distilled water. The solutions were autoclaved at 121°C for 20 minutes. The pH of the solution was adjusted to 6.5 prior to autoclaving for all the experiments.

3.2.3 Electrical Conductometry of the Calcium Free Treatment Solution

The bacterial cells were inoculated into the calcium free treatment solution. The initial concentration of the bacterial cell in the solutions was adjusted to be 10^6 , 10^7 , or 10^8 cell/ml. The bacterial solution taken for inoculation was earlier centrifuged (at 4000 rpm for 15 minutes) and the supernatant was also replaced with fresh calcium free treatment solution. Pellets were mixed in the fresh solution using vortex mixer. The centrifugation process was found to have negligible effect on bacterial cell loss by counting the bacterial cells in the solution using serial dilution method before and after centrifugation. A probe was then dipped into the *S.pasteurii*-inoculated solution in order to simultaneously measure the temperature and electrical conductivity (EC). Time-domain changes in conductivity of the treatment solution in the absence of CaCl_2 (i.e. calcium-free or calcium exclusive treatment solution) were recorded during incubation at the given constant temperature. The change in conductivity is due to ammonium production by microbial activity.

Electrical conductivity of the solution was found to be temperature-dependent per se. Therefore, the electrical conductivity readings were corrected to the fixed given temperature in order to eliminate the small errors which may arise from temperature

oscillation by incubator ($\pm 3^{\circ}\text{C}$) or initial time required for the solution to reach the desired temperature. The following graphs were used for this correction (see Figure 3.1). These graphs were obtained through recording the electrical conductivity of non-inoculated solution at different temperatures.

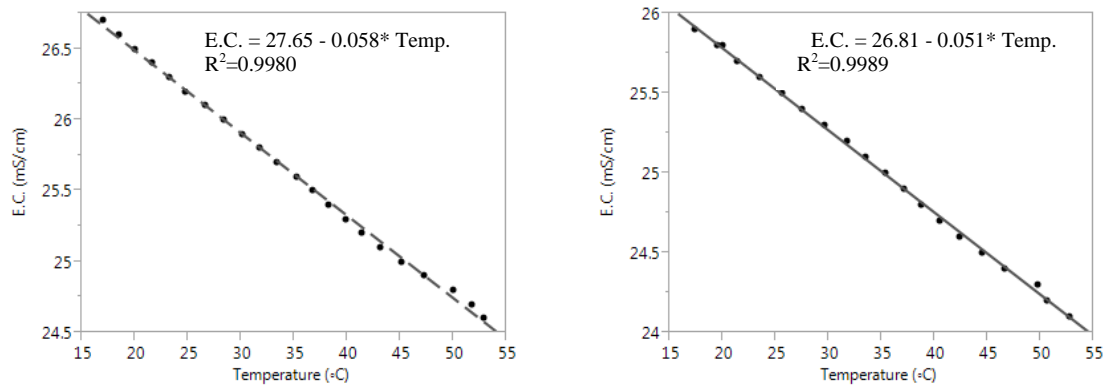


Figure 3.1. Electrical conductivity (EC) of treatment solution containing 0.1M urea (left) and 1M urea (right) versus temperature.

3.2.4 CaCO_3 Precipitation Mass Measurement

Calcium carbonate precipitation progress was also investigated through measuring the mass of solids precipitated in treatment solution at different time intervals of incubation period (60, 180, 360, 720, 1440, 2880 and 5760 minutes after test onset). The treatment solution and temperature were the same as what were used for conductivity measurement but in presence of calcium chloride. Prior to measuring the mass, the precipitates were vacuum filtered, thoroughly washed with distilled water to remove soluble phases and impurities, and then dried at 50°C . A similar abiotic solution was also incubated in parallel to each test as a control test.

3.2.5 Measuring the Bacterial Cell Concentration

Bacterial growth in both culture solution and calcium free treatment solution was estimated through measuring the optical density of solution at the wavelength of 600 nm (OD_{600}) by using spectrophotometry. In order to eliminate the effect of color changes caused by various levels of hydrolyzed urea in calcium free solutions, the solutions were earlier centrifuged and the supernatants were replaced with normal saline solution.

Serial dilution method was used to find population of the bacterial cells corresponding to each optical density in the culture solution. It was obtained by counting the single colonies grown on solid medium which has the same recipe as bacterial culture solution as well as 1.5% agar.

3.2.6 Design of Experiments, Analysis of Variance, Regression Analysis

Two-level full factorial design of experiments was applied to evaluate the microbial $CaCO_3$ precipitation pattern and bacterial growth at different initial bacterial cell concentrations, initial Ca^{2+} /urea concentrations and temperatures. Two center points was added to check the stability and nonlinearity in analysis of variance of change in bacterial growth. Each factor and its levels were presented in Table 3.1. The tests were run randomly. Considering seven time intervals for each $CaCO_3$ precipitation test and repetition, a total of more than 150 tests were performed. Table 3.2 shows the design matrix and the averaged results obtained for each response.

Table 3.1. Factors and their experimental range of amount and level.

Factors	Range of amount and concentration		
Initial cell concentration (cell/ml)	10 ⁶	10 ⁷	10 ⁸
Ca ²⁺ /Urea concentration (M/M)	0.07/0.1	0.37/0.55	0.67/1
Temperature (°C)	20	35	50
Level coded	-1	0	+1

The "Design Expert" software (Stat-Ease, Inc., USA) was utilized to calculate the significance level of each factor and their interactions in a full factorial model using the analysis of variance (ANOVA, *F-test*). Those effects with the values of $p < 0.05$ and $0.05 < p < 0.10$ were respectively accepted as significant and marginally significant (Le, 2003).

The "JMP 11" software (SAS Institute, Inc., USA) was employed to perform a nonlinear regression analysis and find the best fit model to the conductivity and precipitation data points. Considering the nature of microbial systems, different types of logistic, Gompertz and exponential functions as well as Michaelis-Menten model (Equations 3.1-3.8) were separately fitted to each series of data points. The best model was then chosen through comparing both R^2 -value and corrected Akaike Information Criterion (AICc) as the R^2 does not merely represent the most accurate model (see Appendix A). Burnham and Anderson (2004) discussed using AICc for model selection. The best model has the smallest value, as discussed in Akaike (1974).

$$\text{Logistic 5P: } y = c + \frac{d-c}{(1+e^{-a(x-b)})^f} \quad (3.1)$$

(a: growth rate, b: inflection point, c: lower asymptote, d: upper asymptote, f: power)

$$\text{Logistic 4P: } y = c + \frac{d-c}{1+e^{-a(x-b)}} \quad (3.2)$$

(a: growth rate, b: inflection point, c: lower asymptote, d: upper asymptote)

$$\text{Logistic 3P: } y = \frac{c}{1+e^{-a(x-b)}} \quad (3.3)$$

(a: growth rate, b: inflection point, c: asymptote, f: power)

$$\text{Gompertz 4P: } y = a + (b - a)e^{-e^{-cx+cd}} \quad (3.4)$$

(a: lower asymptote, b: upper asymptote, c: growth rate, d: inflection point)

$$\text{Gompertz 3P: } y = ae^{-e^{-bx+bc}} \quad (3.5)$$

(a: asymptote, b: growth rate, c: inflection point)

$$\text{Mechanistic Growth: } y = a - abe^{-cx} \quad (3.6)$$

(a: asymptote, b: scale, c: growth rate)

$$\text{Exponential 3P: } y = a + be^{cx} \quad (3.7)$$

(a: asymptote, b: scale, c: growth rate)

$$\text{Michaelis-Menten: } y = \frac{ax}{b+x} \quad (3.8)$$

(a: maximum reaction rate, b: inverse affinity)

Table 3.2. Matrix design of experimental runs and their corresponding results of bacterial growth change ($\Delta(\text{OD}_{600})^*$).

#	Initial cell concentration	Urea/ CaCl ₂ concentration	Temperature	$\Delta(\text{OD}_{600})$
1	-1	1	-1	0.49
2	1	-1	-1	1.135
3	1	-1	1	0.045
4	-1	-1	-1	1.165
5	0	0	0	0.381
6	1	1	1	0.07
7	1	1	-1	0.345
8	-1	1	1	0.051
9	-1	-1	1	0.038
10	0	0	0	0.416

* $\Delta(\text{OD}_{600})$ represents the difference between final cell concentration and initial cell concentration.

3.3 Results and Discussions

3.3.1 Pattern of Change in Electrical Conductivity of the Treatment Solution in the Absence of Calcium

A time-extended electrical conductometry of calcium exclusive *S.pasteurii*-inoculated treatment solution was conducted at each experimental condition. Plotting the conductivity versus time, it was observed that the conductivity change versus time in all the experiments follows a similar pattern as illustrated in Figure 3.2.

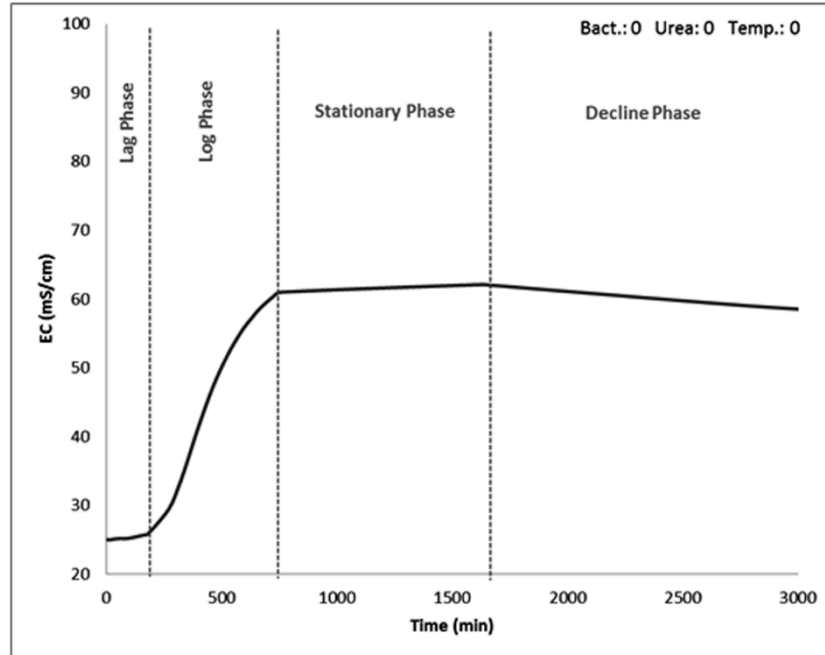


Figure 3.1. Change in conductivity of a calcium exclusive treatment solution versus time.

It was shown that the conductivity change starts exponentially (log phase) after a lag period which varies from a few minutes to some hours at different conditions. The lag duration corresponds to the time required for pH shift to 8 at which the exponential urea hydrolysis is triggered (Whiffin 2004; Parks 2009). The conductivity change exhibits the urea hydrolysis process till the saturation point at which the ammonium ion concentration became constant while the hydrolysis is still progressing at the stationary phase. A slight drop in conductivity after the stationary phase, at decline phase, may be attributed to oversaturation of the system with ammonia, leading off-gassing of ammonia and the apparent decline in ammonium concentration. This is worth to mention that although the conductivity-time pattern is similar to the typical microbial growth curve, it cannot be ascribed to the bacterial growth as the same pattern was also observed in the conditions with no growth.

In the present study, all the conductivity measurements were normalized based on initial urea concentration in order to reduce the uncertainties and make a better comparison. Regression analysis has been performed to fit the best nonlinear model to each normalized conductivity-time series excluding the decline phase which does not occur within the precipitation process. The best fit model was chosen through comparison between the statistics of the various fitted models. It was statistically found that all the experiments were better fitted with a sigmoid function (either logistic or Gompertz) than exponential one. The logistic pattern of the conductivity change versus time may implicitly indicate that the microbial urea hydrolysis reaction follows an autocatalytic kinetics within which ammonium production catalyzes its own formation. Stocks-Fischer et al. (1999) also reported a modified logistic model for the kinetics of calcite precipitation and ammonium production.

3.3.2 Calcium Carbonate Precipitation Progress in Treatment Solution

Mass of calcium carbonate solids precipitated in a treatment solution were measured at the given time intervals. They were also normalized over the initial calcium ion concentration. The same type of function as the best model fitted to the conductivity time series was assigned to the precipitation data points. An R-squared value of around 0.99 for all the experiments suggests an excellent agreement of the precipitation reaction progress with the same type of function as the conductivity fit model.

3.3.3 Comparison between Precipitation Progress and Conductivity Changes in a Treatment Solution at Different Test Conditions

Comparison between precipitation progress and conductivity change curves was presented in Figures 3.3 – 3.9. The results of the tests No. 8 and 9 were not shown, as almost no precipitation and change in conductivity were obtained. Except in the test No.

1 (Figure 3.3), it was interestingly indicated that there is a meaningful coincidence between each precipitation progress curve and its corresponding conductivity pattern at lag phase and log phase. Only a short time extension in the lag phase of the precipitation curve than conductivity curve was monitored in the test No. 4 (Figure 3.6). It was also observed that there is a discrepancy between the upper asymptotes of the precipitation and conductivity curves in all the tests led to precipitation. This difference was less at the minimum concentration of urea.

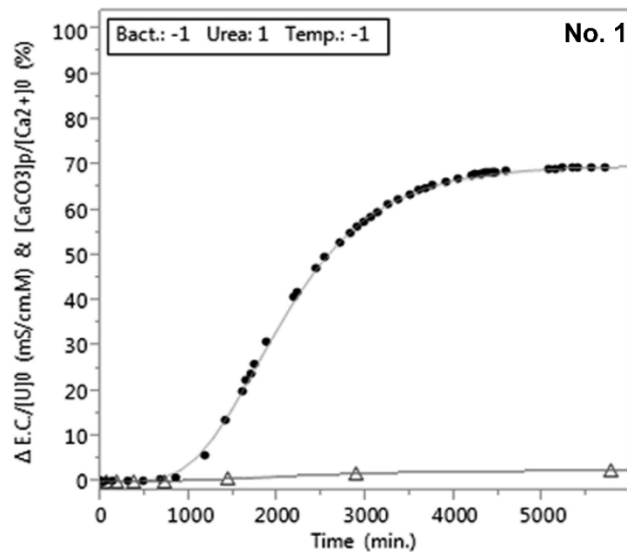


Figure 3.2. Normalized conductivity (●) and precipitation (Δ) data points and their best fitting regression lines at initial cell concentration of 10^6 cell/ml, urea concentration of 1 M, and 20°C .

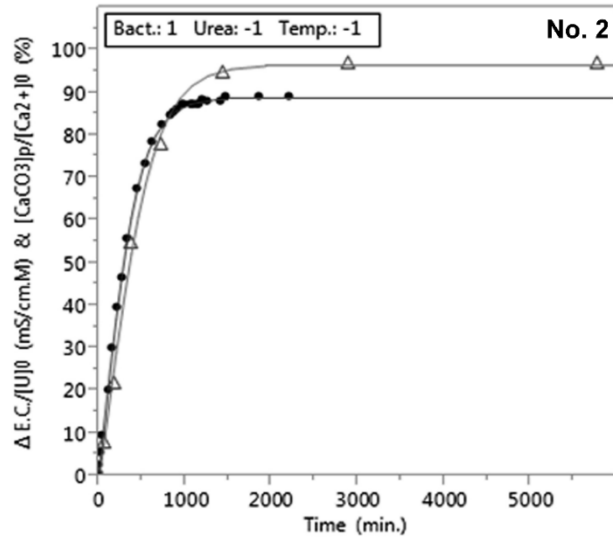


Figure 3.3. Normalized conductivity (●) and precipitation (Δ) data points and their best fitting regression lines at initial cell concentration of 10^8 cell/ml, urea concentration of 0.1 M, and 20°C.

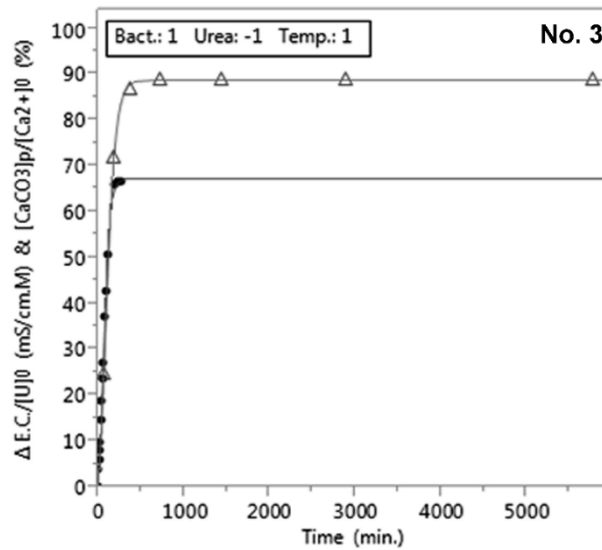


Figure 3.4. Normalized conductivity (●) and precipitation (Δ) data points and their best fitting regression lines at initial cell concentration of 10^8 cell/ml, urea concentration of 0.1 M, and 50°C.

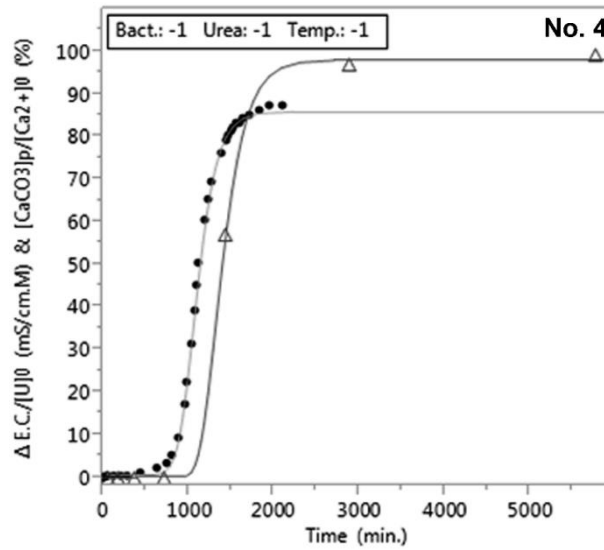


Figure 3.5. Normalized conductivity (●) and precipitation (Δ) data points and their best fitting regression lines at initial cell concentration of 10^6 cell/ml, urea concentration of 0.1 M, and 20°C.

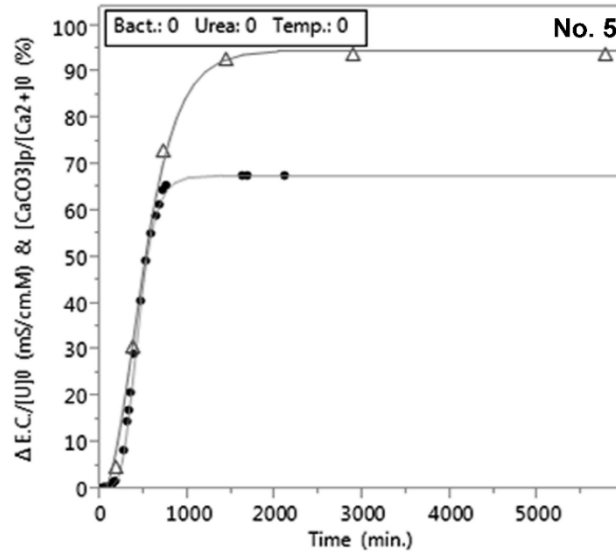


Figure 3.6. Normalized conductivity (●) and precipitation (Δ) data points and their best fitting regression lines at initial cell concentration of 10^7 cell/ml, urea concentration of 0.55 M, and 35°C.

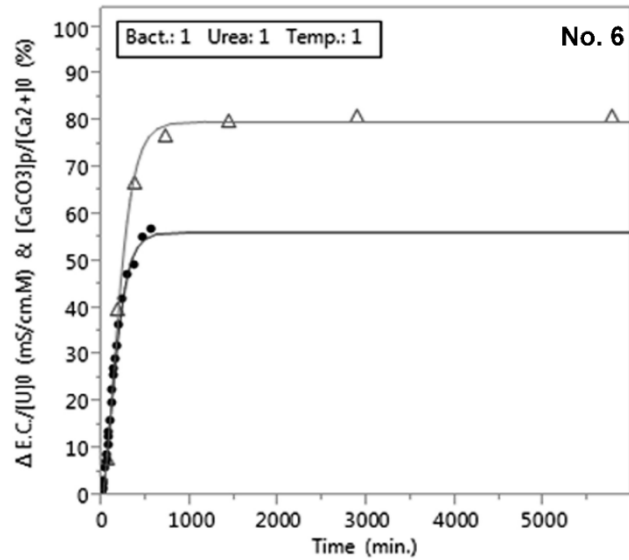


Figure 3.7. Normalized conductivity (●) and precipitation (Δ) data points and their best fitting regression lines at initial cell concentration of 10^8 cell/ml, urea concentration of 1 M, and 50°C .

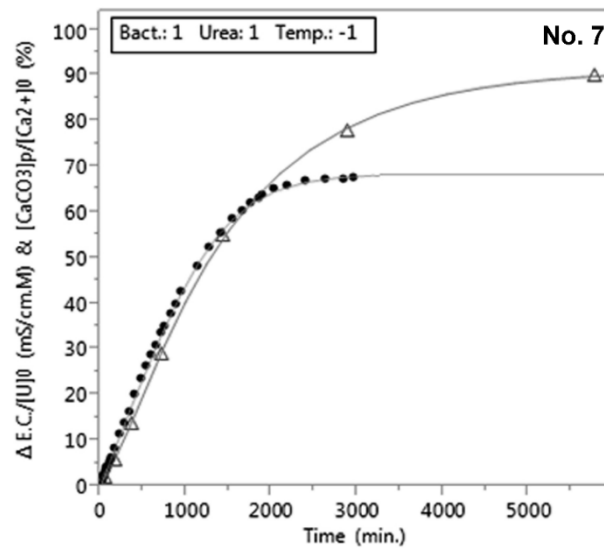


Figure 3.8. Normalized conductivity (●) and precipitation (Δ) data points and their best fitting regression lines at initial cell concentration of 10^8 cell/ml, urea concentration of 1 M, and 20°C .

3.3.4 Microbial CaCO₃ Precipitation Characteristic Curve (MCPCC)

The CaCO₃ precipitation progress curve was designated as microbial CaCO₃ precipitation characteristic curve (MCPCC) in this study since it represents lag duration, precipitation rate and maximum amount of precipitation as three important characteristics describing the progress at each condition.

In the current study, it was detected that the MCPCC for each experimental condition can be obtained by performing an extended time-domain conductometry on the calcium exclusive solution as well as measuring only the maximum amount of precipitation in the calcium inclusive solution. The points at lag phase and (semi-) linear part of log phase from conductometry test are chosen together with the maximum amount of precipitation from mass measurement test. Then the same type of the sigmoid function as the conductivity model is fitted into the new hybrid set of conductivity and mass data points. As conductometry provides more number of points and the type of sigmoid function, more precise regression analysis is resulted. This method is also inexpensive and easy-to-use since there is no need to conduct several precipitates mass measurement tests. A prolongation in lag phase like what occurred in the test No. 4 (Figure 3.6) can be also estimated by visual recording of the approximate onset time of precipitation in the calcium-contained solution.

Generally, estimation of MCPCC for each treatment process can facilitate a better control on precipitation pattern. It can provide designing the most appropriate treatment solution and treatment strategy with existing conditions prior to injection. It can also make an easier process of troubleshooting and retreatment of a corrupted and unwanted

treatment. In other words, the MCPCC estimation helps to modify the precipitation characteristics into desired values by adjusting the controllable influencing factors (e.g. temperature, viscosity and ingredients of treatment solution, etc.). Lag duration creates enough time for spatial distribution of treatment solution within soil. It should be neither too short to cause the near-inlet clogging nor too long to delay the treatment process. Rate of precipitation influences treatment duration and uniformity. Treatment durability is also affected by rate as it mainly determines the type and morphology of the minerals precipitated. Lower rate causes more uniform treatment and stable type of mineral precipitation. Amount of precipitation demonstrates the efficiency of a treatment process. Higher amount leads to less number of treatment cycles.

3.3.5 Variations in Microbial CaCO₃ Precipitation Characteristics

Effects of initial cell concentration, initial Ca²⁺/urea concentration and temperature on variation in microbial CaCO₃ precipitation characteristics and bacterial growth were investigated. Changes in bacterial concentration (Δ (OD₆₀₀)) measurements were presented in Table 3.2. In MCPCCs, upper asymptote of the curves, tangent line on the log phase of the curves, and time-intercept of the tangent lines were considered as the maximum percentage of precipitation, precipitation rate, and lag duration respectively. Figure 3.10 shows variations in the tangent line and lag duration for each experiment.

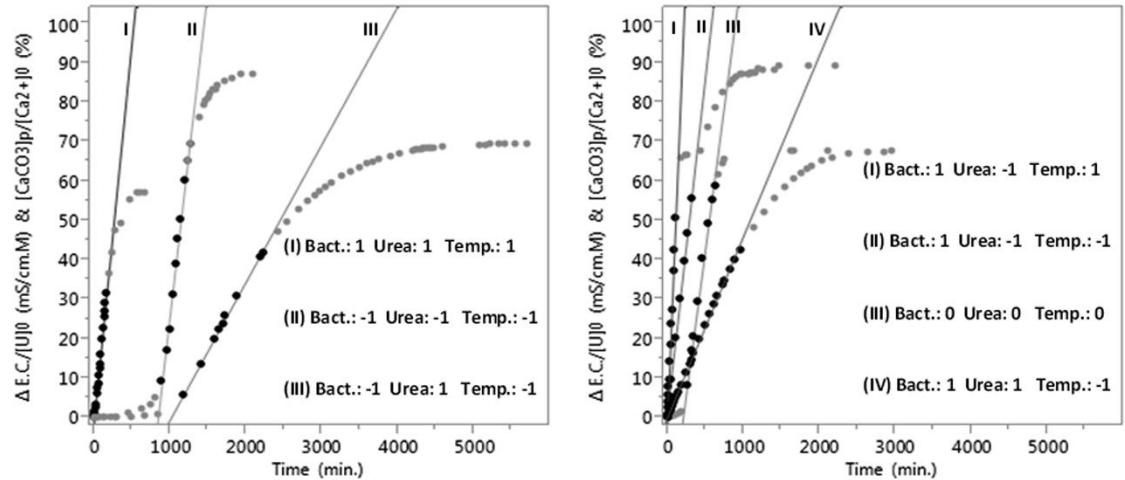


Figure 3.9. Calculating the rate and lag time for each experiment by finding the tangent line on the log phase and its time-intercept (in the legends, Bact., Urea and Temp. represent initial bacterial cell concentration, initial Ca^{2+} /urea concentration and temperature).

Bacterial growth ($\Delta (\text{OD}_{600})$) in calcium-free treatment solution was measured at different conditions. Little growth observed in the conditions of the tests No. 3, 6, 8 and 9 can be attributed to inhibiting effect of the highest level of temperature which is in common in all these four tests. The results of ANOVA indicated the significant negative effect of temperature (p-value= 0.0152) and urea concentration (p-value= 0.0312) and positive effect of their interaction (p-value= 0.0296) on bacterial growth. Insignificant curvature effect (p-value= 0.511) at the range of this study demonstrates that raising temperature or urea concentration linearly hinders the growth. In contrary, an increase up to 70°C or 1.5 M enhances the urease expression of *S.pasteurii* (Whiffin 2004; van Paassen 2009). It can be accordingly realized that the conditions favoring the bacterial growth create an undesirable environment for urease enzyme production. It may be attributed to regulatory effect of *S.pasteurii* in the MICP system by controlling bulk urease generation (Whiffin 2004). The bacteria generally tend to tune-up the system

through enhancing urease production per cell at the harsh condition for bacterial growth or through more cell reproduction at the non-desirable condition for urease generation.

The amounts of precipitation were negligible in the tests No. 1 (Figure 3.3), 8 and 9. In the tests No. 8 and 9, the reason is associated with the lack of growth as explained above. On the other hand, the amount of urease enzyme released by the minimum level of initial cell concentration was not also sufficient enough to speed up the urea hydrolysis reaction. In the test No. 1, there was no precipitation while urea was considerably hydrolyzed with a slow rate in the absence of calcium ions. OD_{600} measurement demonstrated the bacterial growth in the calcium free solution while no bacterial growth was noticed by visual turbidity inspection of the calcium-contained solution. The lack of growth in calcium inclusive medium can be therefore connected to the existence of calcium ions. It is for interaction between minimum cell concentration and maximum calcium ion concentration. The effect of interaction between various concentrations of Ca^{2+} /urea and bacterial cells on precipitation is investigated in detail in the next chapter. It generally seems that the experiments with the desirable growth condition produce higher percentage of precipitation.

Precipitation rate was found independent of the existence of calcium ions in the solution as there is coincidence between log phase of conductivity curve and precipitation curve in all the experiments led to precipitation. Assuming the urea hydrolysis is equal to the conductivity multiplied by a conversion coefficient (Whiffin 2004), it represents that the precipitation rates were always less than the urea hydrolysis rates in the absence of calcium ions at a specific condition. Effect of the factors on precipitation rate is

statistically explained in detail by considering the more number of tests in the next chapter; but it can be implicitly perceived from the figures that increasing initial cell concentration caused an increase in rate. Okwadha and Li (2010) have reported the same effect of initial cell concentration on precipitation rate. It also seems temperature raise led to an increase in precipitation rate provided that its interaction with the minimum level of initial cell concentration does not prevent the bacterial growth and precipitation like tests No. 8 and 9. Excluding the tests with no precipitation, the minimum rate was observed in test No. 7 (Figure 3.9) which may be attributed to the high concentration of urea and low temperature. The maximum rate was observed in test No. 3 (Figure 3.5) at the highest initial cell concentration and temperature and lowest level of urea.

Longer lag duration was observed at the tests with greater change in OD_{600} and less initial cell concentrations. Effect of lower initial cell concentration and temperature on extending lag duration can be realized from the MCPCCs. It indicates that releasing the sufficient amount of urease is prolonged at the suitable conditions for bacterial growth. In the test No. 4 (Figure 3.6), a small shift along time axis points out a prolonged lag phase in the solution containing calcium ions. It manifests that the presence of calcium ions delayed the time corresponding to the starting pH for precipitation (i.e. pH=8.3). Calcium ions probably caused a reduction in the bacterial growth rate at the least temperature and initial cell concentration.

3.4 Conclusion

The hybrid method of conductometry and one precipitation mass measurement test instead of several precipitation mass measurement tests, proposed in this chapter, was found to be a reliable, fast, cheap and non-expert friendly method for monitoring the

precipitation progress in a treatment solution. It was detected that the precipitation pattern in treatment solution follows a logistic function (designated as MCPCC) which describes precipitation lag duration, precipitation rate and maximum amount of precipitation. It provides useful information on describing, interpreting, estimation and steering the precipitation pattern within soil. It can act as an index enabling investigation of the effect of other factors (e.g. temperature, solution ingredients, competing microorganisms, etc.) on precipitation pattern. It also facilitates designing an optimum treatment solution.

It was also observed that initial cell concentration, initial Ca^{2+} /urea concentration, and temperature influence the lag duration, precipitation rate, maximum amount of precipitation and bacterial growth. Hence, the precipitation pattern within soil pores can be controlled by changing these influencing factors. For instance, lag duration, which creates enough time for treatment solution to be well distributed within soil pores and prevents near-inlet clogging, is prolonged at lower temperature and initial cell concentration.

In this study, it was aimed to develop a simple, cheap, fast and non-expert friendly technique for monitoring the ureolysis-based MICP progress in a treatment solution. For this purpose, an extended time-domain electrical conductometry of calcium free treatment solution was assessed. In order to check the reliability of the method, the change in electrical conductivity of the treatment solution as a result of urea hydrolysis (NH_4^+) was compared with real precipitation progress. The real precipitation progress was monitored through precipitation mass measurement in the same treatment solution

containing calcium ions at different time intervals. Finally, a hybrid of conductometry and precipitation mass measurement tests was proposed. A general characteristic pattern was described for precipitation progress. Effect of different initial cell concentrations, Ca^{2+} /urea concentrations and temperatures on precipitation pattern was also investigated.

Chapter 4

EFFECT OF SELECTED ENVIRONMENTAL FACTORS ON MICROBIAL CaCO_3 PRECIPITATION CHARACTERISTICS

4.1 Introduction

In chapter 3, it was qualitatively demonstrated that initial cell concentrations, CaCl_2 /urea concentrations and temperatures as the key adjustable parameter of a treatment solution significantly influence microbial CaCO_3 precipitation characteristics (MCPC), i.e. lag duration, precipitation rate and precipitation ratio. There are many studies which investigated the effect of different environmental factors on precipitation rate and ratio (Al Thawadi 2008; Al Qabany et al. 2011; Chu et al. 2014; Ferris et al. 2004; Martinez et al. 2013; Mortensen et al. 2011; Okwadha and Li 2010; Parks 2009; Stocks-Fischer et al. 1999; van Paassen 2009; Whiffin 2004) but no study was found on lag duration. Those studies on precipitation rate usually explain the effect of environmental factors by changes in urease activity or bacterial growth. Most of them are also biology-oriented studies considering very small concentration of calcium chloride and urea which is not applicable for geotechnical applications. The studies on precipitation ratio are mainly limited to considering the effect of CaCl_2 /urea regardless of other environmental factors. These studies have only tried to report the optimum CaCl_2 /urea based on their own experimental observations without any specific reason. In this chapter, a comprehensive

series of experiments is carried out to evaluate the effect of initial cell concentration, concentration of calcium chloride and urea, proportion of calcium chloride to urea, temperature and their interactions on lag duration, precipitation ratio and precipitation rate. The existing studies on the effect of environmental factors in the literature do not consider the interactions between influencing factors. Statistical analysis is also performed to represent the results (i.e. level of significance of each factor), quantitatively. It is also tried to represent mathematical models correlating the precipitation characteristics to the factors. Effects of some other factors like the presence of seawater, the lack of nutrient broth and the lack of air are assessed.

4.2 Materials and Methods

4.2.1 Bacterial Growth Condition

The bacterial species and its growth condition were described in section 3.2.1.

4.2.2 Treatment Solution

The treatment solution was prepared in the same way as explained in section 3.2.2. A diverse proportions of calcium chloride to urea was also considered in some tests in this chapter, while it was fixed to 2/3 in previous chapter. In order to check the effect of various concentrations of nutrient broth, treatment solutions with 1g/l and no nutrient broth were prepared in some tests, while it was normally 3 g/l at the other test conditions. Some tests were also run at the condition with no aeration ratio. At this condition, the flasks were fully filled with treatment solution and then capped and sealed so that there was no significant amount of air inside except the dissolved air in the solution. The aeration ratio for the other tests at the normal condition was adjusted to 1 portion of treatment solution to 5 portions of air. A few tests were also performed with

the treatment solution containing 50% natural seawater sampled from Mediterranean Sea, Famagusta Bay, Cyprus. Total dissolved solids (TDS) of the seawater were 38600 ppm. To prepare this solution, a given volume of double concentrated treatment solution was mixed with the same volume of filter sterilized seawater after autoclaving.

4.2.3 Monitoring the Microbial CaCO₃ Precipitation Characteristics

The hybrid method of conductometry and precipitation mass measurement tests, which were suggested in the previous chapter, was applied for monitoring the lag duration, precipitation rate and precipitation ratio at each test condition.

4.2.4 Statistical Modelling

Two-level full factorial experimental design studied in the previous chapter is augmented to three-level full factorial design for modelling the response surface, which correlates the microbial calcium carbonate precipitation characteristics to the effect of initial bacterial cell concentrations, initial Ca²⁺/urea concentrations and temperatures. The tests were run randomly and repeated twice. The "Design Expert" program (Stat-Ease, Inc., USA) was utilized to identify the best model fitted to response data points and perform ANOVA (*F-test*) for estimation of the model parameters.

The "JMP 11" software (SAS Institute, Inc., USA) was used to perform a nonlinear and response surface regression analysis on precipitation ratio data points by using the least square method.

4.3 Results and Discussions

4.3.1 Effect of Initial Cell Concentration, CaCl₂/urea Concentration and Temperature on Microbial CaCO₃ Precipitation Characteristics

In order to refine the effect of the influencing factors and their interactions on microbial CaCO₃ precipitation characteristics (MCPC), a three-level full factorial design was performed. Each factor is evaluated at the lowest level, mid-level and the highest level in the new design. Table 4.1 shows the three-level design of experiments and their corresponding results for each characteristic. This augmentation enables more detailed analysis and fitting a response surface model.

4.3.1.1 Precipitation Rate, r

Design Expert program was used to identify the best model fit to the precipitation rate data. The significant model ($p\text{-value} > 0.05$) with higher order and insignificant lack of fit ($p\text{-value} < 0.05$) is chosen as the best model for further in-depth analysis. Summary of the fit statistics for four models was shown in Table 4.2. The 2FI model which is composed of the effect of main factors (i.e. initial cell concentration, urea concentration and temperature) and their second order interactions (i.e. interactions between initial cell concentrations and urea concentration, initial cell concentrations and temperature, and urea concentration and temperature) was identified as the best fit into the precipitation rate data. The results of ANOVA (*F-test*) for this model (Table 4.3) indicate the significant influence of the main factors and the interaction between initial cell concentrations and temperature on precipitation rate. Insignificant lack of fit also suggests that the model is well fitted to the data. Equation 4.1 represents the model after reduction of insignificant terms. The R²-value around 0.73 indicates that the model can

Table 4.1. Three-level full factorial experiments and their corresponding response*.

#	Initial cell concentration (cell/ml)	Urea/ CaCl ₂ (M/M)	Temperature (°C)	r (min ⁻¹)	P _{max} (%)	T _{lag} (min)
1	10 ⁶	1/0.67	20	0	2	∞
2	10 ⁸	0.1/0.07	20	0.17	97	0
3	10 ⁸	0.1/0.07	50	0.47	89	0
4	10 ⁶	0.1/0.07	20	0.17	99	875
5	10 ⁷	0.55/0.37	35	0.17	94	300
6	10 ⁸	1/0.67	50	0.19	81	0
7	10 ⁸	1/0.67	20	0.05	90	0
8	10 ⁶	1/0.67	50	0	2	∞
9	10 ⁶	0.1/0.07	50	0	1	∞
10	10 ⁷	0.55/0.37	35	0.15	97	220
11	10 ⁶	1/0.67	35	0	3	∞
12	10 ⁶	0.1/0.07	35	0.18	100	410
13	10 ⁶	0.55/0.37	35	0.14	19	465
14	10 ⁶	0.55/0.37	20	0.19	34	1070
15	10 ⁶	0.55/0.37	50	0	0	∞
16	10 ⁸	1/0.67	35	0.19	94	0
17	10 ⁸	0.1/0.07	35	0.21	100	0
18	10 ⁸	0.55/0.37	35	0.17	99	0
19	10 ⁸	0.55/0.37	20	0.16	97	0
20	10 ⁸	0.55/0.37	50	0.39	88	0
21	10 ⁷	0.55/0.37	50	0.23	51	0
22	10 ⁷	0.55/0.37	20	0.16	97	380
23	10 ⁷	1/0.67	35	0.14	27	290
24	10 ⁷	1/0.67	20	0.17	21	470
25	10 ⁷	1/0.67	50	0.26	9	0
26	10 ⁷	0.1/0.07	35	0.18	99	110
27	10 ⁷	0.1/0.07	20	0.16	100	215
28	10 ⁷	0.1/0.07	50	0.36	73	0

* Responses are r, P_{max} and T_{lag} which represent precipitation rate, precipitation ratio and lag duration, respectively.

explain 73% of the variability in the response. An adequate response surface model should have an R^2 -value above 0.60, and the bigger R^2 -value the more statistically accurate is the model (Montgomery et al. 2011). The other statistics were also considered for checking the adequacy of the model (see Appendix B). The results of predicted values by this model and actual values of five verification tests are in an acceptable agreement with each other (Table 4.4). Three dimensional surface and counter plots of the model are illustrated in Figure 4.1. It is shown that an increase in urea concentration leads to a decrease in precipitation rate. It may be attributed to the suppressing effect of higher concentration of urea on bacterial growth (explained in previous chapter). Initial cell concentration and temperature were found to have interdependent influence on precipitation rate. An increase in initial cell concentration was found to have no influence on precipitation rate at the lowest temperature while it shows an increasing influence on the rate by raising the temperature. This behavior can be explained by favoring and hindering effect of lower temperature on bacterial growth and urease activity, respectively. It seems that the cell concentration at the end of the lag duration (at the beginning of the log phase) in the solutions with different initial cell concentrations is nearly the same at the lowest temperature. In other words, at the lower temperature, each bacterial cell prefer to be reproduced instead of enzyme generation in order to hydrolyze the minimum required amount of urea for reaching the pH triggering log phase. That is why longer lag duration is also observed at the lower temperature and initial cell concentration. On the contrary, at the highest temperature, the existing cells in the solution can only generate enzyme as the condition is desirable for enzyme production not growth. Higher initial cell concentration causes bigger precipitation rate at this condition. That is why no precipitation was observed at the conditions with the

highest temperature and the lowest initial cell concentration (tests No. 8, 9, 15). Actually, the enzyme produced by the smallest population of the bacteria was not sufficient for triggering the log phase and considerable amount of precipitation. Moreover, there are a few other conditions at which no precipitation was observed (tests No. 1 and 11). These are the conditions with the lowest initial cell concentration and the highest CaCl_2 /urea concentration. As described in the previous chapter, this condition, which cannot be monitored in conductometry of the calcium free solution, happened when CaCl_2 is added into the solution. It seems that a low concentration of enzyme generated by a small number of bacterial cells is affected by electrical conductivity of the treatment solution resulted from high concentration of CaCl_2 (it is discussed in detail in the next section). This effect represents an interaction between the initial cell concentration and CaCl_2 /urea concentration, which cannot be explained by the model presented here for precipitation rate (Equation 4.1) due to the rare number of occurrences within the experimental runs in this study. This drawback of the model can be somewhat eliminated through coupling with the model presented for precipitation ratio in the next section. To do this, the rate of precipitation obtained from Equation 4.1 is corrected to zero if a precipitation ratio equal to zero was achieved from Equation 4.2.

Table 4.2. Summary statistics of different models applied to the precipitation rate data.

Source	Sequential p-value [†]	Lack of Fit p-value [‡]
Linear	0.0012	0.1245
2FI [*]	0.0024	0.1616
Quadratic	0.2099	0.1680
Cubic	0.1832	0.1867

^{*} 2FI corresponds to the factorial model with second order interactions.

[†] Sequential p-value is the probability that the order terms are modeling noise instead of helping explain the trend in the response.

[‡] Lack of fit is measuring how well the model fits the data.

Table 4.3. Table of ANOVA for 2FI model applied to the precipitation rate data.

Source	F Value	p-value Prob > F
Model	15.43	< 0.0001*
A-Initial cell conc.	21.66	< 0.0001*
B-Urea	10.07	0.0046*
C-Temperature	5.58	0.0279*
AB	0.091	0.7654
AC	19.78	0.0002*
BC	0.19	0.6703
Lack of Fit	23.41	0.1616

$$\begin{aligned}
 \text{Precipitation rate} = & 0.24 - (2.42 * 10^{-10} * \text{Initial cell conc.}) - (0.050 * \text{Urea}) - \\
 & (2.68 * 10^{-3} * \text{Temperature}) + (1.16 * 10^{-11} * \text{Initial cell conc.} * \text{Temperature}) \geq 0 \\
 & (R^2 = 72.8\%) \qquad \qquad \qquad (4.1)
 \end{aligned}$$

Design-Expert® Software

Factor Coding: Actual

Precipitation rate (min⁻¹)

● Design points above predicted value

○ Design points below predicted value

0.47

0

X1 = A: Initial cell conc.

X2 = C: Temperature

Actual Factor

B: CaCl₂/urea = -1

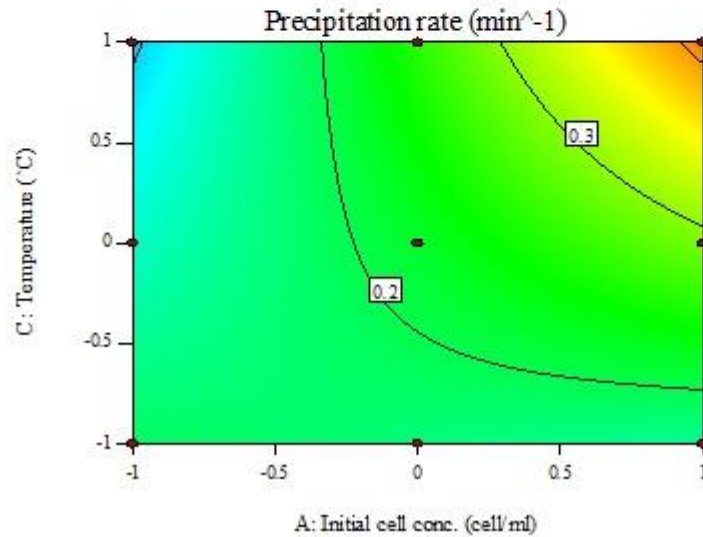
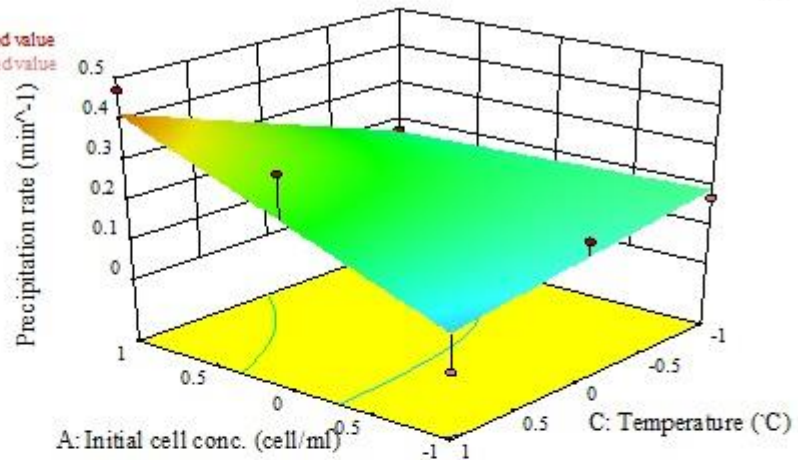


Figure 4.1. Response surface (3D and counter plots) of the precipitation rate at the (a) lowest, (b) mid and (c) highest level of urea concentration.

b

Design-Expert® Software

Factor Coding: Actual

Precipitation rate (min⁻¹)

● Design points above predicted value

○ Design points below predicted value

0.47

0

X1 = A: Initial cell conc.

X2 = C: Temperature

Actual Factor

B: CaCl₂/urea = 0

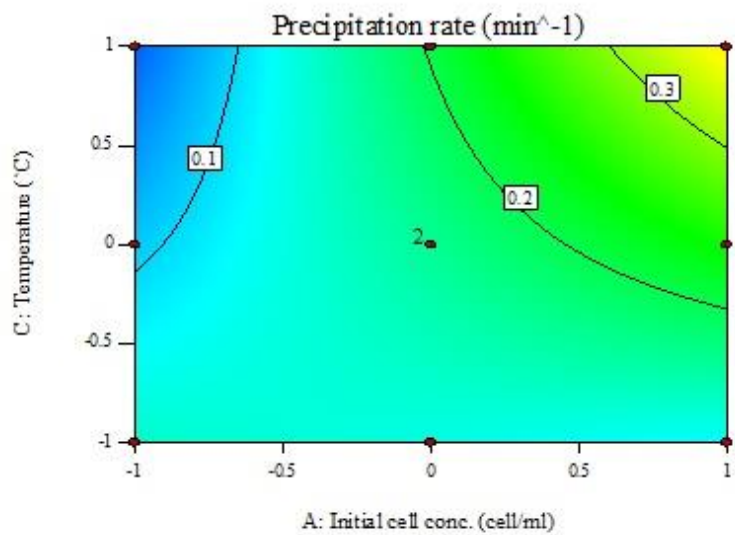
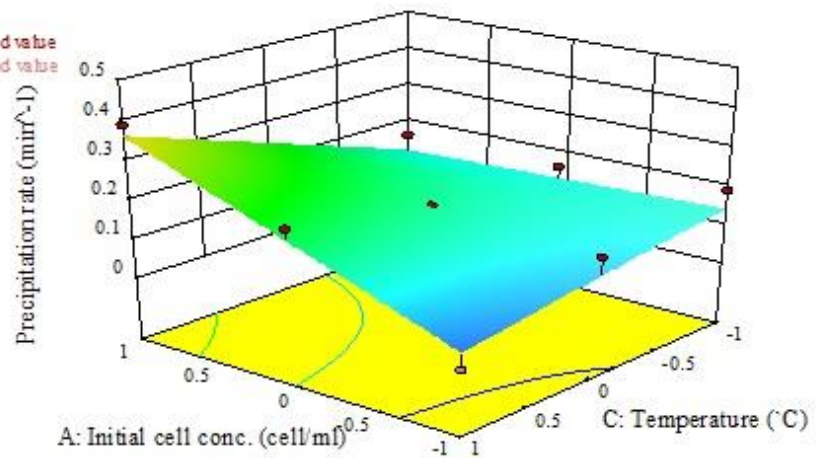


Figure 4.1. (Cont.)

C

Design-Expert® Software

Factor Coding: Actual

Precipitation rate (min^{-1})

● Design points above predicted value

○ Design points below predicted value

0.47

0

X1 = A: Initial cell conc.

X2 = C: Temperature

Actual Factor

B: CaCl₂/urea = 1

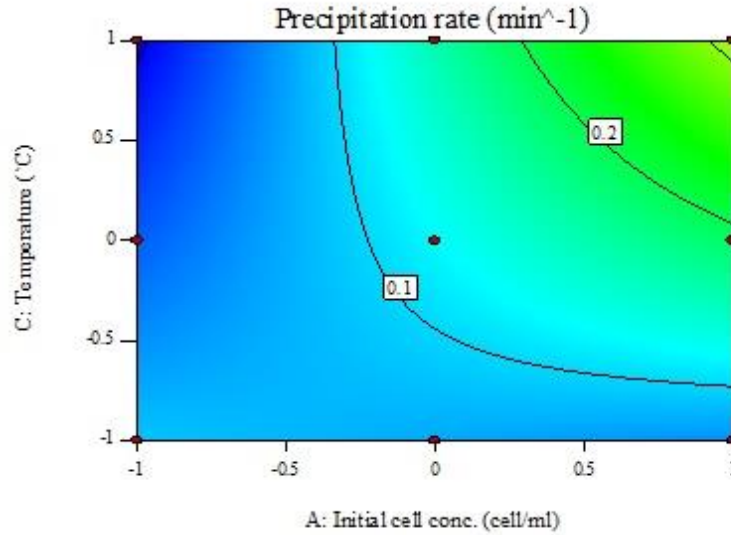
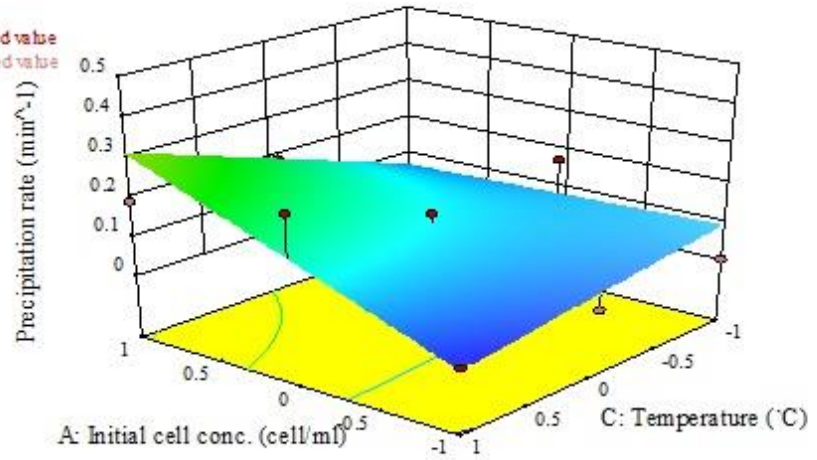


Figure 4.1. (Cont.)

Table 4.4. Comparison between actual values from verification tests and predicted values by presented model for precipitation rate.

Initial cell conc. (cell/ml)	Urea (M)	Temperature (°C)	Predicted rate (min ⁻¹)	Actual rate (min ⁻¹)
10 ⁸	0.90	45	0.35	0.32
10 ⁸	0.75	30	0.22	0.17
10 ⁷	0.35	25	0.16	0.14
10 ⁶	0.15	25	0.17	0.19
10 ⁷	0.30	50	0.12	0.15

4.3.1.2 Precipitation Ratio, P_{max}

It has also been tried to fit a model describing the precipitation ratio. For this purpose, four models (linear, 2FI, quadratic and cubic) were assigned to the response data presented in Table 4.1. As shown in Table 4.5, although sequential p-values for linear and 2FI models suggest that the models are properly representing the data rather than noise, their marginally significant ($0.1 > p\text{-value} > 0.05$) lack of fit indicates that the models are not well fitted to the data. Therefore, more number of tests might be required to get a good fit. On the other hand, all the tests in Table 4.1 were performed with a constant proportion of CaCl₂/urea (i.e. equal to 2/3), which means that even a well-fitted model may not be applied to the other possible proportions of CaCl₂/urea. Hence, a new set of experiments with various proportions of CaCl₂/urea and initial cell concentrations were designed for developing a model for precipitation ratio. Temperature was kept constant at 35°C in this series of tests. The reason of keeping the temperature constant is due to its non-interacting effect with the other factors, perceived from ANOVA of the

previous full factorial experiments. It reveals that temperature raise causes a decrease in precipitation ratio. The results of ANOVA were presented in Table 4.6. The new set of tests and their corresponding results of precipitation ratio at each initial cell concentration were shown in Table 4.7. Considering the electrical conductivity of each solution before adding bacteria, it was interestingly observed that there is a correlation between conductivity of each solution and the precipitation ratio at each initial cell concentration. Electrical conductivity of the treatment solution is a function of CaCl_2 and urea concentration. The results detect an interdependent relation between initial cell concentration and CaCl_2 /urea concentration. Significant interaction between initial cell concentration and CaCl_2 /urea concentration in ANOVA of previous full factorial experiments (Table 4.6) confirm this observation statistically. Plotting precipitation ratio versus electrical conductivity reveals that the data points are following a trend line for each initial cell concentration (see Figure 4.2). In order to model this trend, a regression analysis has been carried out to fit the best function to the data points. It was then found that the corresponding points of each initial cell concentration can be accurately described by a logistic equation (Equation 4.2). This model correlates the precipitation ratio to the electrical conductivity of the solution prior to adding bacterial cells at 35°C . Electrical conductivity of a solution varies with temperature; that is why temperature was found to have significant effect on precipitation ratio in ANOVA of previous full factorial experiments. In order to estimate the electrical conductivity of the treatment solution containing different concentrations of CaCl_2 and urea, a regression analysis was performed to fit a quadratic surface to the conductivity data in Table 4.7 by using the least square methods. Table 4.8 shows the significance of the model parameters. It demonstrates that all the parameters except the second order effect of urea have a non-

zero coefficient. The model and its fit statistics were presented in Equation 4.3 and Table 4.9, respectively. A good agreement between the predicted and the actual values verifies these models (Table 4.10).

Table 4.5. Summary statistics of different models applied to the precipitation ratio data.

Source	Sequential p-value	Lack of Fit p-value
Linear	< 0.0001	0.0707
2FI	0.0280	0.0813
Quadratic	0.1700	0.0857
Cubic	0.2192	0.0931

Table 4.6. Table of ANOVA which represents the significance level of each factor and their second order interactions on precipitation ratio.

Source	F Value	p-value Prob > F
A-Initial cell conc.	45.77	< 0.0001*
B-CaCl ₂ /urea	25.48	< 0.0001*
C-Temperature	8.18	0.0094*
AB	6.14	0.0218*
AC	2.33	0.1416
BC	2.60	0.1215

As highlighted in Table 4.7, for each initial cell concentration, there is a specific electrical conductivity above which the precipitation ratio drops. This specific point was designated as critical electrical conductivity ($EC_{critical}$) in this study. $EC_{critical}$ was considered as the biggest conductivity value corresponding to the precipitation ratio of more than 85%. Bigger conductivity than $EC_{critical}$, the less amount of precipitation ratio.

Table 4.7. Set of experiments performed for finding the precipitation ratio at different CaCl₂, urea and initial cell concentrations.

CaCl ₂ (M)	Urea (M)	EC (mS/cm)	P _{max} (%) at different cell concentrations		
			10 ⁶	10 ⁷	10 ⁸
1.5	1.5	159	1	0	59.6
1.4	1.5	155.5	0	0	64
1.25	1.5	147.4	0	1	61
1.17	1.75	141.7	1	1	34.7
1	1	137.8	0	0	65.4
1	1.25	135.8	1	1	67
1	1.5	134	1	4	70.3
0.67	0.67	111.7	0	25.1	81.1
0.67	1	110.1	3	27.4	94
0.67	1.5	105.7	0	29.1	88
0.55	0.55	101.3	1	30.8	93
0.55	0.825	99	0	38.4	95
0.52	0.78	95.5	3.4	44.3	98
0.5	1	92.4	11	51.3	96
0.39	0.78	80.4	21	86	98
0.37	0.37	79.8	18.9	88.4	100
0.37	0.55	79	19.3	94	99
0.37	0.825	77.9	38	91.1	97
0.33	0.33	74.5	51	97	97.6
0.33	0.49	74	54	99	99
0.22	0.22	61.4	97	98	100
0.22	0.325	59.5	98	97.5	100
0.22	0.49	59.4	98	100	98
0.22	1	58.6	100	96.8	99
0.17	0.78	52.3	99	99	97.8
0.12	0.55	44.1	100	100	100
0.07	0.1	38.6	100	99	100

It was demonstrated that a treatment solution containing less initial cell concentration has less $EC_{critical}$. It was also found that the precipitation ratio in a treatment solution with a conductivity value below around 61 mS/cm is almost 100% even for 10^4 cell/ml initial cell concentration (Table 4.11). There are some studies which have investigated the effect of different concentrations of $CaCl_2$ and urea in order to find the optimum proportion for obtaining highest amount of precipitation (Whiffin 2004; Al Thawadi 2008; van Paassen 2009) but none of them have reported a certain reason for their findings. This study, which attributes the effect of various concentrations of $CaCl_2$ and urea on precipitation ratio to the electrical conductivity of the solution, can explain all the current findings in the literature. The dependency of the precipitation ratio to the conductivity of the solution can be ascribed to denaturation of less concentration of urease enzyme in a solution with high ionic strength.

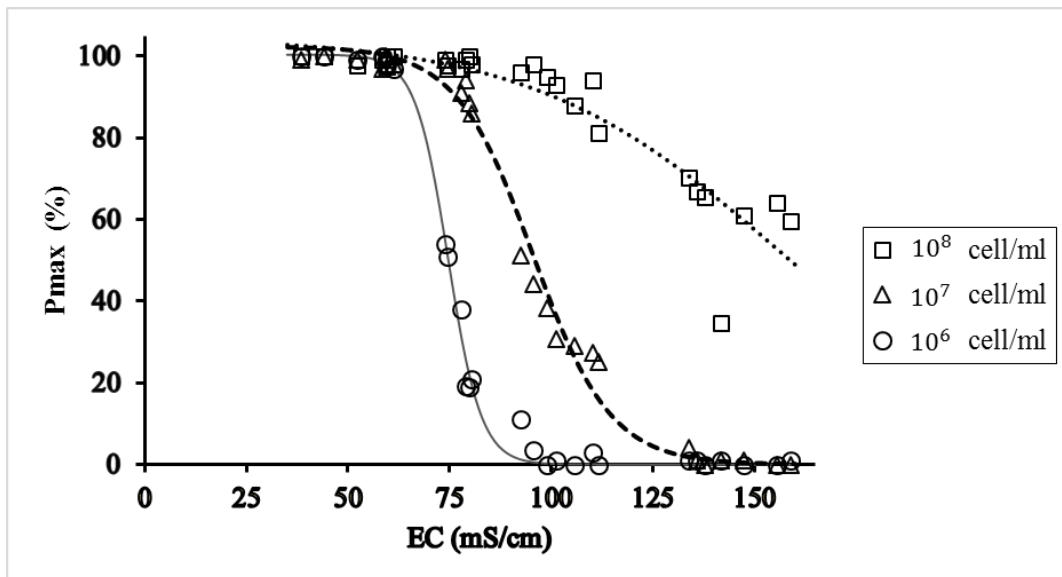


Figure 4.2. Trend line for precipitation ratio versus electrical conductivity of the treatment solution at different initial cell concentrations.

$$P_{max} = \begin{cases} \frac{100.4}{1 + e^{0.246 (EC-74.6)}} \leq 100, & \text{for } 10^6 \frac{\text{cell}}{\text{ml}} & (R^2 = 99.5\%) \\ \frac{102.3}{1 + e^{0.105 (EC-95.5)}} \leq 100, & \text{for } 10^7 \frac{\text{cell}}{\text{ml}} & (R^2 = 98.8\%) \\ \frac{104.8}{1 + e^{0.033 (EC-155.8)}} \leq 100, & \text{for } 10^8 \frac{\text{cell}}{\text{ml}} & (R^2 = 83.6\%) \end{cases} \quad (4.2)$$

Table 4.8. Significance of parameters of the response surface model fitted to the electrical conductivity data points.

Term	Prob> t
Intercept	<0.0001*
CaCl2	<0.0001*
Urea	<0.0001*
(CaCl2 - 0.59)*(CaCl2 - 0.59)	<0.0001*
(CaCl2 - 0.59)*(Urea - 0.87)	0.0187*
(Urea - 0.87)*(Urea - 0.87)	0.7150

$$EC = 45.5 + (106.08*CaCl2) - (6.24*Urea) - [37.68*(CaCl2 - 0.59)^2] - [8.80*(CaCl2 - 0.59)*(Urea - 0.87)] \quad (4.3)$$

Table 4.9. Fit statistics of the electrical conductivity model resulted from the least square method analysis.

Source	DF	Sum of Squares	Mean Square	F Ratio	R ²	R ² Adj.
Model	4	32806.850	8201.71	22561.57	0.999756	0.999712
Error	22	7.998	0.36	Prob > F		
C. Total	26	32814.847		<0.0001*		

Table 4.10. Comparison between actual values from verification tests and predicted values by presented models for electrical conductivity and precipitation ratio.

CaCl ₂ (M)	Urea (M)	Initial cell conc. (cell/ml)	Predicted EC (mS/cm)	Actual EC (mS/cm)	Predicted P _{max} (%)	Actual P _{max} (%)
1.4	1.75	10 ⁸	152.03	152.99	55.7	51.6
1.25	1.75	10 ⁷	145.58	146.7	0.5	0
0.75	1	10 ⁷	117.66	119.01	9.1	6.5
0.75	0.75	10 ⁶	119.57	120.36	0	0
0.45	0.45	10 ⁸	89.18	88.49	94.3	97
0.45	1	10 ⁷	86.43	85.31	73.8	75.2
0.9	1.1	10 ⁷	129.83	130.52	2.7	0.5
0.2	0.55	10 ⁶	56.49	55.94	99.2	97.3

Table 4.11. Precipitation ratio below the minimum EC_{critical} at 10⁴ and 10⁵ cell/ml initial cell concentration

CaCl ₂ (M)	Urea (M)	EC (mS/cm)	P _{max} (%) at different cell concentrations	
			10 ⁵	10 ⁴
0.22	0.22	61.2	100	98
0.07	0.1	38.6	100	100

4.3.1.3 Lag Duration, T_{lag}

As explained in detail in the previous chapter, lag duration represents the time period between the beginning of the test when no precipitation occurred and onset of the log phase when precipitation starts exponentially. As shown in Table 4.1, the amount of lag duration varies between zero and infinity. Zero values correspond to those tests with

immediate precipitation (within some minutes) after adding bacterial cells into the solution. Infinite values describe the tests which have never experienced the precipitation within time at that condition. Considering this wide range of change in lag duration, no model can be found to fit the data. Even more number of tests cannot be helpful since the range is too wide to be filled by an affordable number of tests. In other words, numerous tests are required to get a model fit with insignificant lack of fit. Therefore, the best and easiest way for getting estimation on lag duration is the visual inspection of a precipitation process, as suggested in Chapter 3. It can be clearly perceived from the test results that longer lag duration is expected at the conditions favoring the bacterial growth. As discussed earlier, it seems lag duration corresponds to the condition at which the system required reproduction of more number of cells to hydrolyze the minimum amount of urea for shifting the pH to around 8.3, required for precipitation. Visual examination of the solution within lag duration confirmed bacterial growth (i.e. increasing turbidity of the solution) with no precipitation.

4.3.2 Effect of the Presence of Seawater on Precipitation Ratio

In order to see the effect of ionic strength caused by other salts as well as urea and calcium chloride on precipitation ratio, 50% (by volume) of the distilled water used for preparation of treatment solution was replaced with natural seawater. The concentrations of calcium chloride and urea in each solution were adjusted in a way that the EC did not exceed the corresponding $EC_{critical}$ of the initial cell concentration in the solution. In other word, the concentration of calcium chloride and urea were adjusted in a way that approximately a full precipitation ratio is expected for each solution. Table 4.12 shows the test conditions and results. In contrast to what was expected from the results in Section 4.3.1.2, the results here (highlighted in the table below) represents a value much

less than the full precipitation ratio. It manifests that the models for precipitation ratio in Section 4.3.1.2 is applicable when EC of the treatment solution is only resulted by general ingredients (nutrient broth, ammonium chloride, sodium bicarbonate and hydrochloric acid) as well as calcium chloride and urea. The EC caused by the presence of seawater reduced the precipitation ratio at lower initial cell concentration.

Table 4.12. Effect of 50% seawater (by volume) on precipitation ratio; temperature was kept constant at 35°C within the tests.

CaCl ₂ /Urea	EC (mS/cm)	Cell concentration (cell/ml)	P _{max} (%)
0.06/0.49	57.8	10 ⁶	36
		10 ⁷	91
		10 ⁸	99
0.1/0.55	65.4	10 ⁷	49
		10 ⁸	100
0.23/0.78	90	10 ⁸	54

4.3.3 Effect of Various Concentration of Nutrient Broth on Microbial CaCO₃ Precipitation Characteristics

Excluding nutrient broth from treatment solution provides a more selective medium for contribution of ureolytic bacteria in soil environment which includes many species of microorganism. The same two-level full factorial experiments as in Chapter 3 were carried out in the absence of nutrient broth. As depicted in Table 4.13, no significant change in precipitation characteristics was observed except at the tests including considerable lag duration. Lack of nutrient broth led to an increase in precipitation rate and reduction in precipitation ratio and lag duration at the conditions with lag duration.

Montoya (2012) has also reported no change in precipitation rate in the absence of nutrient broth as she had not considered the test conditions with lag duration. Effect of lack of nutrient broth at the conditions with lag duration can be attributed to its influence on bacterial growth. It seems that the lack of nutrient broth disturbs the bacterial growth. That is why lag duration, as a characteristic corresponding to the bacterial growth, is reduced. On the other hand, it was observed earlier that the conditions suppressing the bacterial growth can cause more urease activity. Increase in precipitation rate in the absence of nutrient broth can be attributed to this issue. Some other tests were also performed to check the effect of different concentrations of nutrient broth on precipitation ratio at the corresponding $EC_{critical}$ of 10^6 , 10^7 and 10^8 cell/ml initial cell concentrations (see Table 4.14). Temperature was fixed at $35^{\circ}C$ in all the experiments. Although it was expected to achieve around 100% precipitation ratio in all conditions due to $EC \leq EC_{critical}$, much less ratio was observed at $EC=61.4$ mS/cm, 10^6 cell/ml and $EC=74$ mS/cm, 10^7 . These are the conditions which are anticipated to show a long lag period. These results demonstrate that the model for precipitation ratio cannot be applied for lower concentration of nutrient broth.

Table 4.13. Effect of lack of nutrient broth on microbial CaCO₃ precipitation characteristics.

Initial cell concentration (cell/ml)	Urea/ CaCl ₂ (M/M)	Temperature (°C)	with NB			without NB		
			r min ⁻¹	P _{max} (%)	T _{lag} (min)	r min ⁻¹	P _{max} (%)	T _{lag} (min)
10 ⁶	1/0.67	20	0	2	0	0	0	0
10 ⁸	0.1/0.07	20	0.17	97	0	0.16	99	0
10 ⁸	0.1/0.07	50	0.47	89	0	0.49	90	0
10 ⁶	0.1/0.07	20	0.17	99	875	0.21	8	340
10 ⁷	0.55/0.37	35	0.17	94	300	0.29	34	135
10 ⁸	1/0.67	50	0.19	81	0	0.17	76	0
10 ⁸	1/0.67	20	0.05	90	0	0.07	93	0
10 ⁶	1/0.67	50	0	2	0	0	0	0
10 ⁶	0.1/0.07	50	0	1	0	0	0	0
10 ⁷	0.55/0.37	35	0.15	97	220	0.28	29	160

Table 4.14. Effect of various concentrations of nutrient broth on precipitation ratio; temperature was kept constant at 35°C during the tests.

CaCl ₂ /Urea (M/M)	EC (mS/cm)	Initial cell concentration (cell/ml)	P _{max} (%) at different concentrations of NB		
			3 g/l	1 g/l	0 g/l
0.22/0.22	61.4	10 ⁶	98	4.1	0
		10 ⁷	100	97	94
		10 ⁸	98	97.8	91.4
0.33/0.49	74	10 ⁷	98	28.6	52.3
		10 ⁸	99	95.9	91
0.67/1	110.1	10 ⁸	96	97	97.9

4.3.4 Effect of Lack of Air on Precipitation Ratio

Air concentration drastically drops within soil pores along depth. Some tests were carried out to see the effect of lack of air on precipitation ratio. The tests and their results were presented in Table 4.15. It shows that the precipitation ratio decreases in the treatment solution containing CaCl₂/urea=0.33/0.49, 10⁷ cell/ml and CaCl₂/urea=0.67/1, 10⁸ cell/ml. It seems that these concentrations of bacterial cells cannot grow or produce enough enzyme to precipitate the existing calcium ions. It also seems that the amount of dissolved air in the solution containing CaCl₂/urea=0.22/0.22 is enough for 10⁶ cell/ml of bacterial cells to grow and produce enzyme for precipitating calcium ions.

Table 4.15. Effect of lack of air on precipitation ratio.

CaCl ₂ /Urea (M/M)	EC (mS/cm)	Initial cell concentration (cell/ml)	P _{max} (%) at different aeration ratios	
			0 to 1	5 to 1
0.22/0.22	61.4	10 ⁶	95.7	98
		10 ⁷	98.5	100
		10 ⁸	100	98
0.33/0.49	74	10 ⁷	35.4	98
		10 ⁸	100	99
0.67/1	110.1	10 ⁸	28.5	96

4.4 Conclusion

Statistical model for precipitation rate in this chapter shows that the precipitation rate is significantly influenced by initial cell concentration, CaCl₂ and urea concentration, temperature and the interaction between initial cell concentration and temperature. Comparison between observed and predicted results at some test conditions (with the highest concentration of calcium chloride and urea and the lowest initial cell concentration) represents that the presented model cannot explain the precipitation rate at the condition with no precipitation caused by interaction between the lowest initial cell concentration and the highest concentration of calcium chloride and urea. This was attributed to the high conductivity of the solution at the maximum calcium chloride and urea concentration. Therefore, it was suggested to use the model for precipitation rate when the result obtained from the model for precipitation ratio is not zero.

Precipitation ratio was observed to be a function of initial cell concentration and electrical conductivity of the treatment solution mainly caused by calcium chloride and urea. It was demonstrated that the precipitation ratio drops when the electrical conductivity of the treatment solution is above a specific value ($EC_{critical}$) corresponding to each initial cell concentration.

Statistical model cannot be presented for the lag duration as the conditions with no precipitation (i.e. infinite lag duration) act as outliers. Visual examination of precipitation solution was suggested as the best way for estimation of lag duration. Excluding the tests with no precipitation, which can be realized through the model for precipitation ratio, longer lag duration is expected to occur at the lowest initial cell concentration and temperature.

Seawater was found to cause a reduction in precipitation ratio in the treatment solution with $EC_{critical}$ corresponding to each initial cell concentration. It was found with no influence at EC less than $EC_{critical}$ corresponding to each initial cell concentration. It suggests that the precipitation ratio is just a function of EC caused by calcium chloride and urea not by other saline.

Lack of nutrient broth was observed to increase the rate and decrease the precipitation ratio and lag duration at the conditions with longer lag duration. It did not influence the conditions with no considerable lag duration. This behavior corresponds to the effect of nutrient broth at the conditions favoring bacterial growth.

It was perceived that precipitation happens even at the conditions with lack of air although the precipitation ratio drastically dropped at the conditions with $EC_{critical}$ corresponding to 10^7 and 10^8 cell/ml initial cell concentrations.

Chapter 5

POTENTIAL MORPHOLOGY AND TYPE OF *S.PASTEURII*-INDUCED CALCIUM CARBONATE PRECIPITATION IN TREATMENT SOLUTION

5.1 Introduction

It has been well recognized that morphology and type of calcium carbonate play key roles in its applications for different industries. Mechanical properties of the MICP-treated soil can also be affected by precipitation of different types and morphologies of CaCO_3 . Rhombohedral calcite crystal is the mainly reported mineral in microscale analysis of the studies in the literature since the ideal treatment conditions are usually applied. No study was found to investigate the precipitation of other possible kinds of CaCO_3 in the soil pores within MICP treatment process. It seems there is a lack of mineralogical insight among geotechnical engineers working in this field of research.

To date, six different types of calcium carbonate have been identified: calcite, aragonite, vaterite, monhydrocalcite, ikaite and amorphous calcium carbonate (in decreasing stability). Calcite is the most desirable one for geotechnical applications due to its thermodynamic stable nature. Unstable mineral does not result in ultimate mechanical properties since it may transform to another type of mineral. Al-Thawadi (2008) attributed the ultimate compressive strength of the biocemented sand to the calcite

crystals and not to the vaterite crystals. Aragonite formation is favored at high temperature and pH below 12 or at low temperature in the solution containing magnesium ions and pH less than 11 (Tai and Chen 1998). In water, vaterite transforms to calcite and aragonite at low and high temperature, respectively (Plummer and Busenberg 1984). However, it may be stabilized in the presence of some additives and organic matter in the aqueous solution (Plummer and Busenberg 1984). Electrostatic interaction of calcium ions on the surface of crystal and negatively charged sites of ions and molecules in the solution is responsible for thermodynamic stability of the vaterite (Saikia et al. 2012). Monohydrocalcite is hydrous form of calcium carbonate which appears during dehydration process of ikaite and in the environment containing inhibitors such as magnesium and polyphosphates (Swainson 2008). Small quantity of magnesium is incorporated into its crystal lattice. Monohydrocalcite will more likely form than the water free modifications (calcite, aragonite, vaterite) as there is no need for full dehydration of Mg ions prior to their incorporation into the crystal lattice (Rodriguez-Blanco et al. 2014). It has been reported that this mineral is decomposed to aragonite and calcite in the exposure of air and water, respectively (Swainson 2008). Existence of this mineral in moonmilk of the caves and some beachrocks and lacustrine deposits has been documented (Stoffers and Fischbeck 1974 and 1975; Krumbein 1975; Taylor 1975; Onac 2000). Ikaite forms in presence of inhibitors, like monohydrocalcite, but in near-freezing water (Hu et al. 2012). That is why it is naturally found in cold marine environment. It rapidly disintegrates into more stable phases when removed from cold water. Amorphous calcium carbonate (ACC) is the least stable and the most soluble phase. This is the immediate product of the precipitation process. It usually transforms to more stable phases after seconds of formation (Rodriguez-Blanco et al. 2014). Presence

of high concentration of magnesium may cause stability of ACC (Cobourne et al. 2014). Long term stable ACC can also be synthesized (Bentov et al. 2010). Only biological systems allow coexistence of stabilized ACC and crystalline phases (Jack et al. 2000).

Morphology represents shape and size of the precipitated particles. Calcite has different shapes of crystals. They are usually precipitated as individual or agglomerates of rhombohedral crystals. Spherical calcite crystals have also been observed (Al-Thawadi 2008). Aragonite is precipitated as short to long prismatic, acicular with chisel-like termination, dipyramidal or thick tabular single crystals. It can also be precipitated as columnar, globular, pisolitic, reniform, stalactitic and coralloidal aggregates of crystals and crusts (Anthony et al. 2001). Vaterite precipitates as very finely fibrous crystals. It typically appears in the form of aggregates of spheres and plates (Niedermayr et al. 2013; Anthony et al. 2001). Monohydrocalcite is commonly found as spheroids and crusts. It is also rarely formed as aggregates of rhombohedral crystals (Anthony et al. 2001). Ikaite is normally precipitated as tabular crystals or pseudomorphous after rhombohedral carbonate minerals (Anthony et al. 2001). ACC usually appears as single or aggregated spheroids. It may exhibit various surface textures, depending on the kind of stabilizer used for its synthesis. Mechanism of increasing particle size is dominated by agglomeration of previously individually formed crystals although the primary crystal growth also causes an increase in size (Hostomsky and Jones 1991). Agglomeration pattern varies with precipitation conditions (Hostomsky and Jones 1991). It reveals the weakness and the potential breakage points of a particle at micro level. In most of the previous studies on micro structure of the microbial CaCO_3 precipitates, the experimental conditions were chosen in a way that no crystal agglomeration occurred.

Many studies confirmed that variations in the formation of biogenic CaCO_3 crystals are attributed to several factors. Microorganisms and presence of seawater are two of those factors. Microorganisms can influence the rate of precipitation controlling the formation of CaCO_3 crystal polymorphs (Okwadha and Li 2010). They may act as nucleation sites through causing localized supersaturation in solution (Bosak and Newman 2005). Al-Thawadi (2008) reported well spherical arrangement of rhombohedral calcite crystals in the presence of bacterial cells (localized supersaturation) and poorly arranged ones in the precipitation solution containing pure plant urease (uniform supersaturation). Based on the hypothesis that each bacterial cell can act as a nucleus for an individual crystal formation, it is expected to observe more but smaller individual crystals at higher concentration of bacterial cells. Al-Thawadi's (2008) observations were in contrast with this hypothesis. Formation of various polymorphs of calcium carbonate by different species of bacteria was reported in the literature (Ferris et al. 2004; Sanchez-Moral et al. 2003; Kaur and Mukherjee 2013). There may also be a case of application of the MICP technique into sands with a more complex solution like seawater in the pores. Adding seawater in parent solution results in co-precipitation of various inorganic compounds, which depends on its composition, salinity and temperature (Zuddas and Mucci 1994 and 1998; Lopez et al. 2009; Ries et al. 2008). An increase in ionic strength strongly increases calcite precipitation rate (Zuddas and Mucci 1998) although it may disturb viability of exogenous microorganisms. Natural inorganic seawater constituents, especially magnesium and sulfate ions, hinder calcite precipitation at a given ionic strength (Zuddas and Mucci 1994 and 1998). It is well known that morphology of microbial CaCO_3 in seawater is mainly controlled by Mg:Ca ratio in seawater (Ries et al. 2008). In contrast to calcium ions, magnesium ions stabilize unstable, hydrated and

amorphous phases (Loste et al. 2003). The adsorption and incorporation of foreign ions like magnesium into biogenic calcite crystal structure are significantly correlated with temperature and total ionic strength of parent solution (Zuddas and Mucci 1998; Lopez et al. 2009; Chave 1954). This incorporation inhibits rhombohedral crystal formation (Loste et al. 2003). It should be noted that the results of the literature regarding the effect of Mg:Ca ratio on CaCO₃ precipitation may not be exactly applicable for MICP treatment of soil in presence of seawater because the concentration of calcium as substrate within this technique is much more than the ranges presented in these studies.

This chapter investigates the potential changes in morphology and type of CaCO₃ mineral precipitated in treatment solution, which is commonly used as biogROUT in geotechnical studies, at different conditions. It focuses on the effect of initial cell concentrations, initial Ca²⁺/urea concentrations, temperatures, lack of nutrient broth, and presence of seawater in treatment solution. The crystals were allowed to be agglomerated. In order to see the effect of aging, the precipitates containing unstable phase of mineral at the early ages of precipitation were examined after one year. Light microscopy, SEM, XRD and FTIR were applied as micro-scale identification tools.

5.2 Materials and Methods

5.2.1 Bacterial Culture

Species and growth conditions of the bacterium used at this part of the study are the same as what explained in Section 3.2.1.

5.2.2 Harvested Calcium Carbonate Precipitates

Calcium carbonate precipitates harvested from three kinds of solutions were examined in this study. The first solution was the same treatment solution explained in Section 3.2.2.

This solution is addressed as NB-urea-NH₄Cl solution hereafter in this chapter. A two-level full factorial design of experiments were applied to consider the effect of change in initial cell concentration, initial CaCl₂/urea concentration and temperature on micro-scale properties of the precipitates harvested from NB-urea-NH₄Cl solution. Two center points (tests No. 7 and 10) were also added to check the process stability. The tests were run randomly and repeated twice. Levels of each variable and the experimental design were presented in Table 5.1.

Calcium carbonate precipitation in the same experimental condition as the tests number 1 and 4, corresponding to the lowest and the highest rate of precipitation respectively (Table 5.1), but without nutrient broth (urea-NH₄Cl solution) was also investigated. Excluding the nutrient broth provides a more selective medium for the urea hydrolyzing microorganism.

The precipitates harvested from two treatment solutions containing 50% filter-sterilized seawater (SW-urea-NB-NH₄Cl solution) were also examined. The initial cell concentration in both solutions was adjusted to 10⁸ cell/ml. Initial concentrations of urea and CaCl₂ were respectively equal to 0.1 M and 0.55 M in one solution and 0.23 M and 0.78 M in another one. The values were chosen so that the ionic strength of the medium does not hinder the microbial precipitation. These solutions were incubated at 35°C. Seawater used in this study was sampled from eastern part of the Mediterranean Sea, Famagusta Bay, Cyprus. Its composition was presented in Table 5.2.

Table 5.1. Full factorial design of the experiments for examining the effect of three variables at two levels on micro-scale properties of the precipitates harvested from NB-urea-NH₄Cl solution.

#	Initial bacteria concentration (cell/ml)	Urea/ CaCl ₂ concentration (M)	Temperature (°C)	r (min ⁻¹)
1	10 ⁸	1/0.67	20	0.05
2	10 ⁶	1/0.67	20	NP*
3	10 ⁶	0.1/0.07	20	0.17
4	10 ⁸	0.1/0.07	50	0.47
5	10 ⁶	1/0.67	50	NP
6	10 ⁸	0.1/0.07	20	0.17
7	10 ⁷	0.55/0.37	35	0.15
8	10 ⁸	1/0.67	50	0.19
9	10 ⁶	0.1/0.07	50	NP
10	10 ⁷	0.55/0.37	35	0.17

* NP: No precipitation occurred.

Table 5.2. Composition of seawater used in this study (the ion concentrations are in mg/l).

Cl ⁻	Na ⁺	SO ₄ ²⁻	Mg ²⁺	K ⁺	Ca ²⁺	Br ⁻	C (as CO ₂)	BO ₃ ³⁻
21200	11800	2950	1404	461	425	149	101	66

In order to investigate the agglomeration pattern, a continuous precipitation in each solution was allowed till there was no longer an increase in precipitation mass. Prior to identification analysis, all the precipitates obtained from the solutions were collected using ash-less filter paper, thoroughly rinsed with distilled water to remove impurities, and then dried overnight at 50°C. The dried samples were kept in capped flasks at room temperature for later analysis.

5.2.3 Precipitation Rate Measurement

The rate of calcium carbonate precipitation in each urea-NB-NH₄Cl solution was estimated through the change in electrical conductivity of the same solution in the absence of calcium ions as explained in Chapter 3.

5.2.4 Micro-scale Identification Methods

Light and scanning electron microscopy (SEM) were used to visualize morphology of the calcium carbonate precipitates at different magnifications. For SEM, the clean and completely dried samples were earlier coated with gold in an ion sputter.

X-ray diffraction (XRD) analysis was employed to identify the crystal structure of the precipitated calcium carbonate. For this purpose, the diffracted Cu-K α radiation from dried powders was scanned at the range between 3° to 90° with the speed of 0.5 degree per minute.

Fourier Transform Infra-Red (FTIR) Spectroscopy was applied to identify the molecular structure of the precipitates. The peak position in IR spectrum of each sample reveals an effective mass of vibrating group of atoms, the vibration geometry and the vibrational species in the neighborhood. The powder samples were prepared using attenuated total

reflection (ATR) technique. This technique enables powder samples to be examined directly without pre-treatment.

5.3 Results and Discussions

5.3.1 In Urea-NB-NH₄Cl Solution

The rates of precipitation in urea-NB-NH₄Cl solutions at each test condition are presented in Table 1. Except the tests No. 1 and 4 with the lowest and highest rate, respectively, the other tests show almost a similar rate. As explained in the previous chapter, initial cell concentration, initial Ca²⁺/urea concentration, temperature, and the interaction between initial cell concentration and temperature were statistically found to have significant effect on the precipitation rate.

XRD and FTIR analyses and microscopy of the precipitates deposited in urea-NB-NH₄Cl solution indicated that the morphology and spectra of the samples change when the precipitation rate has significantly changes. Figures 5.1-5.6 compare the results of micro-scale identification analyses at the maximum (0.47 min⁻¹), medium (~0.17 min⁻¹) and minimum (0.05 min⁻¹) rates of precipitation. This observation suggests that the precipitation rate is the most determining factor on morphology and type of the microbially induced calcium carbonate minerals. It means that the initial cell concentration, initial Ca²⁺/urea concentration and temperature influence the morphology and type of mineral through affecting the rate of precipitation.

In the IR spectra, three prominent absorption maxima at ~1391, ~870, ~712 cm⁻¹ and two minor peaks at 2511 and 1795 cm⁻¹ demonstrate the presence of calcite in all the samples (Figures 5.1a-5.1c). These peaks are related to the CO₃ groups in the crystals.

Appearance of two minor peaks at ~ 1090 and ~ 850 cm^{-1} may suggest the existence of aragonite at the precipitation rates of 0.05 and 0.17 min^{-1} . However, the hypothesis can be rejected as the most characteristic peak of aragonite between the absorption bands of 1493 and 1429 cm^{-1} (Huanc et al. 1960) was not observed. So, these two features may be assigned to incorporation of constituents of bacterial growth medium into the biogenic CaCO_3 . The XRD pattern of the samples verifies the presence of calcite crystal phase and the absence of aragonite phase at 0.05 and 0.17 min^{-1} (Figures 5.2a and 5.2c). Two salient peaks at 1074 and 743 cm^{-1} in the IR spectrum of the sample harvested at the highest rate (Figure 5.1b), representing the characteristic peaks of vaterite (Wang et al. 2010), indicate coexistence of vaterite and calcite at the highest rate of precipitation. This is also in agreement with XRD analysis which represents calcite and vaterite phases together at the highest rate (Figure 5.2b). Generally, it was found that precipitation of calcite as the most stable phase of calcium carbonate occurs at all the rates in the range of this study, whereas vaterite as the least stable phase formed only at the highest rate.

The precipitates harvested at the rates of minimum and ~ 0.17 min^{-1} were perceived as granular particles under naked eyes (Figure 5.3a). They were assessed under both light and electron microscope (Figures 5.4 and 5.5). The micrographs exhibit the appearance of agglomerates of calcite rhombs at both conditions, as it was demonstrated by XRD and FTIR analysis. Although the particles precipitated at both conditions have approximately a similar diameter, they exhibit different forms and surface textures. The particles obtained at the lowest rate are denser agglomerates of calcite crystals with sharp edges on the surface, which formed in spherical assembly (Figure 5.4) while those ones obtained at the higher rate are agglomerates of smooth surface rhombohedral

calcite crystals with rounded edges, which formed in irregular polygonal assembly (Figure 5.5). The denser particles are expected to produce stronger bonds between soil grains.

At the highest rate, the precipitates were beheld to be thread-like under naked eye (Figure 5.3b). The light and electron micrographs show a mixture of spherical, unshaped and rod-shaped particles in the precipitates (Figure 5.6). The spherules can be attributed to vaterite which its existence at the highest rate was earlier confirmed by XRD and FTIR analysis. The hollow detected within each spherule (Figures 5.6d and 5.6h) is probably the place where bacterium was trapped into the growing crystal lattice. Al-Thawadi (2008) and van Paassen (2009) also reported the formation of hollow spherules within the microbially induced calcium carbonate precipitation. Light micrographs display the existence of cracks on the spherules surface (Figure 5.6d and 5.6e). The spherules are the initial production of the cementation process. They can be degenerated and then transformed to calcite and aragonite. The unshaped particles are likely those degenerated spherules which had no time or chance to transform (Figures 5.6b and 5.6c). Stabilization of these unshaped particles may be attributed to the presence of organic matter in the precipitation medium. It was also detected that the spherules were clustered together in collinear arrangement (Figure 5.6b). The formation of the rhombohedral crystals in rod-shaped arrangement is maybe a result of degeneration and consequently transformation of the collinearly arranged spherules to calcite. The non-gibbous faces of the crystals are due to the lack of sufficient time for growth (Figure 5.6j). Degeneration of the spherules attached to the crystal surface caused redundancies on the rod-shaped crystals (Figures 5.6j). The rod-shaped crystalline unites can be linked to each other by

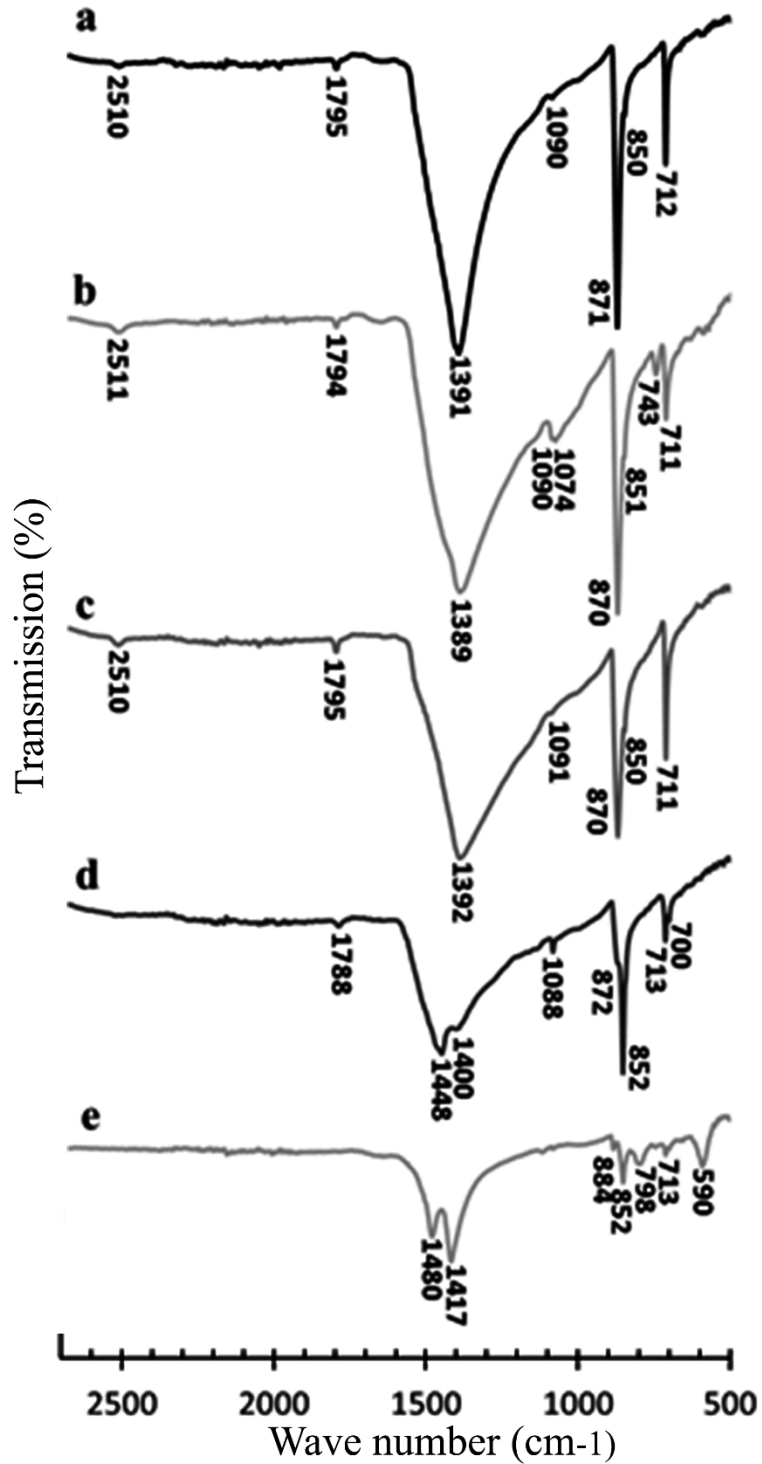


Figure 5.1. FTIR spectra of the precipitates harvested from urea-NB-NH₄Cl solutions at the rates of 0.05 min⁻¹ (a), 0.47 min⁻¹ (b) and 0.17 min⁻¹ (c); and from SW-urea-NB-NH₄Cl solutions with [CaCl₂] = 0.1 M (d) and 0.23 M (e).

the spherules (Figures 5.6e and 5.6k). The linkages can be the potential breakage points of each rod-shaped assembly. There is another type of rod-shaped particles which seems to be the collinearly arranged spherules covered by the degenerated calcium carbonates (Figure 5.6i). Overall, the solids precipitated at the highest rate seem to be not desirable for soil strengthening since they are susceptible to transformation and/or breakage.

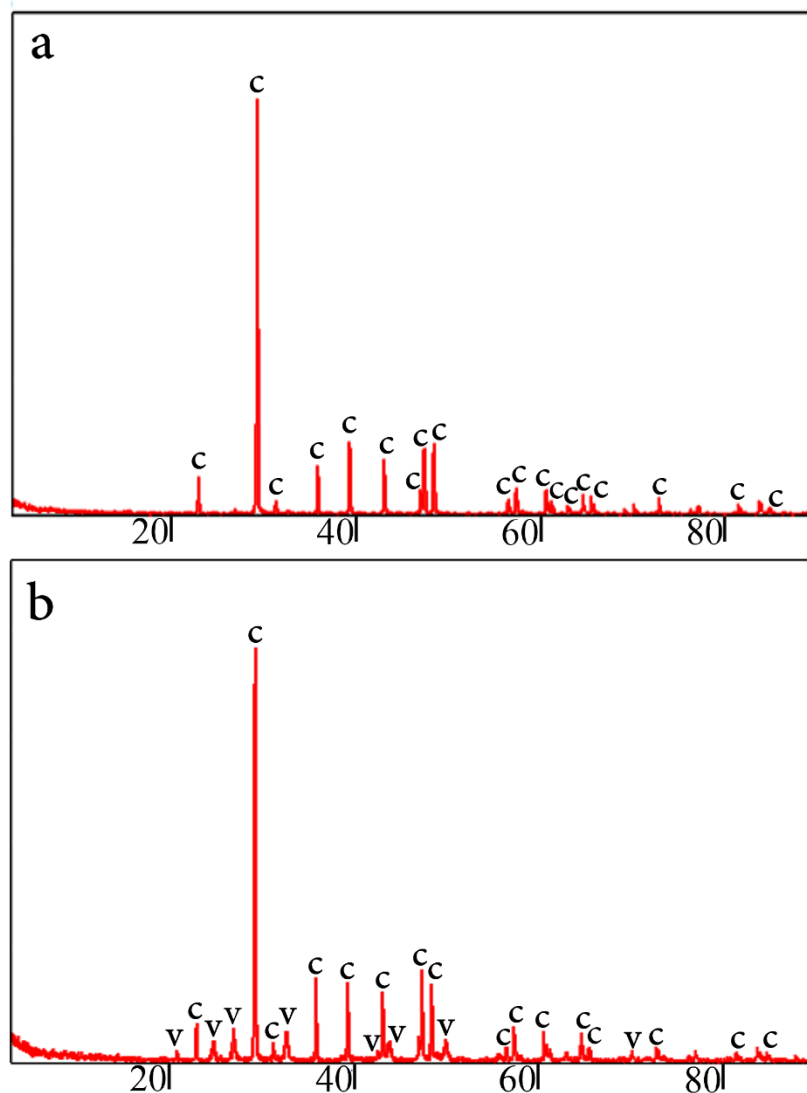


Figure 5.2. XRD spectra of the precipitates harvested from urea-NB-NH₄Cl solutions at the rates of 0.05 min⁻¹ (a), 0.47 min⁻¹ (b) and 0.17 min⁻¹ (c); and from SW-urea-NB-NH₄Cl solutions with [CaCl₂] = 0.1 M (d) and 0.23 M (e); (A: aragonite; C: calcite; M: monohydrocalcite; V: vaterite).

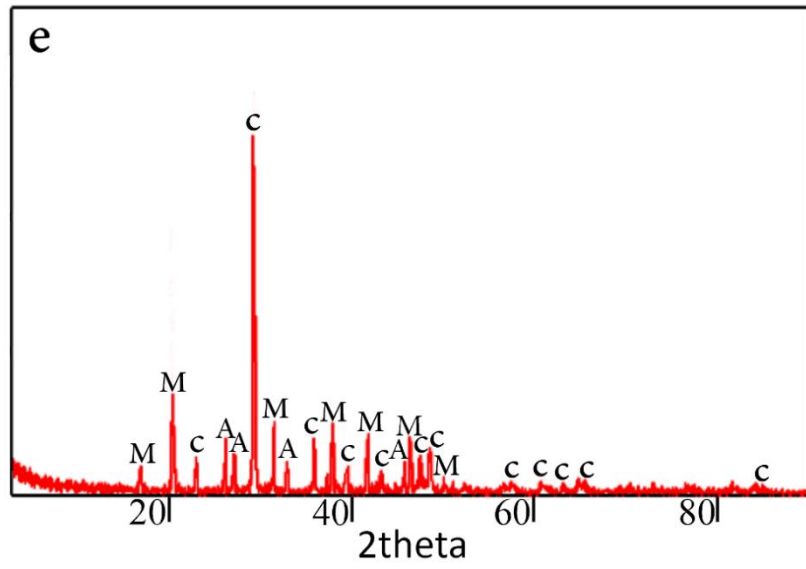
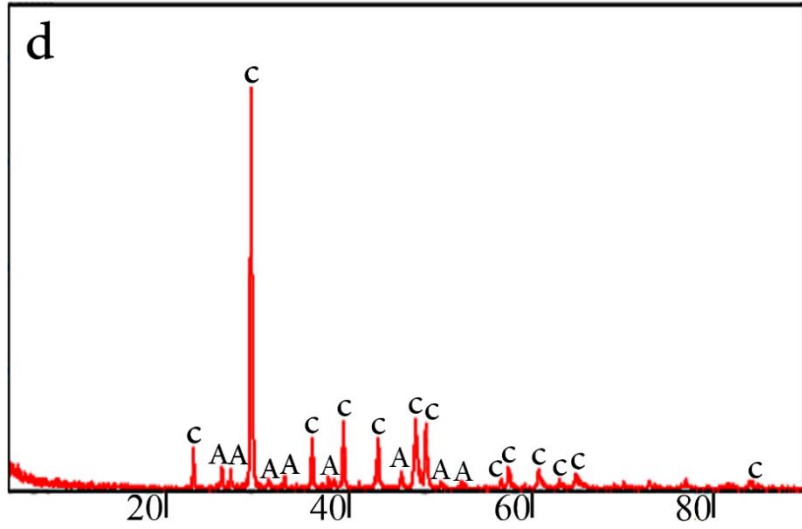
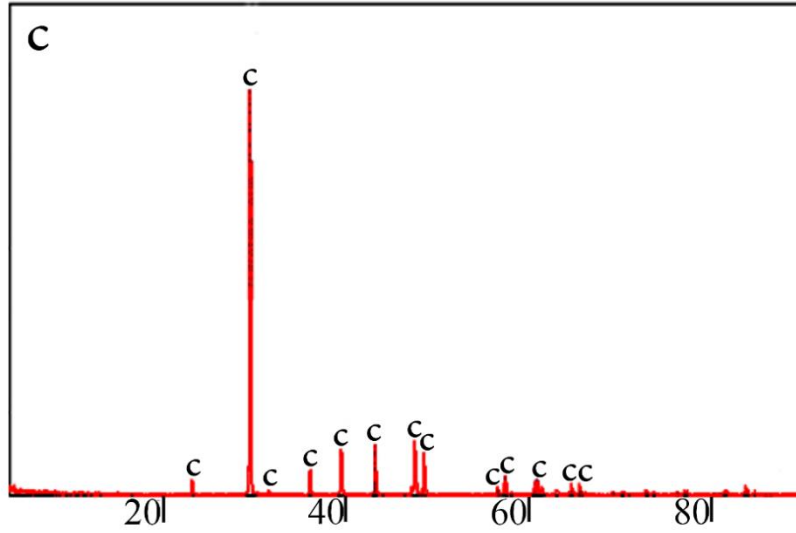


Figure 5.2. (Cont.)

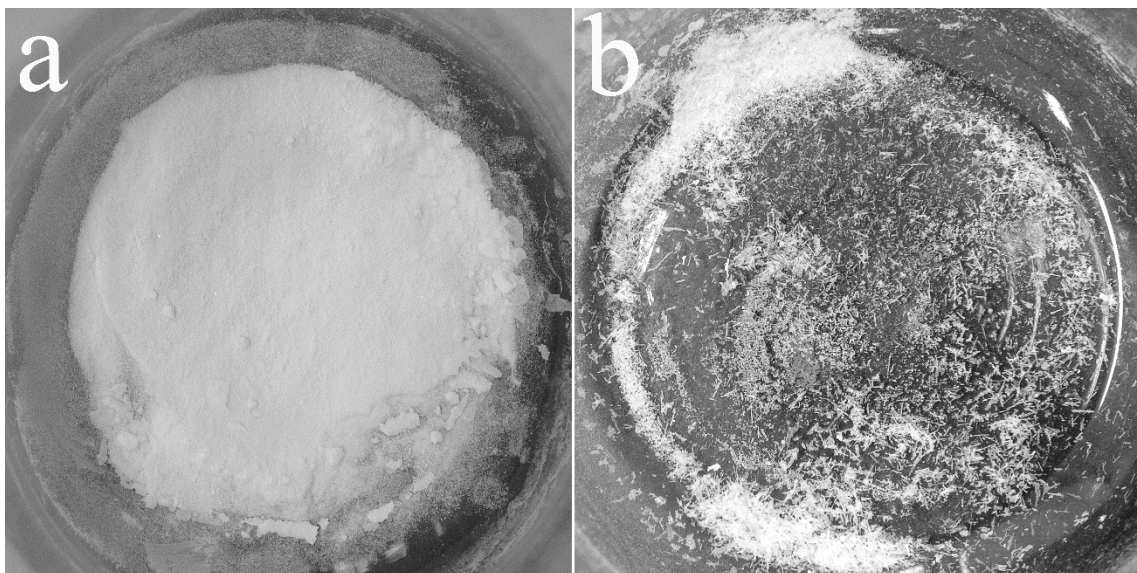


Figure 5.3. Visual appearance of the precipitates under naked eyes: granular particles obtained at the rates of 0.05 and $\sim 0.17 \text{ min}^{-1}$ (a) and thread-like particles acquired at the 0.47 min^{-1} rate (b).

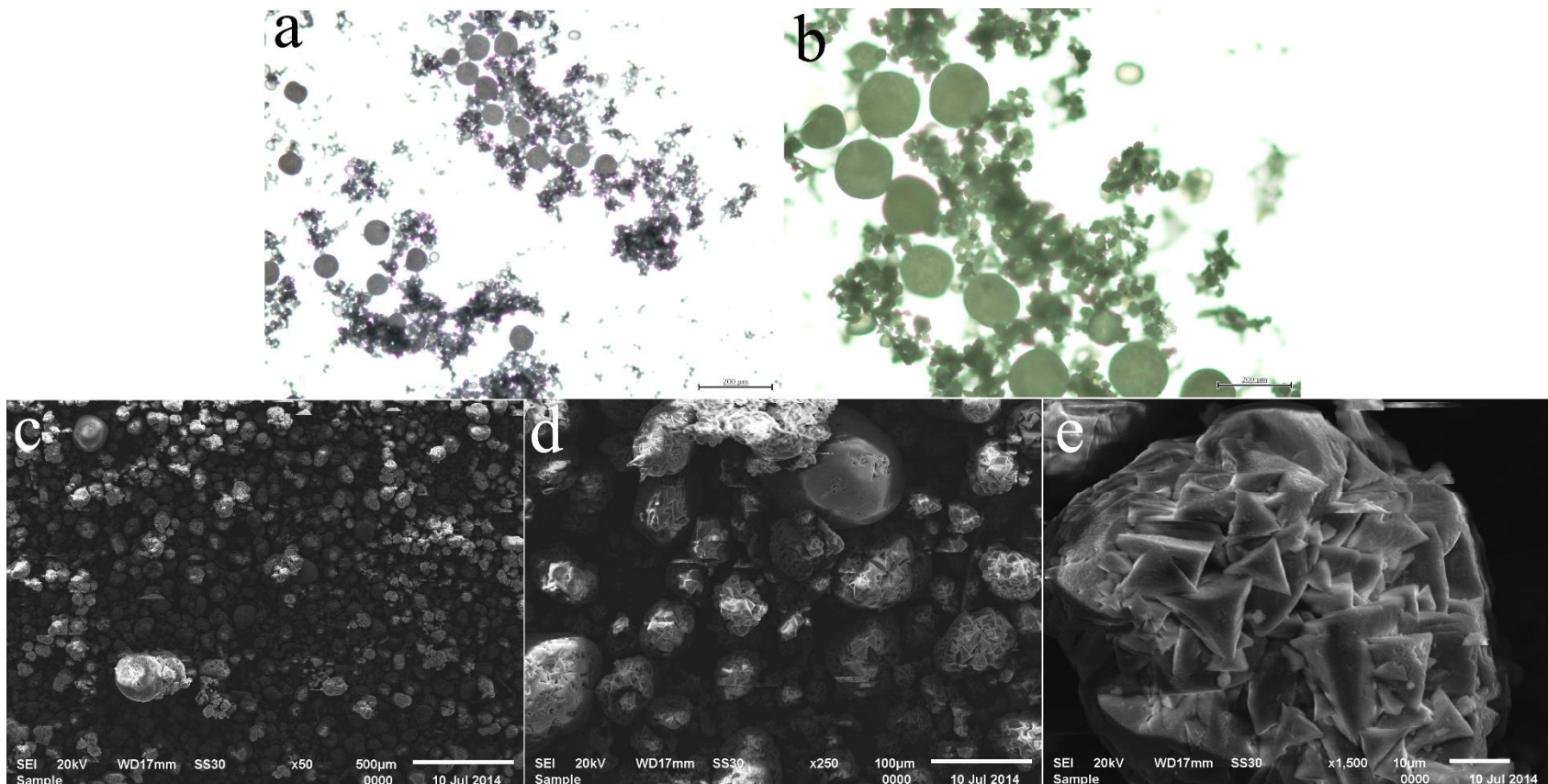


Figure 5.4. Light (a and b) and electron (c-e) micrographs of the precipitates obtained at the precipitation rate of 0.05 min^{-1} .

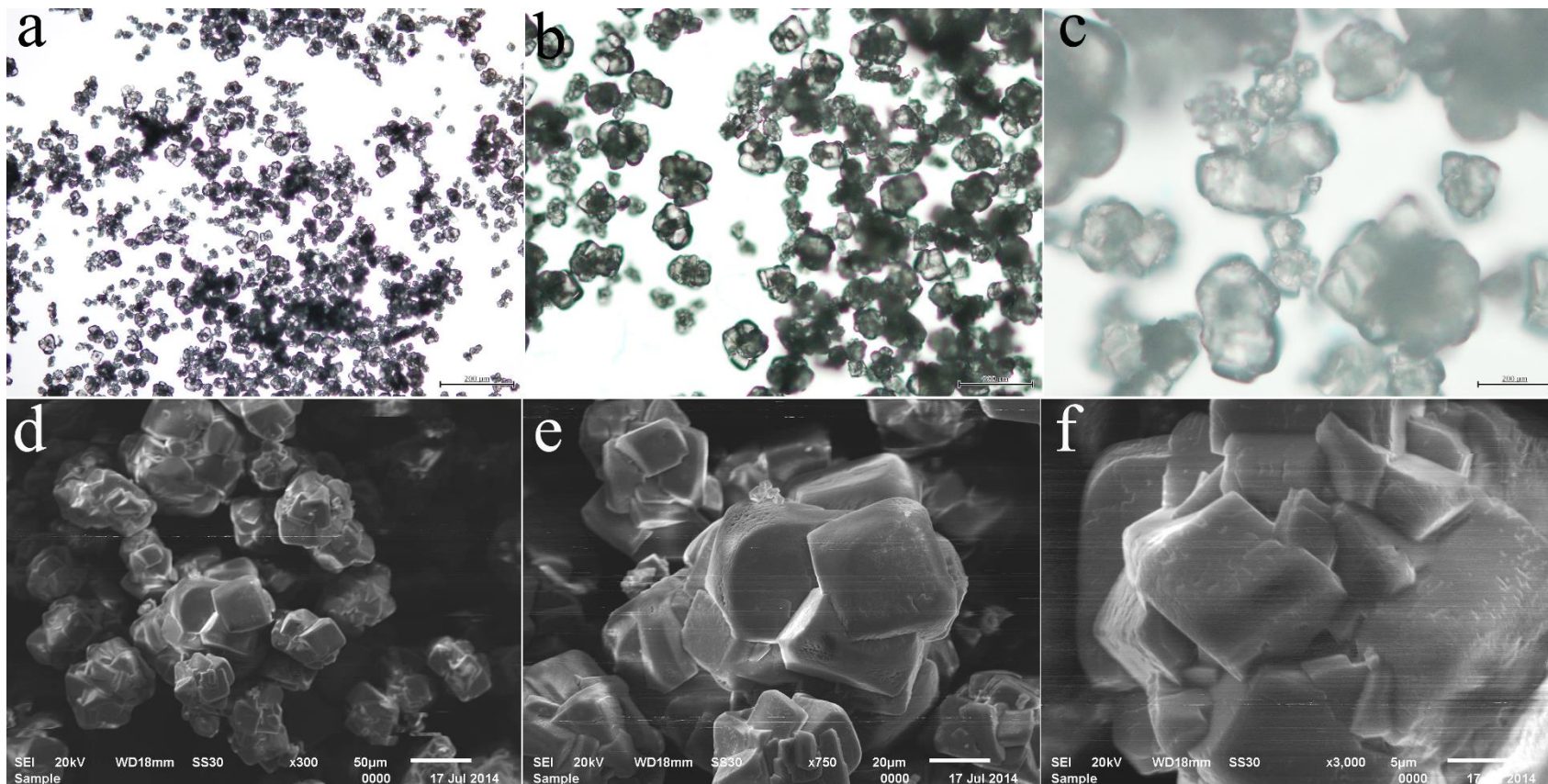


Figure 5.5. Light (a-c) and electron (d-f) micrographs of the precipitates obtained at the precipitation rate of $\sim 0.17 \text{ min}^{-1}$.

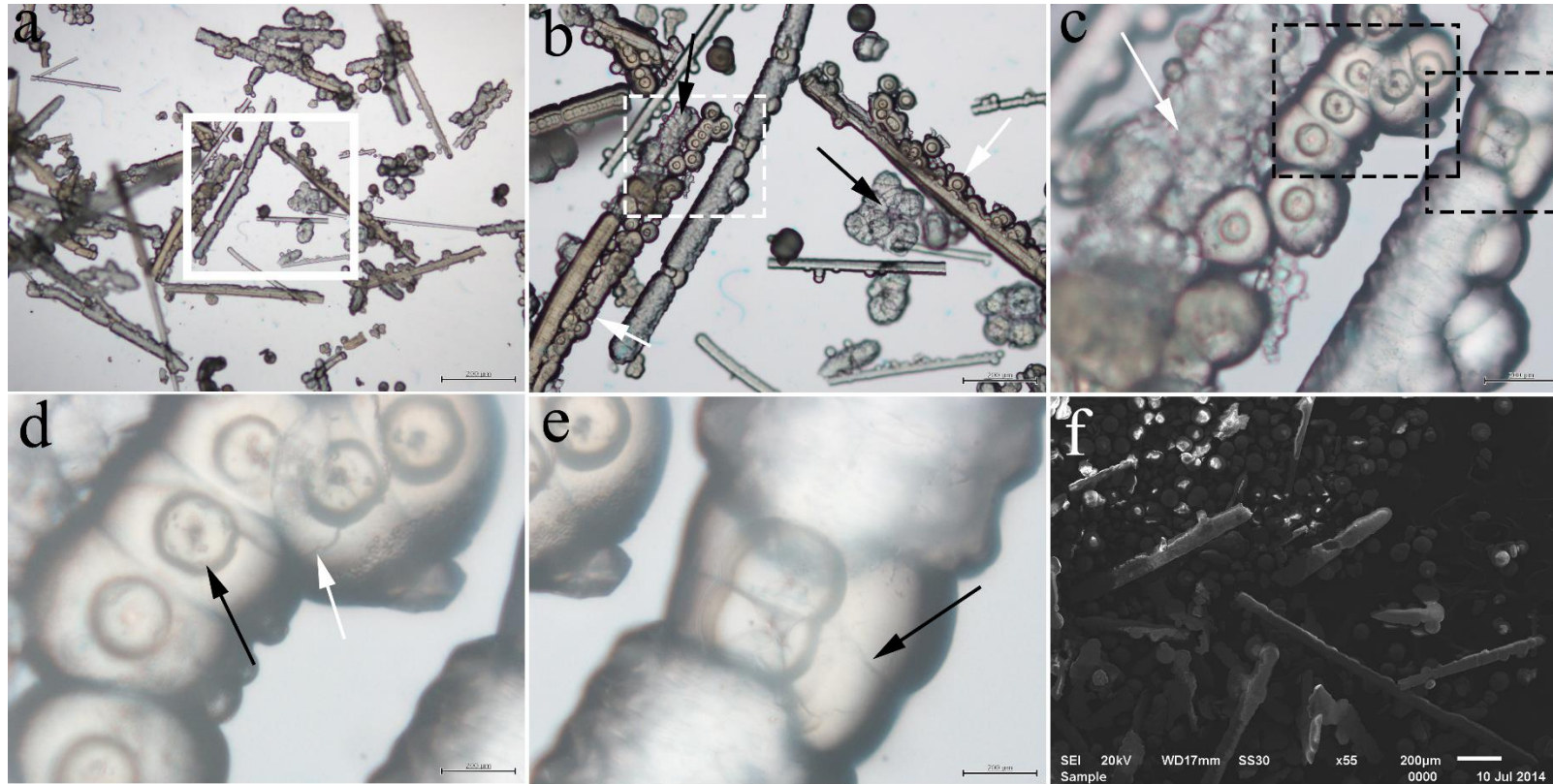


Figure 5.6. Light (a-e) and electron (f-l) micrographs of the precipitates obtained at the precipitation rate of 0.47 min^{-1} . The solid arrows in (b) and (c) point out the degenerated spherules. The dashed arrows in (b) indicate the collinear arrangement of the spherules. The arrows in (d) and (h) signalize the presence of hollow in the spherules. Existence of redundancies, linkage between rod-shaped crystals by the spherules, and trace of degenerated spherule on crystal surface were respectively marked in (j), (k) and (l).

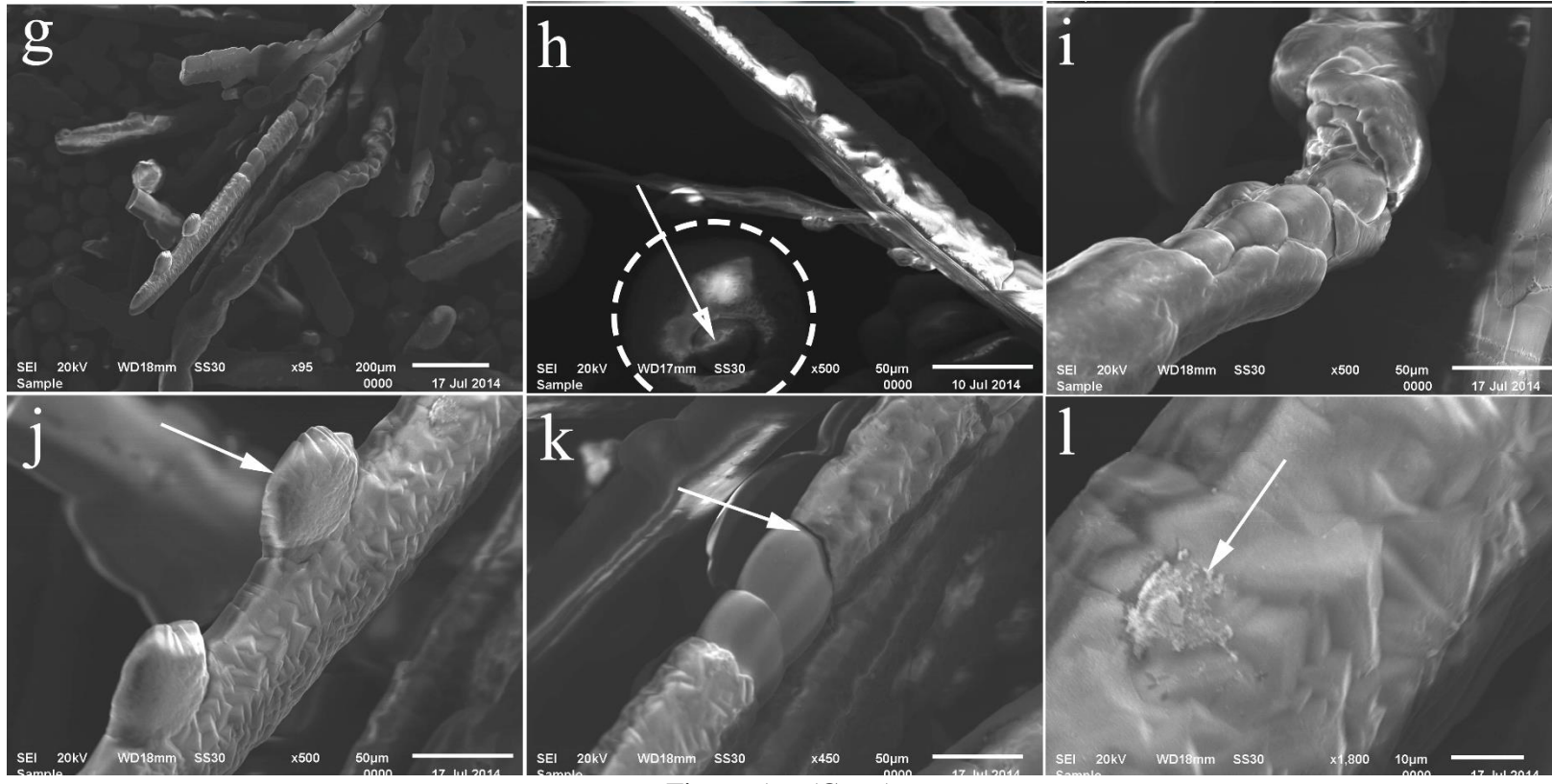


Figure 5.6. (Cont.)

5.3.2 In Urea-NH₄Cl Solution

The tests No. 1 and 4 were performed in the absence of nutrient broth. The precipitation rates were respectively recorded as 0.07 min⁻¹ and 0.49 min⁻¹ for the tests No. 1 and 4 in urea-NH₄Cl solution. The results show no significant change in precipitation rate in comparison with similar conditions in NB-urea-NH₄Cl solutions (as explained in Chapter 4), which indicates that there is no considerable difference between the micro structure of the precipitates harvested from urea-NH₄Cl solution and NB-urea-NH₄Cl solution. This similarity in micro structure can be attributed to the neutral contribution of nutrient broth in precipitation rate at these conditions.

5.3.3 In SW-Urea-NB-NH₄Cl Solution

XRD and FTIR spectra of the precipitates acquired in the existence of seawater were shown in Figures 5.1d, 5.1e, 5.2d and 5.2e. IR spectrum of the solids from the solution containing 0.1 M CaCl₂ represent presence of calcite and aragonite together as it includes all their characteristics peaks (Figure 5.1d). Absence of absorption bands between 720 and 770 cm⁻¹ can suggest insignificant incorporation of magnesium in crystal structure of the precipitates (Huanc et al. 1960) and the lack of formation of vaterite (Wang et al. 2010). Together appearance of a single peak at 1088 cm⁻¹ and double peaks at the absorption bands 900-830 and 714-660 cm⁻¹ indicate aragonite formation (Huanc et al. 1960). The major peaks at 713, 872 and 1400 cm⁻¹ corresponds to calcite. A slight shift in characteristic peaks of calcite in comparison with previous conditions may be for placement of tiny amount of magnesium in its crystal structure (Huanc et al. 1960). More prominent characteristic peak of calcite at 713 cm⁻¹ than the characteristic peak of aragonite at 700 cm⁻¹ reveals the higher amount of calcite in the mixture. Comparing the intensities of the other major peaks of aragonite and calcite do

not provide any quantitative estimation since they overlap each other. XRD spectrum of the sample also indicates a mixture of calcite and aragonite with higher amount of calcite (Figure 5.2d). IR spectrum of the sample from the solution containing 0.23 M CaCl_2 (Figure 5.1e) does not decidedly represent the existing phases. Actually, some peaks appeared in the IR spectrum of this sample does not very closely match with the available IR spectra of the expected occurring compounds (e.g. Mg-contained, hydrated and amorphous calcium carbonates) in the literature. This difference can be ascribed to the different precipitation medium. No study investigating microbial calcium carbonate precipitation in seawater with this much concentration of Ca^{2+} was found in the literature. XRD spectrum of the sample is more determining here. It clearly exhibits the presence of calcite, aragonite and monohydrocalcite in the sample (Figure 5.2e). So, considering the IR characteristic peaks of calcite and aragonite, the absorption bands at 590, 743, 798 and 884 cm^{-1} for this sample can be only attributed to monohydrocalcite. The other absorption bands of monohydrocalcite have overlap with the absorption bands of calcite and aragonite. Neumann and Epple (2007) reported the absorption bands of 590, 700, 727, 766, 873, 1068, 1408 and 1487 cm^{-1} for pure monohydrocalcite. Generally, the observations suggests that presence of seawater in the soil pores can lead to formation of less stable phases of calcium carbonate at higher concentration of calcium ions.

Images of light microscopy of the precipitates harvested from seawater represent agglomerates of solid spherules (Figures 5.7a and 5.7b). Figures 5.7 and 5.8 show the arrangement, micro-structure and texture of the spherules under SEM. It was exhibited that the spherules obtained from the solution containing 0.1 M CaCl_2 are made of calcite

and interwoven needle-shaped aragonite crystals in spherical assembly (Figures 5.7d-5.7g). Those acquired at 0.23 M CaCl_2 seems to be aggregates of calcite rhombs covered by cauliflower-like surface texture in spherical assembly (Figure 5.8). Each particle is an agglomerate of the spherules which are attached to each other. The attachment points can be the potential breakage points at micro level as they have less concentrated texture.

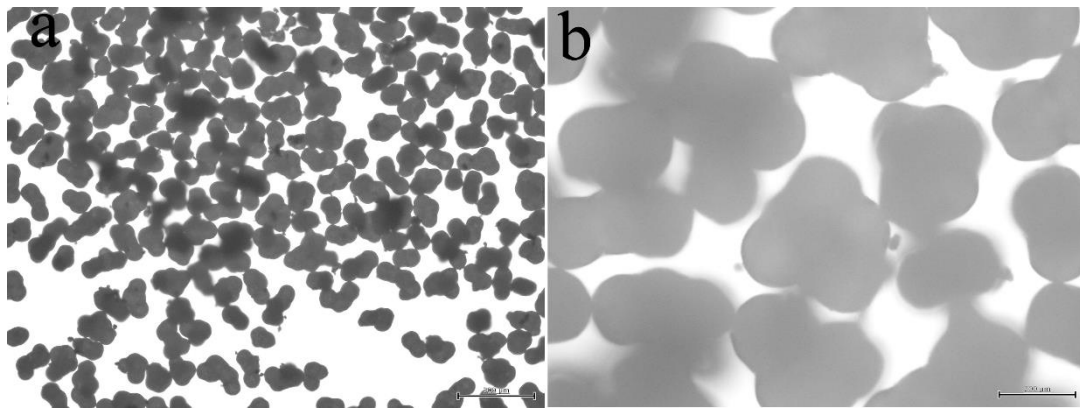


Figure 5.7. Light (a and b) and electron (c-g) micrographs of the precipitates acquired from SW-urea-NB- NH_4Cl solution containing 0.1 M CaCl_2 .

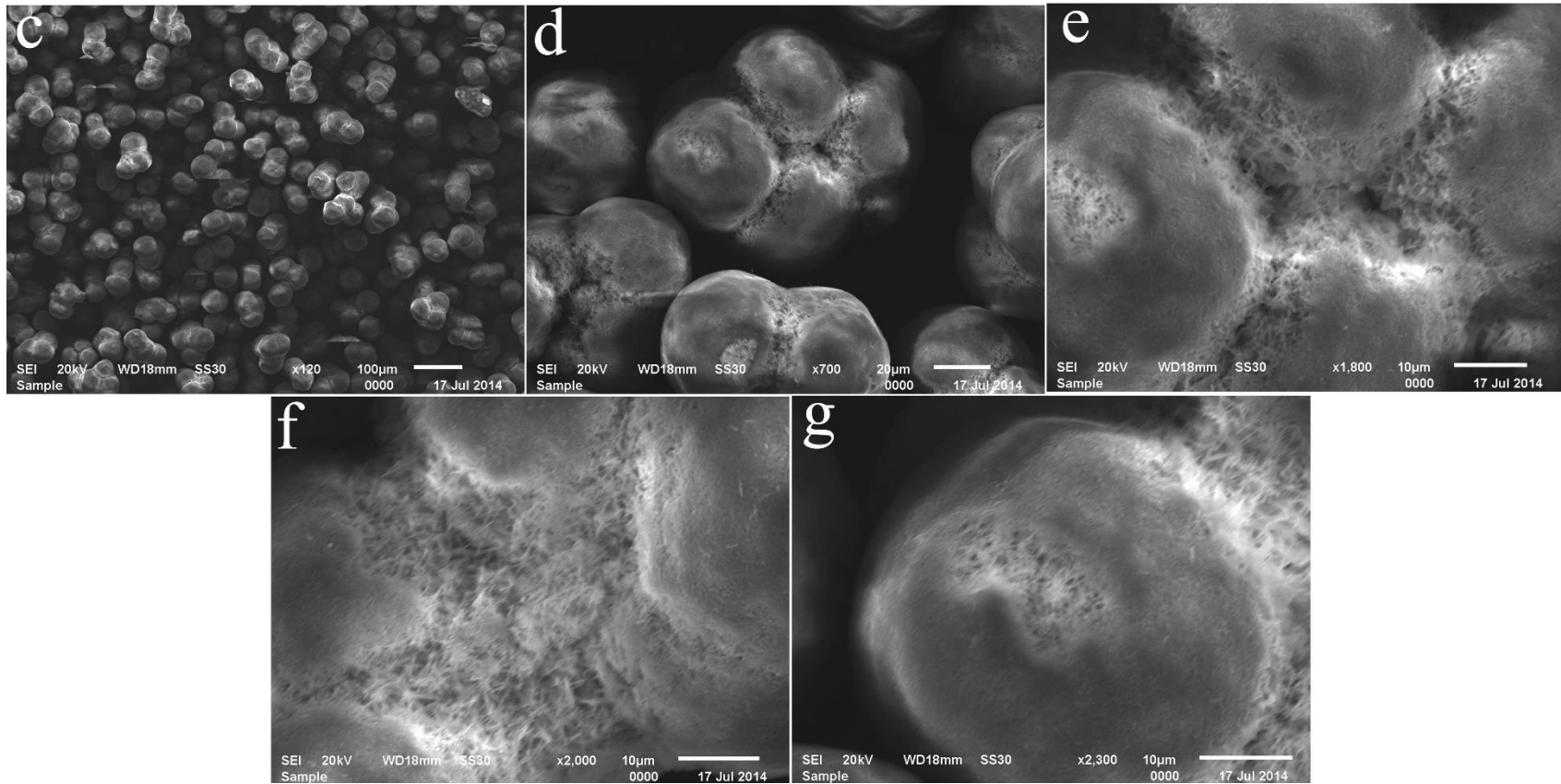


Figure 5.7. (Cont.)

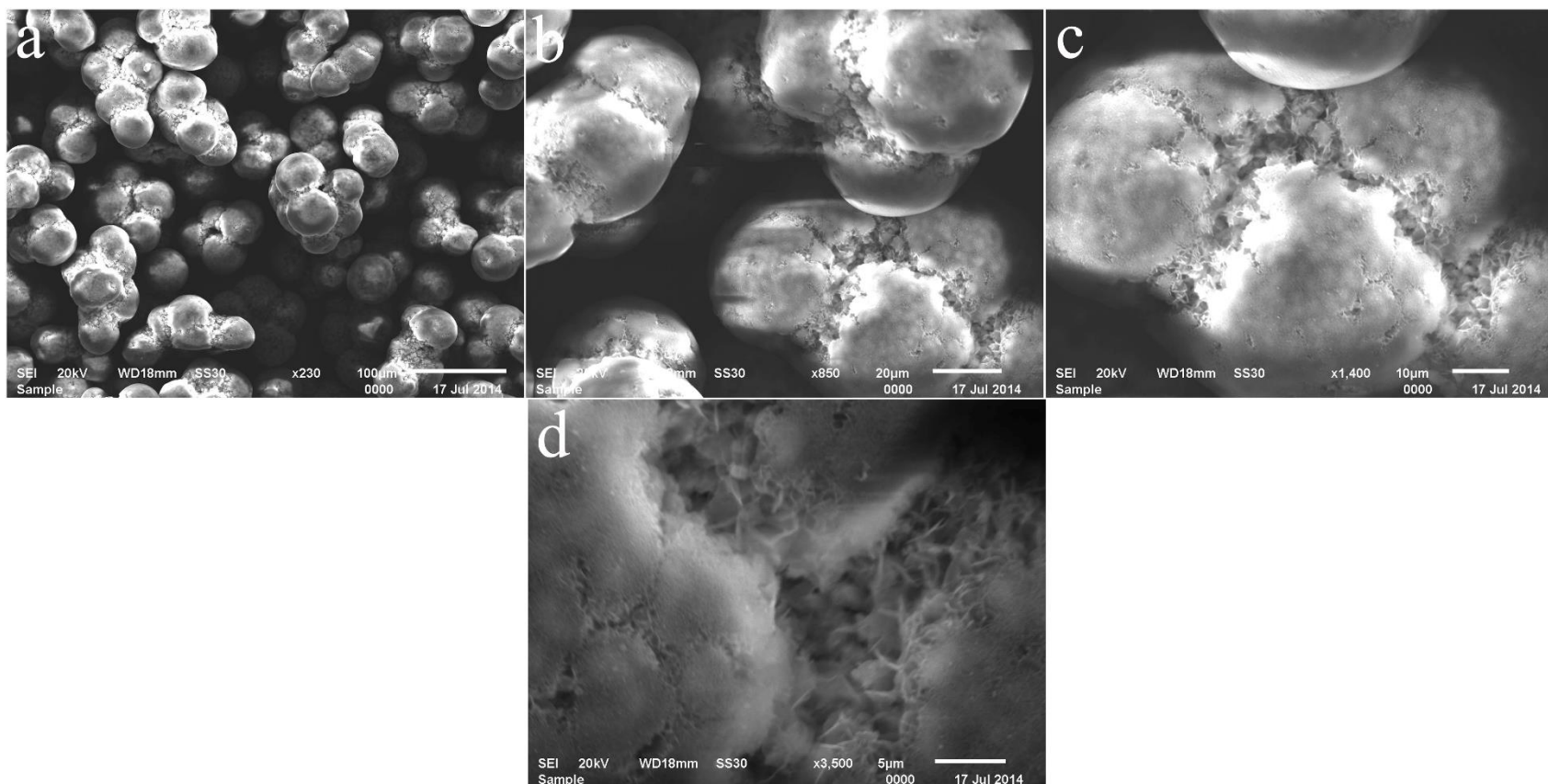


Figure 5.8. Electron micrographs of the precipitates acquired from SW-urea-NB-NH₄Cl solution containing 0.23 M CaCl₂.

5.3.4 Effect of Aging

In order to examine the effect of aging on type and morphology of the precipitated minerals, the samples containing less stable phases (i.e. sample from urea-NB-NH₄Cl solution at the highest rate and the samples from SW-urea-NB-NH₄Cl solutions) were inspected after around one year of keeping in a capped flask at room temperature.

No change in XRD spectrum of the sample obtained from urea-NB-NH₄Cl solution at the highest rate indicates stability of vaterite, which is a non-stable phase of calcium carbonate, at the storage condition (Figure 5.9a). The stabilization may be attributed to high concentration of organic matter by maximum amount of bacterial cells at the test condition. The electron micrographs illustrate different morphology of the particles than before. All the spherical and rod-shaped particles were fractured into smaller pieces after this while (Figure 5.10). It reveals that formation of vaterite and even calcite at the highest rate of precipitation in the soil pores results in time-dependent mechanical properties due to unstable morphology. In other words, the mechanical properties of a treated soil at the highest rate change within time.

The XRD analysis and electron microscopy of the solids harvested from SW-urea-NB-NH₄Cl solution containing 0.1 M CaCl₂ show no significant change in type and morphology of the precipitates after a year (Figures 5.9b and 5.11). Very slow transformation of aragonite as metastable phase can be due to the lack of solution environment within storage period. Of course presence of inhibitor-contained solution prevents this transformation.

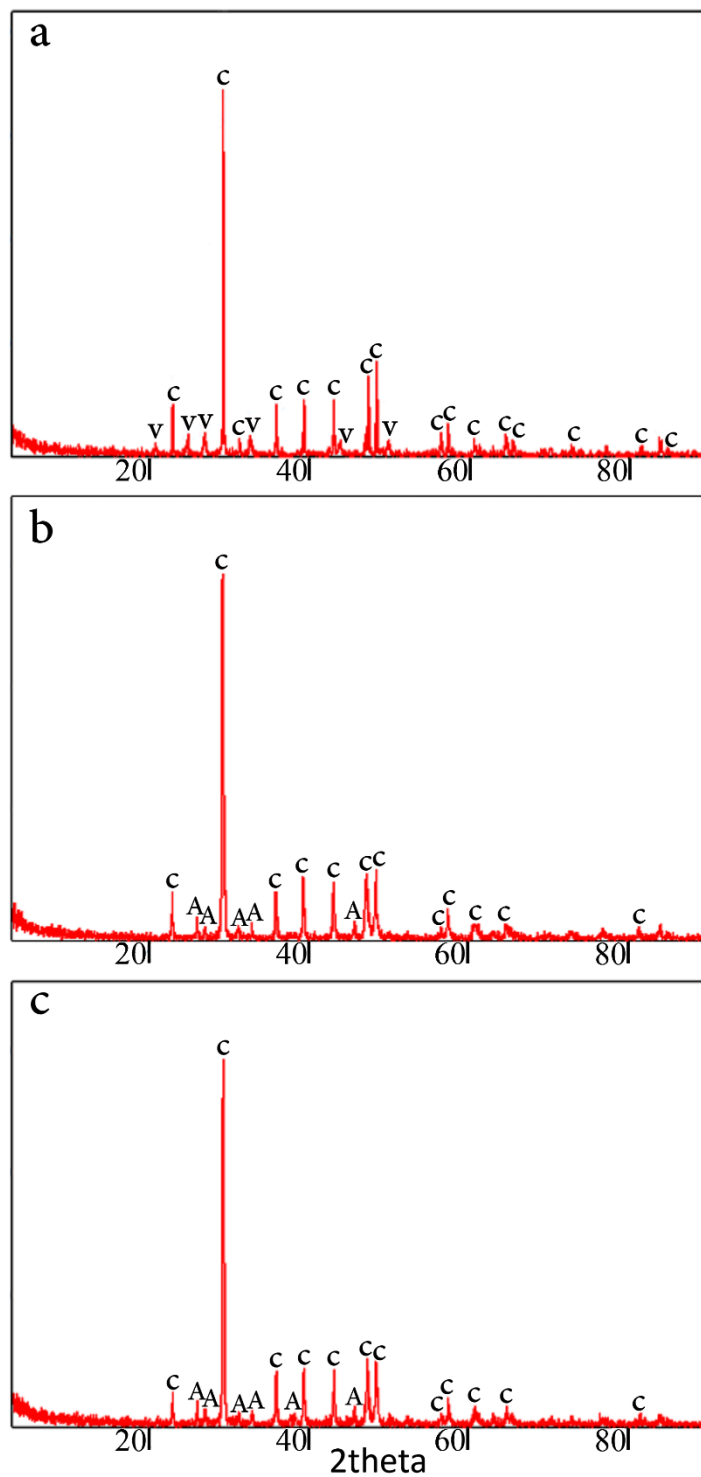


Figure 5.9. XRD spectra of the precipitates harvested from urea-NB-NH₄Cl solutions at the rate of 0.47 min⁻¹ (a) and from SW-urea-NB-NH₄Cl solutions with [CaCl₂] = 0.1 M (b) and 0.23 M (c) after one year; (A: aragonite; C: calcite; V: vaterite).

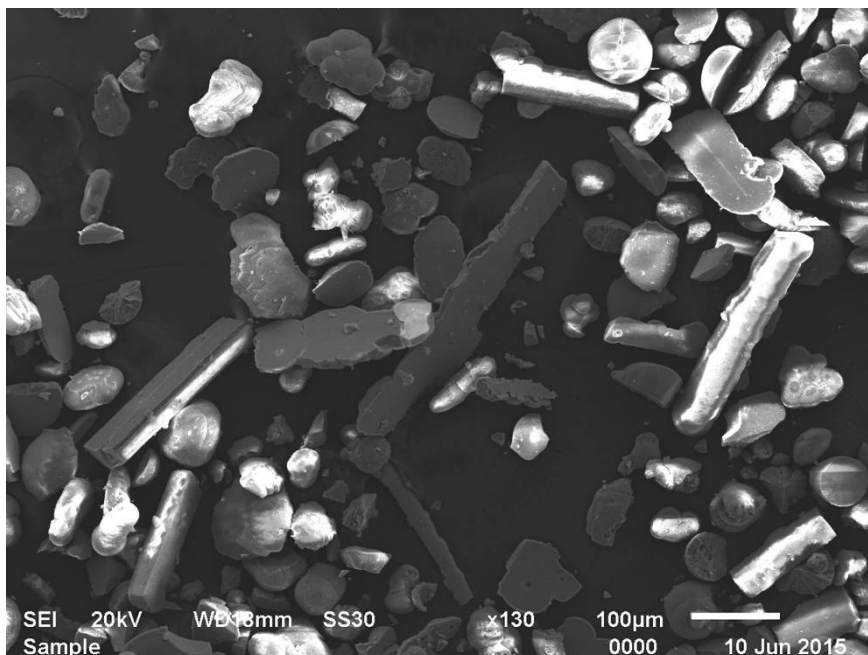


Figure 5.10. Electron micrograph of the precipitates obtained at the precipitation rate of 0.47 min^{-1} after one year on keeping at room condition.

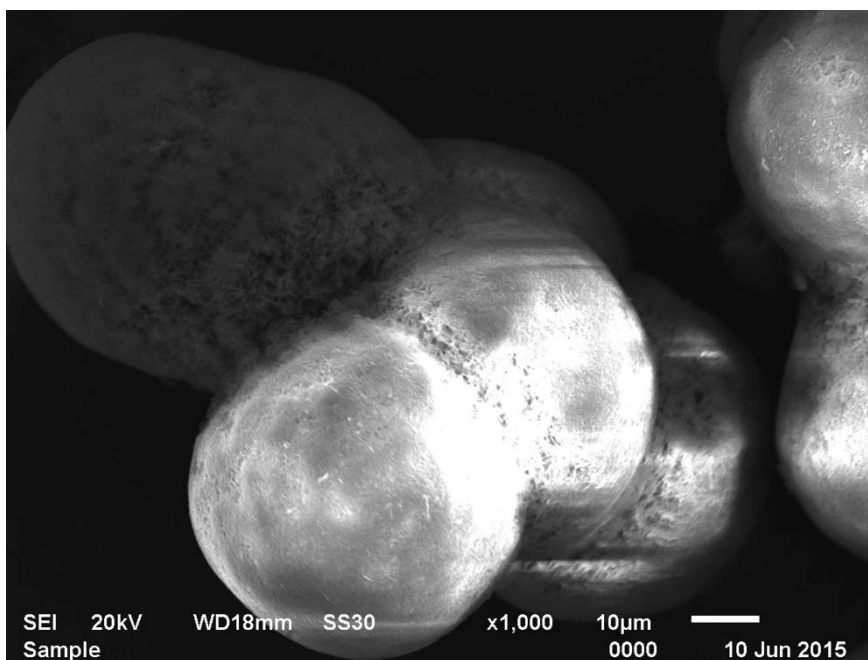


Figure 5.11. Electron micrographs of the precipitates acquired from SW-urea-NB-NH₄Cl solution containing 0.1 M CaCl₂ after one year.

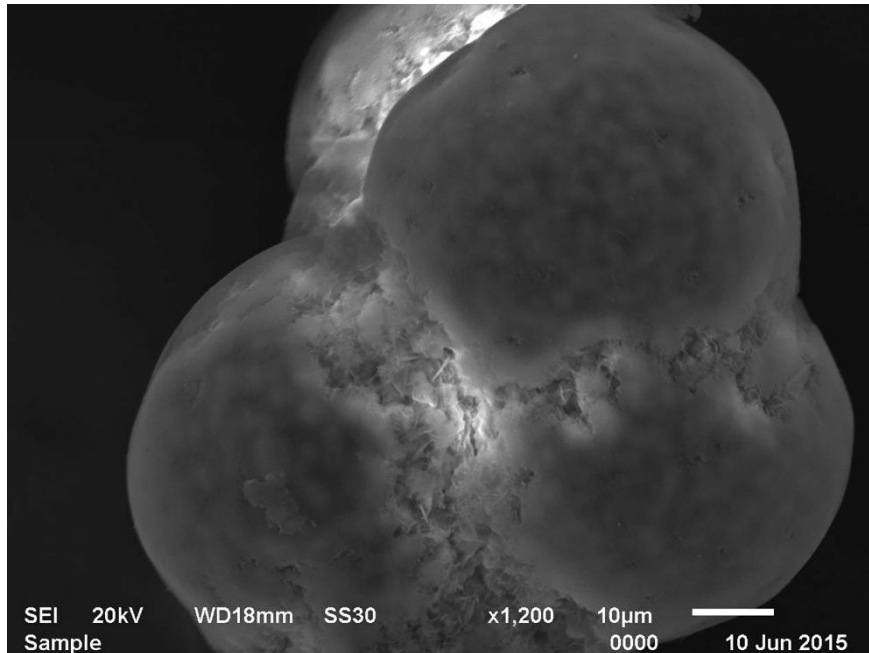


Figure 5.12. Electron micrographs of the precipitates acquired from SW-urea-NB-NH₄Cl solution containing 0.23 M CaCl₂ after one year.

The XRD spectrum of the sample acquired from SW-urea-NB-NH₄Cl solution containing 0.23 M CaCl₂ (Figure 5.9c) exhibits vanishing monohydrocalcite phase after about one year although results of SEM interestingly show no considerable change in appearance of the particles (Figure 5.12). Transformation of monohydrocalcite to aragonite and calcite was expected as it is an unstable phase of calcium carbonate. This transformation within time suggests probable variation in mechanical properties of the soil treated in presence of seawater at high concentration of calcium ions.

The results of this study on the solids precipitated in urea-NB-NH₄Cl solution at the highest rate and in SW-urea-NB-NH₄Cl solution containing 0.23 M CaCl₂ reveal that both XRD and SEM analysis are required for monitoring the effect of aging. Using just one of these analytical methods may lead to an improper interpretation.

5.4 Conclusion

This chapter reported some potential types and morphologies of calcium carbonate precipitates within MICP treatment solution for soil improvement. Type and morphology of the precipitated minerals and aging are three important parameters which influence the mechanical properties of MICP-treated soil:

- Precipitation of calcite as the most stable phase of calcium carbonate is more desirable for geotechnical applications. Precipitation of non-stable phases causes change in mechanical properties as they tend to transform to more stable phases. It also influences durability of the treatment since they are more sensitive to dissolution in water and acidic environment. Although non-stable phases can get sometimes stabilized in a given condition, they may transform again by changing the biochemical conditions of soil environment. Stabilization of vaterite and aragonite was observed in this study at the presence of organic matter and Mg content of seawater.
- Particles precipitated within MICP process were observed to be hollow or solid, densely or loosely agglomerated, rod-shaped, spherical or irregular. It is obvious that each kind of these morphologies produces different mechanical properties. For instance, solid and densely agglomerated particles are expected to create stronger bonds between grains or increase the shear wave velocity at a higher extent; loosely agglomerated particles are more susceptible to breakage at micro level; hollow particles can retain water inside of themselves.
- Aging may cause change in type and/or morphology of the minerals precipitated in the pores. Vaterite was fractured into small pieces at room temperature after

around one year. Monohydrocalcite was also transformed into aragonite at room temperature within a year.

The ultimate mechanical properties of a MICP-treated soil is achieved when there will be no longer change in type and morphology of the precipitates within the pores. Type and morphology of the precipitated minerals can be modified to desirable ones through some curing considerations within treatment process, right after treatment, or later at the time of need.

Chapter 6

MICP-TREATMENT OF SAND THROUGH INJECTION AND SOAKING METHODS AT THE LOWEST AND HIGHEST RATE OF PRECIPITATION

6.1 Introduction

Preparing a representative soil sample at element laboratory scale is essential for studying the in situ mechanical behavior of the soil. Two kinds of methods have been employed in the literature for MICP-treatment of soil samples: injection and soaking. In injection method, the bacterial solution and treatment solution are introduced into the soil through either an injection line by a small non-disturbing pressure or pouring the solution on the soil surface and letting it to penetrate by gravity, also known as percolation in the literature. Lateral surfaces of the soil body are confined by rigid boundaries (e.g. tube and tank) in the injection method. Near inlet clogging due to non-uniform distribution of bacterial solution and treatment solution within soil body were always the main concern in this method. Many efforts have been made to eliminate this problem, such as applying different injection rate, changing the chemical concentration, etc. (see Chapter 2). In the same regard, soaking method has been developed to provide a better way of distribution of the solution within the soil pores for obtaining a uniform treatment. In the soaking method, all the soil surfaces are exposed to the treatment solution. For this purpose, the soil is placed into the open boundaries (e.g. mesh and

geotextile) instead of rigid boundaries. It is then soaked into the tank containing treatment solution. The most recent soaking treatment strategy has been reported by Amini et al. (2014). Although this method is faster and easier to use, it is less cost efficient than the injection method as a large volume of treatment solution is consumed at each cycle of treatment. A considerable proportion of calcium ions are precipitated as calcium carbonate in the treatment tank instead of soil pores. In both injection and soaking treatment method in the literature, chemical concentration and required amount of bacterial solution and treatment solution are overestimated to ensure the preparation of highly treated sample. Actually, the amount of precipitation was the main concern of the treatment process in the studies and no attention was paid to controlling the rate and type of precipitates during treatment.

In this chapter, both injection and soaking method were employed for MICP-treated sample preparation. Treatments were carried out through each method at the highest and the lowest rate of precipitation in order to check the efficiency of these two methods for a rate-controlled treatment. The soaking method used in this study is a new developed method with some advantages to the recent one in the literature. It is a thermostated bath which provides bigger precipitation ratio. The samples treated here were examined using SEM. S-wave measurement and unconfined compression tests were performed on the samples treated at different levels in order to see the relation between the amount of precipitation, shear wave velocity and unconfined compressive strength.

6.2 Materials and Methods

6.2.1 Soil Properties

Clean ASTM 20-30 Ottawa sand with the following specifications was used in this study (see Table 6.1). Mass of soil for each size of sample was adjusted based on the relative density of around 40%.

Table 6.1. Specifications of ASTM 20-30 Ottawa Sand.

Mineral	Hardness (Mohs)	pH	G_s	e_{max}	e_{min}	C_c	C_u	D_{50} (mm)
Quartz	7	7	2.65	0.742	0.502	1	1.2	0.72

6.2.2 Injection Treatment Method

In this method, a given mass of sand was poured into the rigid plexiglass columns by using dry funnel depositional method. A thin layer of nylon liner was earlier placed into the columns in order to enable bringing out the treated samples at the end of the experiments. Inner diameter of the columns was 5 cm and the height of the soil was adjusted to 10 cm. The columns were shut with plastic caps at top and bottom. Each cap had inlet fittings for injection lines. Sponge pads were placed on top and bottom of the soil columns to facilitate uniform distribution of solution at the surface and prevent washing off the soil grains and precipitates. A total of ten soil columns in two batches of six and four samples were separately treated at the highest and lowest rate of precipitation, six samples at the lowest rate and four samples at the highest rate. Two 7.5 cm × 15 cm samples were also treated for monitoring the shear wave velocity at varied levels of precipitation at the highest and lowest rates. These two samples were earlier

prepared by deposition of dry sand into membrane-lined split-plexiglass columns embedded with bender element (BE)-equipped platens at top and bottom. Figure 6.1 shows the schematic design of the treatment columns. Treatment process was performed through pretreatment, injection of bacterial cells, and injection of treatment solution (cementation solution) into the soil at a low constant flow rate by using peristaltic pump. Bacterial cells were injected as a suspension in normal saline. It was prepared through centrifugation of the required amount of bacterial solution and then suspending the pellets into normal saline. This process of separating bacterial cells from biological waste increases bacterial activity (Chu et al. 2014). Bacterial solution and treatment solution were prepared according to Section 3.2.1 and 3.2.2 respectively.

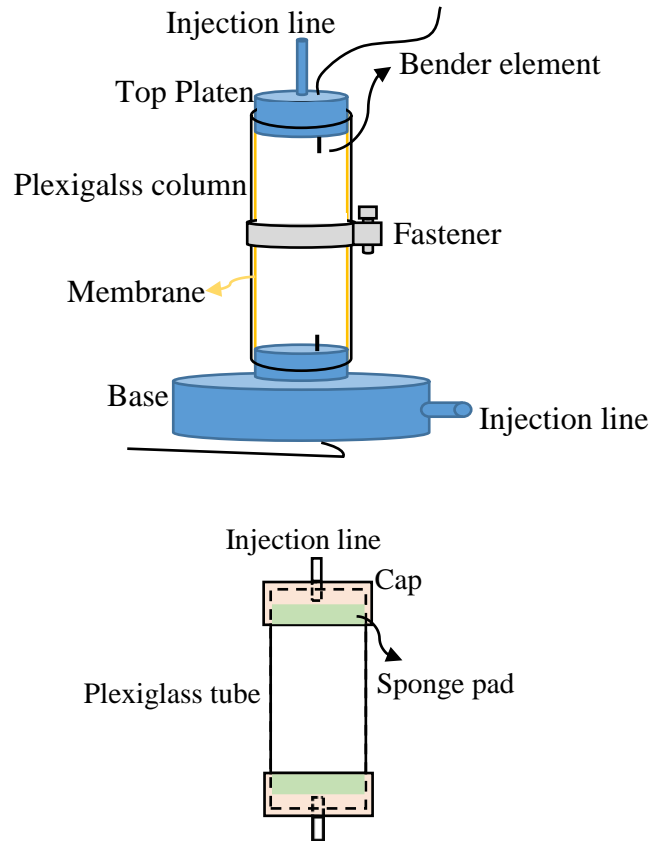


Figure 6.1. The columns used for injection treatment: (top) BE-equipped column, and (bottom) simple treatment column.

The treatment steps used in this section are as below:

- 1- Pretreatment: one pore volume (~80 ml for 5 cm × 10 cm samples and ~260 ml for 7.5 cm × 15 cm samples) pretreatment (fixation) solution was first injected from the top line into soil at the rate of 1.5 ml/min for the small samples and 5 ml/min for the big samples. These rates were applied for all subsequent injections. This solution was composed of the same ingredients as treatment solution with 0.1 M urea, 0.05 M CaCl₂ and bacterial cell concentration of 10⁶ cell/ml. This step was performed at room temperature for all the tests. Precipitation caused by pretreatment facilitates cell attachment to the grains (Whiffin et al. 2007; Harkes et al. 2010). In other words, it prevents washing off

the cells during injection of bacterial solution, which results in better control on concentration of the cells in the treatment matrix. No considerable change in shear wave velocity represents a negligible amount of precipitation after pretreatment.

- 2- After 6 hours of pretreatment, the sample was rinsed with one pore volume of distilled water. The water was allowed to be completely drained off by gravity.
- 3- Bacterial cells suspended in normal saline solution were injected from the top line. The volume of the solution was equal to the volume of the voids, with the cell concentration of 10^8 cell/ml. The solution was let to drain off by gravity after 2 hours. The clear solution from the outlet represents the attachment of the injected bacterial cells to the soil grains.
- 4- One pore volume of the main treatment solution was injected from the bottom line at each cycle of treatment at this step.

For the highest rate of precipitation, treatment solution contained 0.1 M urea and 0.07 M CaCl_2 . All the tests were performed in a temperature controlled chamber at 50°C . Four samples were treated with one, two and three cycles at this condition. The cycles were applied within three days at around 24-hour intervals, i.e. a fresh treatment solution was injected after every 24 hours. The control sample was also separately treated with three treatment cycles at this condition. Shear wave velocity was measured at the time corresponding to treatment period of each sample, i.e. after about 3 hours, 1 day, 2 days and 3 days.

For the lowest rate of precipitation, treatment solution containing 1 M urea and 0.67 M CaCl₂ was injected into each sample. The tests were carried out at room temperature (i.e. ~20°C). Six samples were treated with three cycles of treatment. The cycles were applied within six days at about 48-hour intervals. The control sample was also separately treated at this condition for a period of six days. Shear wave velocity in this sample was measured after 6 and 12 hours and about 1, 2, 4, 6 days.

- 5- At the end of the treatment, each column was immediately washed by injection of two pore volumes distilled water; the remained pore solution was let to be drained off by gravity. The column was then dismantled and the sample was gently brought out. It was put into oven at 50°C to be completely dried for further tests.

6.2.3 Development of Soaking Treatment Method

A new treatment method has been developed in order to provide an ideal condition of treatment which facilitates desirable distribution of microbes and full exposure to treatment solution. In this method, soil was placed into a mesh column in ten equal layers by using the dry depositional method. The mesh column was sewn by polypropylene (PP) mesh sheet (ELKO Filtering Co.) which its specifications presented in Table 6.2. The soil was then inoculated through uniformly dropping a given volume of bacterial solution (with the cell concentration of 10⁹ cell/ml) on the surface of each layer by using micropipette. Volume of the solution dropped on the surface of each soil layer was adjusted to be around a hundredth of the volume of voids (~750 µl for 5 cm × 10 cm samples and ~2.6 ml for 7.5 cm × 15 cm samples) so that a final bacterial concentration of 10⁸ cell/ml was achieved at the fully saturated condition. Surface of

each soil layer was scratched before placing the subsequent layer in order to create sufficient friction between layers. Figure 6.2 illustrates the mesh columns. As shown, two sizes of cylindrical samples (5 cm × 10 cm and 7.5 cm × 15 cm) were used in this study. Two BE-equipped platens were put on top and bottom of the bigger samples in order to measure the shear wave velocity at various levels of treatment.

Table 6.2. Specifications of polypropylene mesh.

Excellent resistance to acids, alcohols, bases and mineral oils.
Good hydrolysis resistance.
Very tough and flexible.
Working temperature is typically around 90°C.
Does not absorb any water.
Mesh Opening: 250 micron
Open Area: 29 %
Thickness: 430 micron

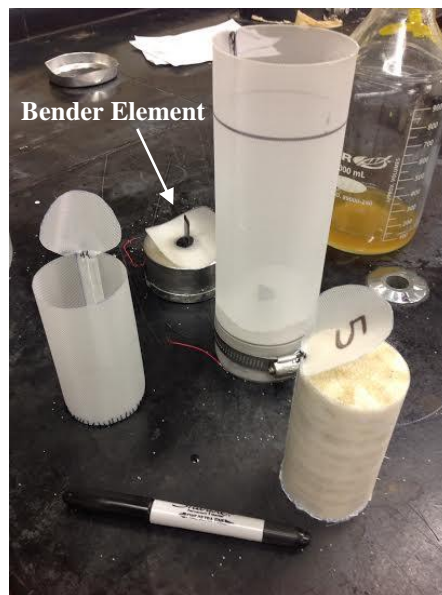


Figure 6.2. Mesh columns used for soaking treatment.

After preparation of the inoculated samples, they were embedded into a 5-liter temperature controlled treatment bath. Figure 6.3 depicts the layout of the treatment bath. The bath was then filled with treatment solution up to a few centimeters above the samples (i.e. ~3.5 liters solution). Temperature adjustment of the treatment solution in the bath provides better control on precipitation rate. Significant effect of temperature on precipitation rate was previously explained in Chapter 3 and 4. A gentle stirring of the treatment solution was applied to create a non-disturbing slow flow within samples.

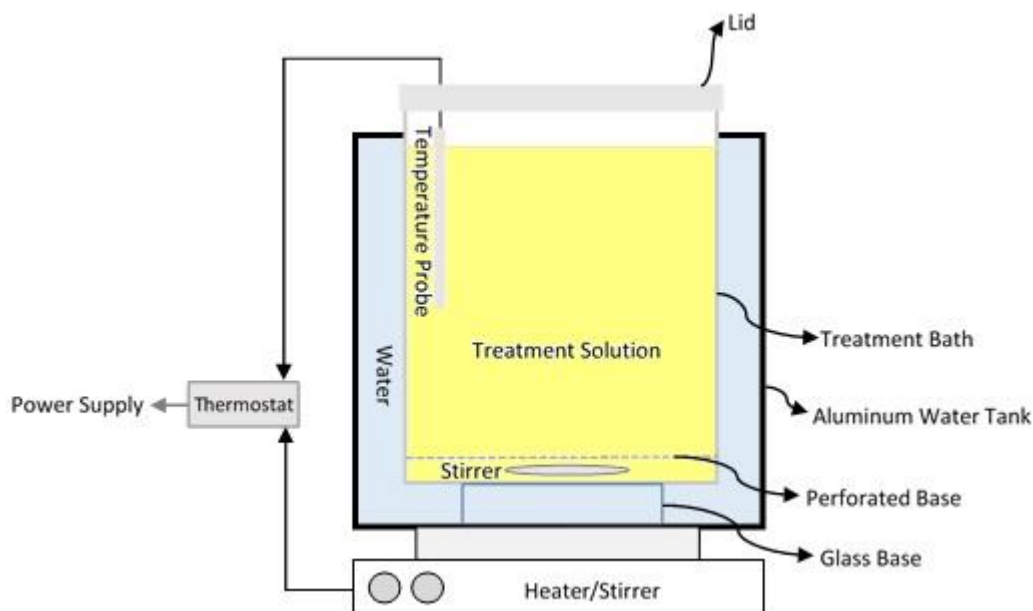


Figure 6.3. Schematic view of temperature-controlled treatment bath.

In order to see the effect of precipitation rate and amount of precipitation, two batches of 6 small samples and 1 big BE-equipped sample were treated at the lowest and highest rate of precipitation separately. The small samples were then successively brought out after given time intervals of treatment. In order to remove impurities and biological wastes, each treated sample were immediately rinsed through soaking into distilled

water at room temperature overnight. After rinsing, the samples were completely dried in 50°C oven. Concurrent with termination of treatment process for each sample, the big sample was also brought out for measuring the shear wave velocity corresponding to each level of treatment. It was then returned to the bath for measuring the shear wave velocity at further levels of treatment.

In order to achieve the treatment at the highest rate of precipitation, initial cell concentration, concentration of calcium chloride, concentration of urea and temperature were adjusted at 10^8 cell/ml, 0.07 M, 0.1 M and 50°C respectively. Three cycles of treatment were applied at 24-hour intervals in this condition, i.e. the treatment solution in the bath was replaced with a fresh one every 24 hours for three times. The samples were successively brought out of the bath after 3 hours and about 1, 2, 3, 4 and 7 days of the beginning of the treatment process.

For treatment of the samples at the lowest rate of precipitation, initial cell concentration, concentration of calcium chloride, concentration of urea and temperature were adjusted at 10^8 cell/ml, 0.67 M, 1 M and 20°C respectively. A single cycle of treatment was applied at this condition within a period of eight days. The samples were successively brought out after around 15, 40, 69, 95, 138 and 192 hours.

6.2.4 Shear Wave Velocity Measurement and Compressive Strength Test

Bender element-equipped platens were used at the top and bottom of the 7.5 cm × 15 cm samples for measuring the shear wave velocity (Figure 6.4). They were fabricated compatible with aggressive environment (Montoya et al. 2012). Visual picking method was used for determination of shear wave arrival time in this study (Chan 2010).

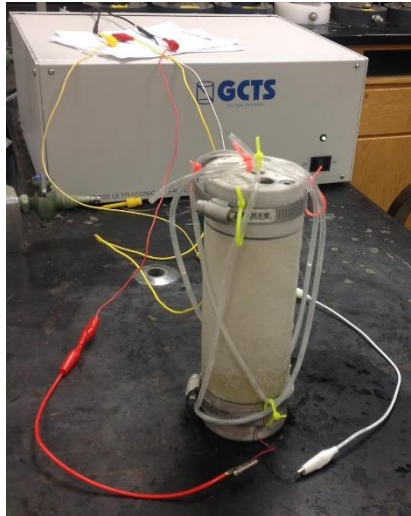


Figure 6.4. Treated sample with BE-equipped platens at top and bottom.

A simple compression test was performed on each treated cylindrical sample to determine its unconfined compressive strength (UCS). In order to apply a uniform axial stress, two end surfaces of the sample were earlier flattened by using a thin layer of Plastic Steel Putty (ITW Devcon, US; see Figure 6.5). The putty becomes rigid after solidification. It is not also dissolved in HCl during acid washing of the samples.

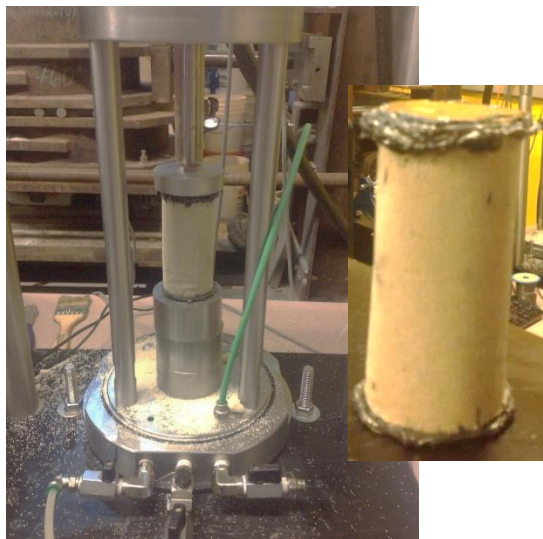


Figure 6.5. Flattening the two end surfaces of the treated sample with putty for unconfined compression test.

6.2.5 Acid Washing of Treated Samples

As CaCO_3 is fully soluble in HCl, treated samples were washed with 4 M HCl. The acid washed samples were rinsed multiple times with distilled water through No. 200 sieve, and then oven dried. The difference between the masses before and after washing was taken as the mass of precipitated calcium carbonate.

6.3 Results and Discussions

6.3.1 Treatment Using Injection Method at the Highest Rate

Table 6.3 represents the results of treatment using injection method at the highest rate of precipitation. As shown, relative density of the samples before treatment (D_r) and initial shear wave velocity were ($(V_s)_0$) were around 40% and 150 m/s respectively. The first sample was treated with one pore volume of treatment solution for around 3 hours ($t_{\text{Treatment}} = 3 \text{ hrs}$). Acid washing of the sample showed that a precipitation mass (m_{CaCO_3}) of 0.35 g out of the stoichiometric maximum of 0.56 g was achieved, as the treatment solution contained 0.07 M calcium chloride. This amount of precipitation corresponds to a precipitation ratio (P_{max}) of about 63% after 3 hours, indicating a high rate of precipitation. This mass of precipitation is only 0.11% of the dry mass of non-treated sand ($M_{\text{CaCO}_3}=0.11\%$). It caused a slight increase in shear wave velocity after treatment ($(V_s)_1$). Unconfined compressive strength (UCS) of the treated soil could not be measured since the amount of precipitation was too small to form a stable soil column for the compression test (Figure 6.6). Treatment of the second sample with the same volume (i.e. one pore volume) of treatment solution but longer treatment period (i.e. around one day) exhibited that 86% of the existing calcium ions in the treatment solution were precipitated as calcium carbonate in the soil pores. However, treatment of the third

and fourth samples with two and three cycles of treatment revealed that the precipitation ratio drastically dropped by increasing the number of treatment cycles. That is why no more cycle of treatment was applied. This reduction in precipitation ratio can be attributed to the harsh condition for bacterial growth at 50°C (see Chapter 4). In other words, the initially injected bacterial cells into the samples could not reproduce more number of cells for contribution in further cycles of treatment. It was also observed that the amount of precipitation in all the samples was not enough for unconfined compression test (Figure 6.6). Change in shear wave velocity (ΔV_s) linearly increased by increasing the precipitation mass percent although it was very small change due to the small amount of precipitation (Figure 6.7). Surprisingly, electron micrographs of the treated soil illustrated rhombohedral calcite precipitation without any other kind of non-stable phase (Figure 6.8), while the precipitation at the highest rate in liquid medium (in the absence of soil) exhibited the formation of non-stable phases (see Chapter 5). It may be attributed to the effect soil on formation of calcium carbonate minerals in exposure of high concentration of organic matters resulted by microbial activity.

Table 6.3. Summary of the treatment of the samples through injection method at the highest rate of precipitation.

sample No.	D_r	$(V_s)_0$	$t_{\text{Treatment}}$	Treatment cycle	$(V_s)_1$	UCS	m_{CaCO_3}	M_{CaCO_3}	ΔV_s	$\Delta V_s/M_{\text{CaCO}_3}$	P_{max}
1	42	151	3	1 (80 ml)	168	NA	0.35	0.11	17	154	63
2	40	149	23	1 (80 ml)	171	NA	0.48	0.15	22	145	86
3	44	154	48	2 (160 ml)	184	NA	0.6	0.19	30	159	21
4	40	148	70	3 (240 ml)	180	NA	0.65	0.21	32	156	9

Table 6.4. Summary of the treatment of the samples through injection method at the lowest rate of precipitation.

sample No.	D_r	$(V_s)_0$	$t_{\text{Treatment}}$	Treatment cycle	$(V_s)_1$	UCS	m_{CaCO_3}	M_{CaCO_3}	ΔV_s	$\Delta V_s/M_{\text{CaCO}_3}$	P_{max}
1	40	148	6	1 (80 ml)	201	NA	0.9	0.28	53	186	17
2	47	156	12	1 (80 ml)	281	NA	2.1	0.66	125	190	39
3	40	150	21	1 (80 ml)	420	139	4.3	1.36	270	198	80
4	40	148	47	1 (80 ml)	453	161	4.8	1.52	305	201	90
5	42	152	94	2 (160 ml)	709	357	9.1	2.87	557	194	85
6	44	153	142	3 (240 ml)	947	584	13.1	4.12	794	193	81

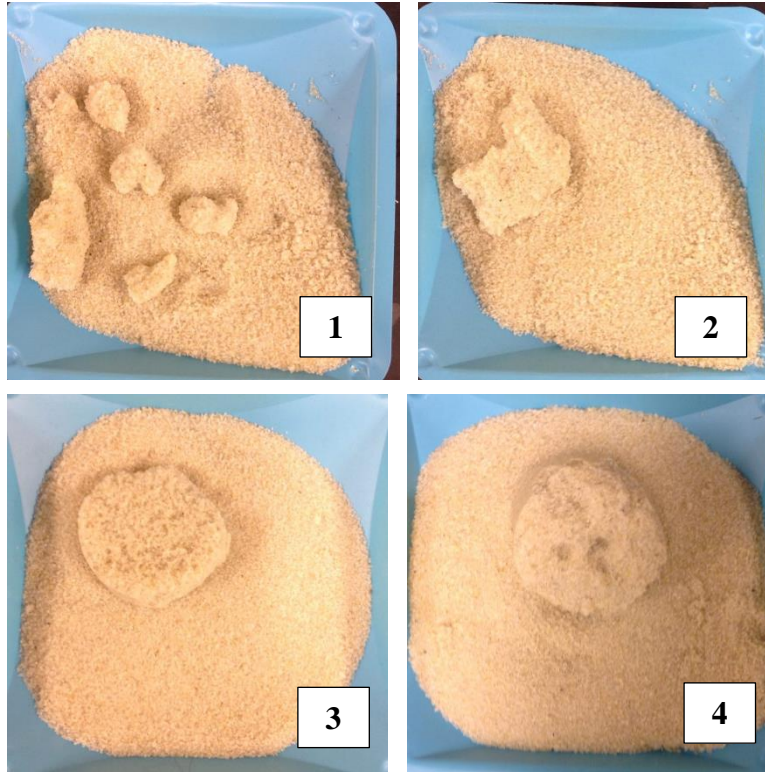


Figure 6.6. Treated samples by using injection method at the highest rate.

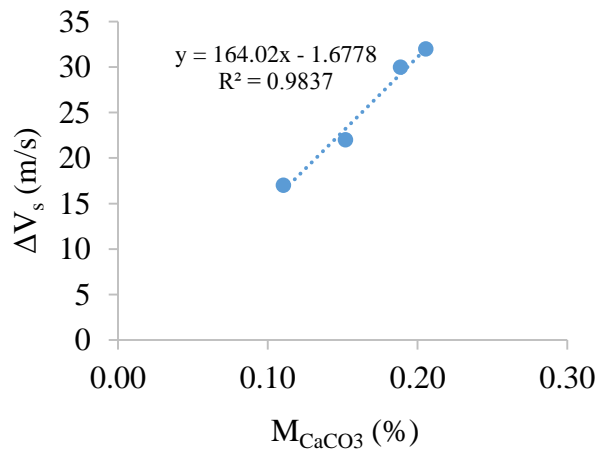


Figure 6.7. Change in shear wave velocity versus precipitation mass percent for the samples treated by injection method at the highest rate.

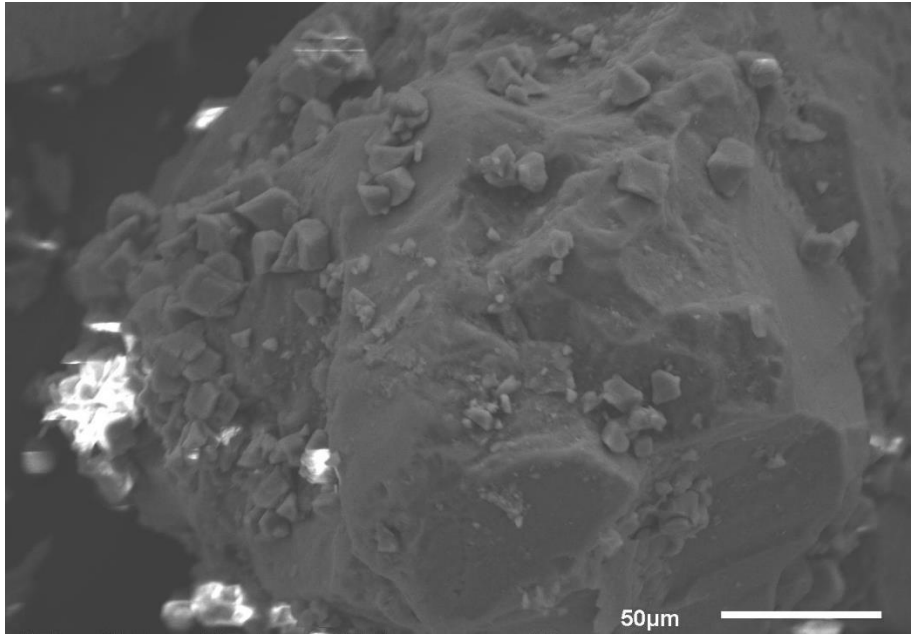


Figure 6.8. Calcite precipitation in the soil treated through injection method at the highest rate of precipitation.

6.3.2 Treatment Using Injection Method at the Lowest Rate

Results of treatment using injection method at the lowest rate were presented in Table 6.4. Four samples were treated with one pore volume of treatment solution for varied treatment periods. Two other samples were treated with two and three cycles for around 2 days per cycle. It was observed that the mass of precipitation increased by time and the number of treatment cycles. There was not considerable reduction in precipitation ratio by increasing the treatment cycles like treatment at the highest rate. Except the samples 1 and 2 with precipitation mass percent below 1%, the amount of precipitation in other samples was enough to form stable soil columns for unconfined compression test (Figure 6.9). A shear wave velocity of 947 m/s and unconfined compressive strength of 0.58 MPa were obtained at precipitation mass percent of 4.1%. Such values are usually observed for soft rocks or very dense soils. The results indicate that there is a linear

correlation between shear wave velocity, unconfined compressive strength and mass of precipitation (Figure 6.10 and 6.11). Using the correlation enables the use of shear wave velocity measurement, as a non-destructive test, for estimation of the amount of calcium carbonate precipitation and the strength of the MICP-treated soil. Al Qabany (2011) has also reported a linear relation between shear wave velocity and the amount of precipitation in MICP-treated soil. Electron micrographs of the precipitates illustrate rhombohedral calcite crystals at the contact points between grains (Figure 6.12).

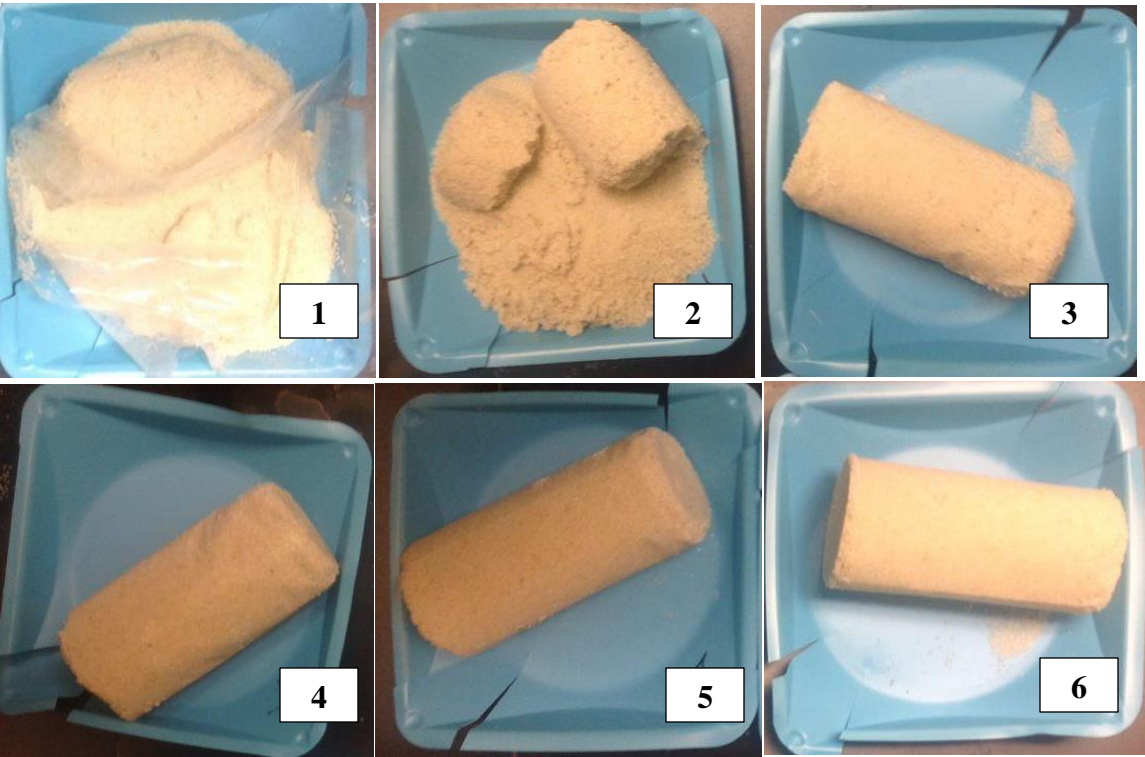


Figure 6.9. Treated samples by using injection method at the lowest rate.

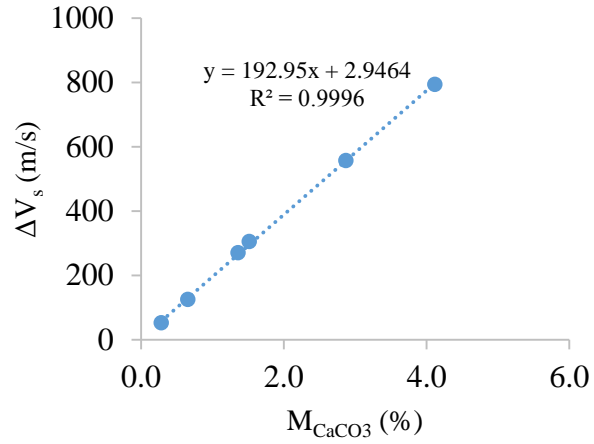


Figure 6.10. Change in shear wave velocity versus precipitation mass percent for the samples treated by injection method at the lowest rate.

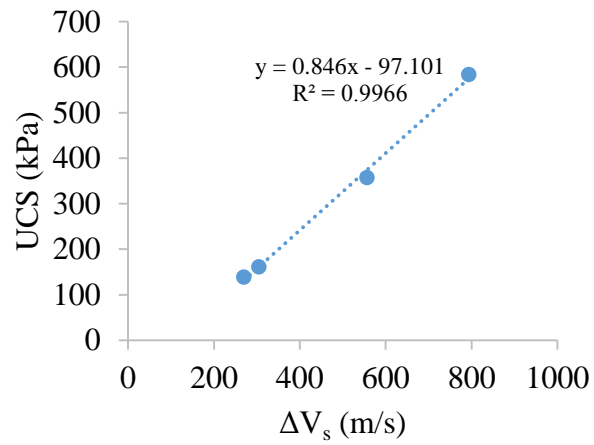


Figure 6.11. Unconfined compressive strength versus shear wave velocity after treatment for the samples treated by injection method at the lowest rate.

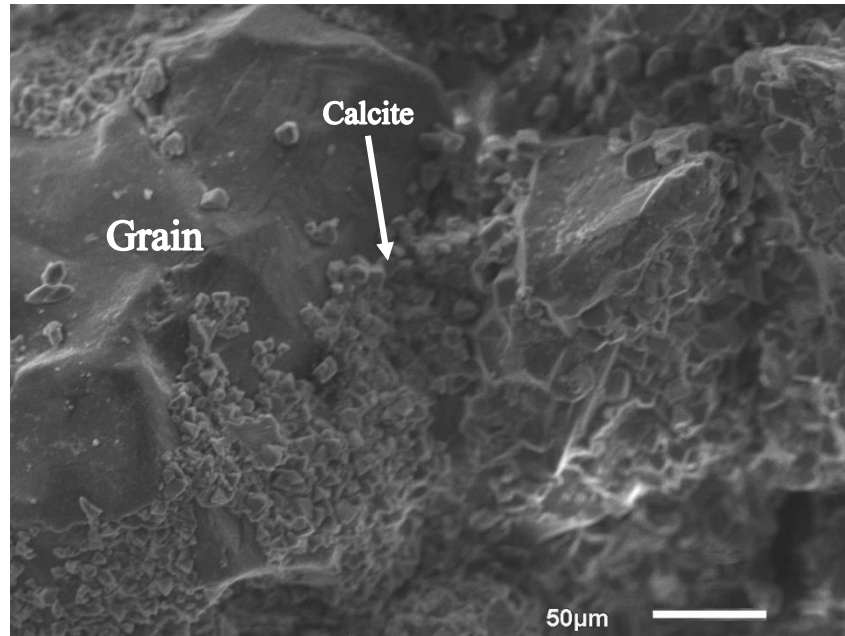


Figure 6.12. High concentration of calcite in the soil treated through injection method at the lowest rate of precipitation.

6.3.3 Treatment Using Soaking Method at the Highest Rate

Table 6.5 shows the results of treatment using soaking method at the highest rate. Samples 5, 6, 4 and 3 were respectively brought out of the bath filled with the first 3.5 liters of treatment solution after treatment periods of 3, 21, 47 and 71 hours. Samples 2 and 1 were taken out of the bath after around 2 days extra treatment in the second and third 3.5-liter volume of fresh treatment solution respectively. It was demonstrated that the mass of precipitation increased by increasing the time and cycles of treatment. Although a bigger amount of precipitation was achieved in comparison with injection treatment method at the highest rate, it should be noted that the amount of treatment solution used at each cycle (i.e. 3.5 liters for a maximum mass of ~2850 g soil) was much more than the amount of treatment solution in injection method (i.e. 80 ml per sample with a mass of ~318 g). In other words, the soil samples in soaking treatment method are in exposure of more amount of treatment solution. Considering the amount

of precipitation to the consumed treatment solution, the soaking method is more costly than the injection method. The amount of precipitates deposited into the bath (not into the soil pores) at the first cycles of treatment was measured around 8 g out of the expected stoichiometric total of 24.5 g, i.e. around 16.5 g of the calcium carbonate precipitation occurred into the soil pores. The amount of the wasted precipitates were even increased in further cycles of treatment as exposure of the soil pores to the fresh treatment solution was declined due to the earlier precipitation. It was interestingly observed that the shear wave velocity does not significantly change by increasing the mass of precipitation in the samples 3, 4, 5, and 6 (Figure 6.13). This behavior can be attributed to the hollow cylindrical pattern of precipitation at this condition (Figure 6.14). It was demonstrated that the precipitation mainly occurred at the lateral surfaces; and the middle zone of the samples, where the influence zone of the S-wave generated by axially-arrayed bender elements is, remained almost non-treated. Very high rate of precipitation is the reason for such a precipitation pattern. Because of the high precipitation rate, nearly all the calcium ions in the treatment solution were quickly precipitated in the lateral surfaces where were directly exposed to the treatment solution. So, there was not considerable amount of calcium ions remained in the treatment solution reaching the middle zone. In other words, precipitation developed from outer surfaces to the inner parts of the sample when there were no more bacterial cells in the outer part of the sample to precipitate the calcium ions. The samples with more treatment period had thicker cemented shells. In contrast with the injection treatment at the highest rate, the SEM images of the treated samples at this condition revealed the presence of non-stable phase of calcium carbonate (Figure 6.15), which can be partially dissolved in water or transformed into more stable phases (see chapter 5). That is why

the treated samples at this condition were very weak and brittle. They lost their form and stability even after soaking into distilled water for a few minutes (Figure 6.16). This can be ascribed to partial solubility of the amorphous phases in water. Unconfined compression test on the samples treated at this condition was not performed, as a stable columnar sample could not be obtained.

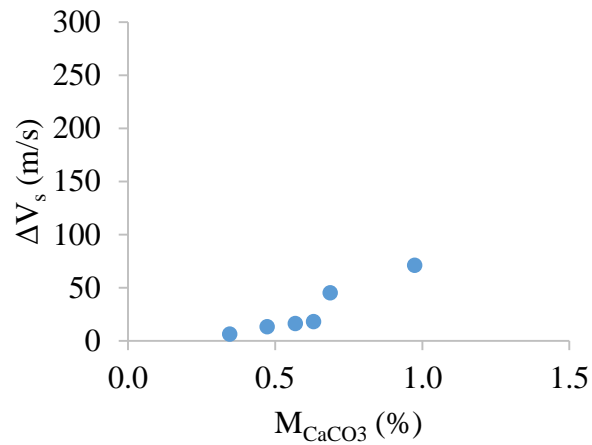


Figure 6.13. Change in shear wave velocity versus precipitation mass percent for the samples treated by soaking method at the highest rate.

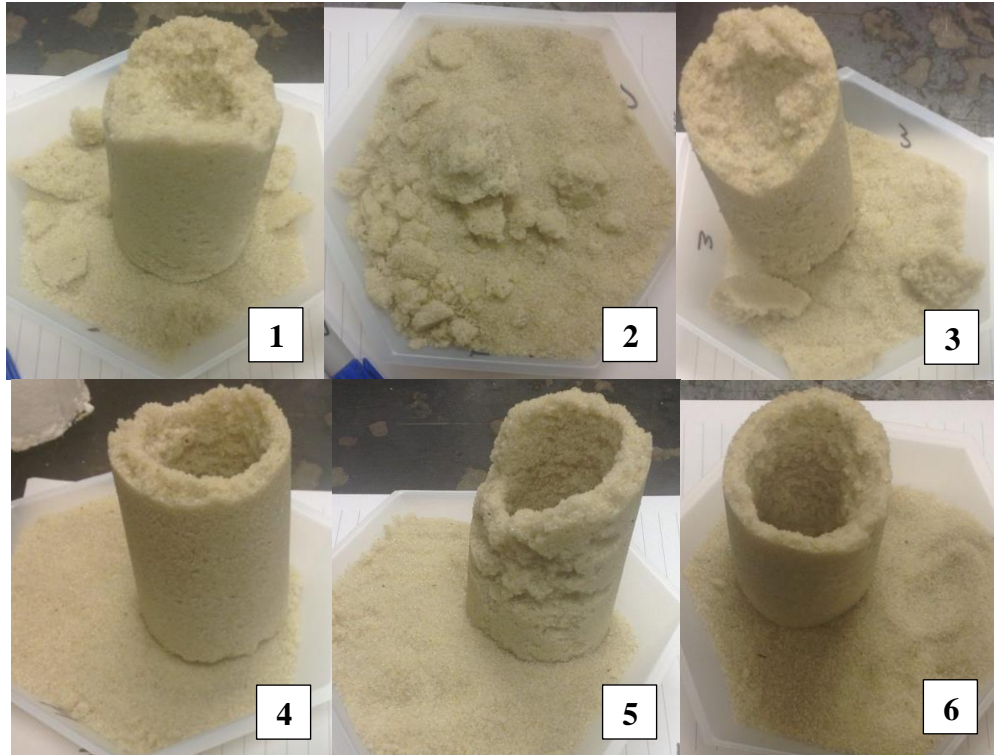


Figure 6.14. Treated samples by using soaking method at the highest rate.

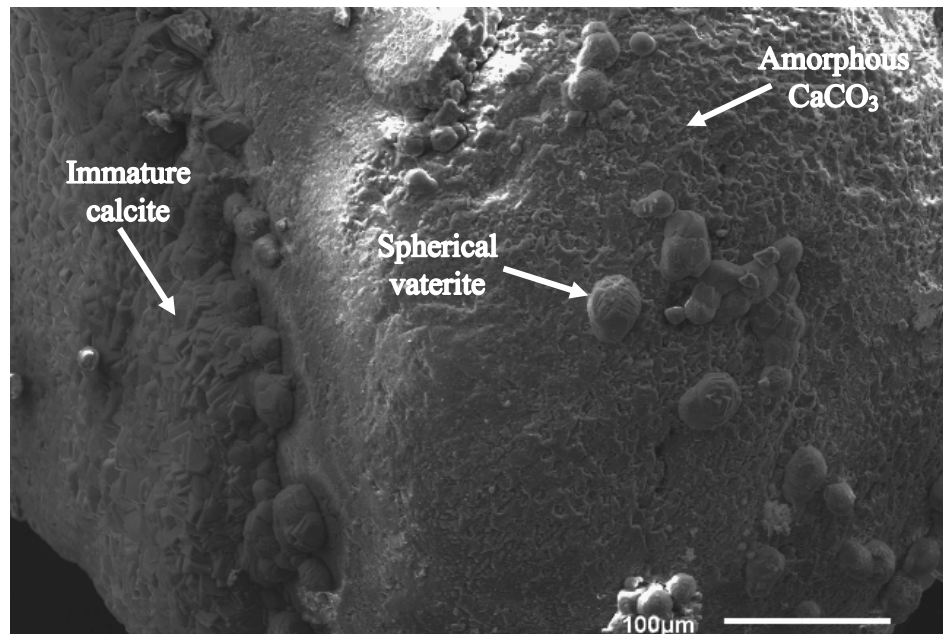


Figure 6.15. Soil grain from the sample by soaking method at the highest rate is covered by amorphous calcium carbonate. Spherical vaterite and immature calcite crystals are also observed on the grain surface.



Figure 6.16. The sample treated through soaking method at the highest rate was crumbled by soaking into distilled water.

6.3.4 Treatment Using Soaking Method at the Lowest Rate

Table 6.6 represents the results of treatment with soaking method at the lowest rate. All the samples were treated in only 3.5 liters of treatment solution (i.e. one treatment cycle) at varied treatment periods. The amount of precipitation increased at longer treatment period. The precipitation mass percent in each sample at this condition was considerably higher than the other conditions above. It varies between 2.68% for only 15 hours treatment period and 7.96% at the end of the experiment. A total of around 161 g calcium carbonate was achieved in all the samples while the 3.5 liters of treatment solution was theoretically susceptible to precipitation of 234.5 g calcium carbonate. A linear increase in shear wave velocity versus mass of precipitation was also observed in this condition (Figure 6.17). The magnitude of the shear wave velocity for the treated samples in this condition corresponds to stiff soils, soft and medium stiff rocks. In spite of such big magnitudes, a stable soil column could not be formed to perform unconfined compression tests. All the samples had very weak lateral surfaces which could be easily crumbled even with very gentle touch, while the middle part of the soil columns was

really stiff that could not be easily broken by hand (Figure 6.18). It should be noted that the middle part of each column was subjected to the shear wave velocity measurement due to axial array of bender elements along the samples. In order to find the reason for the fragility of the lateral surfaces, the soil grains were examined under SEM. It was identified that the grains on the surface are covered with a film of organic matters. No calcite bonds were observed between the grains from the lateral surfaces of each sample. The bonds, if exist, are very weak and unstable (Figure 6.19a). This precipitation pattern can be ascribed to the continuous exposure of the lateral surfaces to the high concentration of biological wastes and organic matters existing in treatment solution. Concentration of biological wastes and organic matters in the treatment solution was high as the environment was desirable for bacterial growth at this condition. High concentration of the organic compounds inhibits the formation of calcite (see Chapter 5). Calcite bonds were beholden on and between the grains from middle part of the sample, where it is not in direct exposure of the treatment solution (Figure 6.19b). Visual inspection of the acid washing process of the samples is also in a logic agreement with the mineralogical examinations. It was observed that the grains on the lateral surfaces of the samples treated at this condition are instantly disintegrated by soaking into the acid solution, while the middle parts might even take some hours to be completely washed with acid. Generally, the samples were treated at the lowest rate were comparatively taking longer time for full dissolution of the precipitates. It suggests the presence of more stable mineral phases (e.g. calcite) in the precipitates.

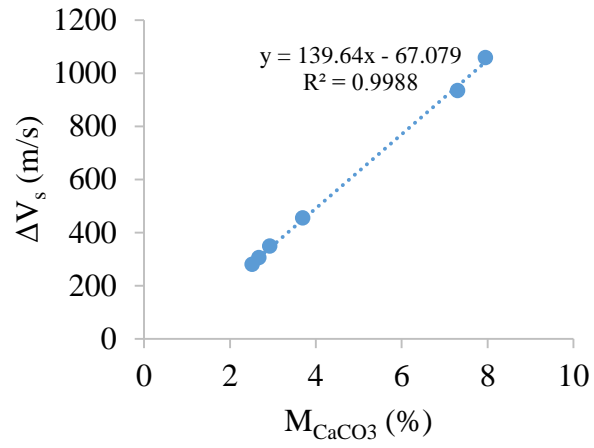


Figure 6.17. Change in shear wave velocity versus precipitation mass percent for the samples treated by soaking method at the lowest rate.



Figure 6.18. Treated samples by using soaking method at the lowest rate.

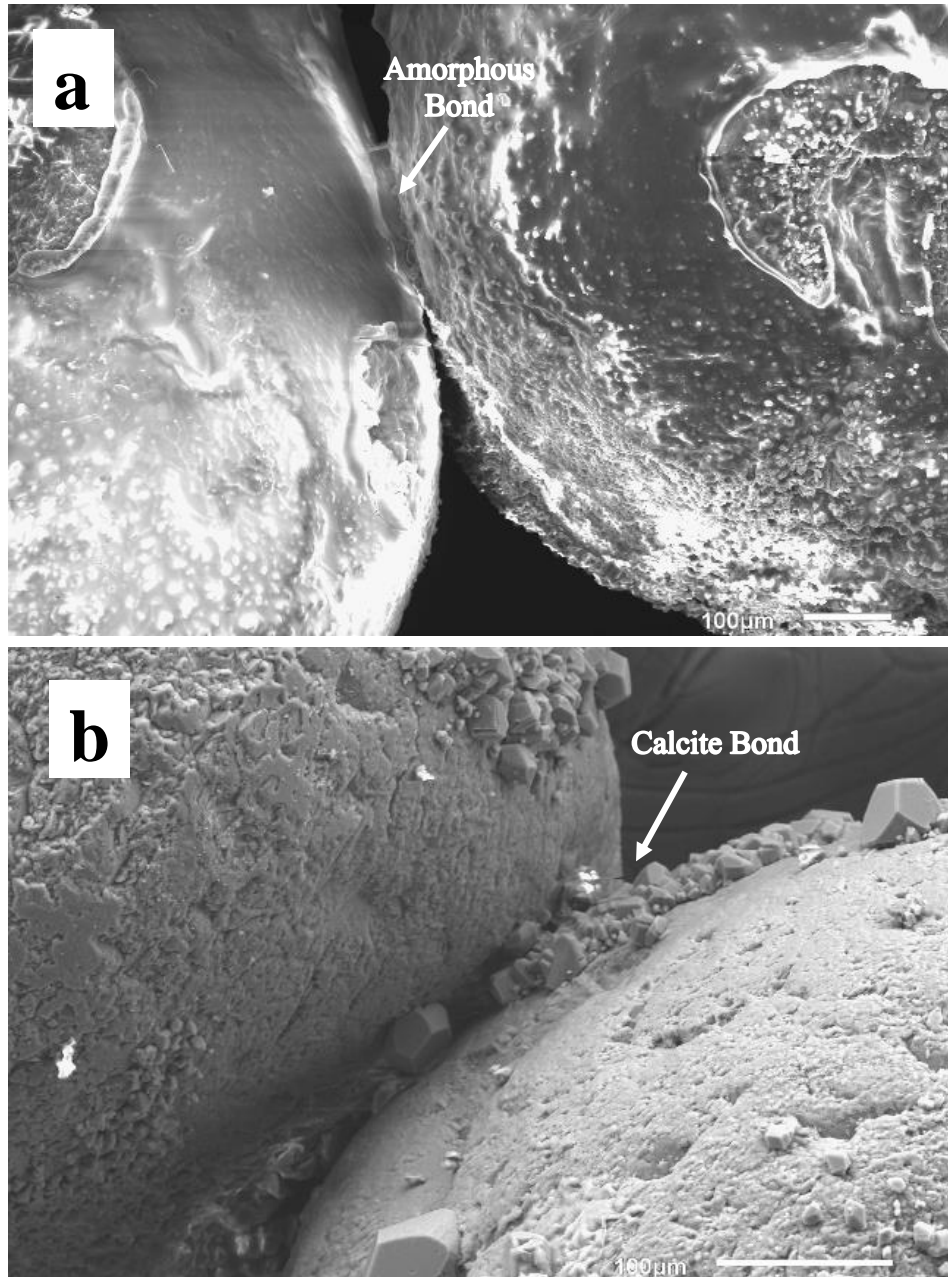


Figure 6.19. SEM images of the grains from (a) lateral surface and (b) the middle part of sample treated by using soaking method at the lowest rate of precipitation.

It was interestingly perceived that the mass-normalized change in shear wave velocity ($\Delta V_s/M_{CaCO_3}$) of the MICP-treated samples varies at different treatment method and rate of precipitation: $(\Delta V_s/M_{CaCO_3})_{Injection, low} > (\Delta V_s/M_{CaCO_3})_{Injection, high} > (\Delta V_s/M_{CaCO_3})_{Soaking}$.

Table 6.5. Summary of the treatment of the samples through injection method at the highest rate of precipitation

sample No.	D_r	$(V_s)_0$	$t_{\text{Treatment}}$	Treatment cycle	$(V_s)_1$	UCS	m_{CaCO_3}	M_{CaCO_3}	ΔV_s	$\Delta V_s/M_{\text{CaCO}_3}$
1	44	150	167	3 (10.5 l)	221	NA	3.1	0.97	71	73
2	44	149	3	1 (3.5 l)	155	NA	1.1	0.35	6	17
3	49	157	95	2 (7 l)	202	NA	2.2	0.69	45	65
4	42	145	71	1 (3.5 l)	163	NA	2	0.63	18	29
5	42	146	21	1 (3.5 l)	159	NA	1.5	0.47	13	27
6	40	142	47	1 (3.5 l)	158	NA	1.8	0.57	16	28

Table 6.6. Summary of the treatment of the samples through injection method at the lowest rate of precipitation

sample No.	D_r	$(V_s)_0$	$t_{\text{Treatment}}$	Treatment cycle	$(V_s)_1$	UCS	m_{CaCO_3}	M_{CaCO_3}	ΔV_s	$\Delta V_s/M_{\text{CaCO}_3}$
1	42	146	40	1 (3.5 l)	451	NA	8.5	2.68	305	114
2	42	146	15	1 (3.5 l)	426	NA	8	2.52	280	111
3	42	144	69	1 (3.5 l)	493	NA	9.3	2.93	349	119
4	40	142	95	1 (3.5 l)	597	NA	11.7	3.70	455	123
5	47	154	138	1 (3.5 l)	1088	NA	23.3	7.30	934	128
6	44	148	192	1 (3.5 l)	1207	NA	25.3	7.96	1059	133

low $> (\Delta V_s/MCaCO_3)$ Soaking, high. Bigger increase was noticed in the samples treated with injection method than the samples treated with soaking method. The samples treated at the lowest rate also showed a higher increase in shear wave velocity. It indicates that different treatment methods and rates of precipitation influence the stiffness of the treated samples even at the same level of precipitation.

6.4 Conclusion

In this chapter, it was demonstrated that MICP-treatment of sand is not only a function of the precipitation rate, which depends on the chemical concentration of the treatment solution and environmental condition per se, but also highly dependent on the treatment method. Two treatment methods, i.e. injection method and soaking method, were evaluated here. Injection method was found more efficient for precipitation of calcite at contact points between grains although only a low level of treatment can be achieved at the highest rate of precipitation using this method. Soaking method produced more amount of precipitation at both low and high precipitation rates in comparison with injection method; but, contrary to expectation, less uniform treatment resulted using soaking method. It indicates that availability and uniform distribution of the treatment solution and bacterial cells are not sufficient for obtaining uniform treatment. Treating the samples by soaking method at the highest rate led to bigger concentration of precipitation at lateral surfaces, while a higher precipitation was observed in the middle zone of the soil column at the lowest rate. Non-stable phases of calcium carbonate were also perceived in the precipitates treated through soaking method due to high organic content produced through bacterial activity in the treatment solution. A confined compression test (e.g. triaxial test) should be applied for measuring the strength of the

samples treated through the injection method at the highest rate and the soaking method, as the samples are easily crumbled cannot be formed at unconfined conditions.

A linear relation between the mass of precipitation and the shear wave velocity was observed in the treated samples. Unconfined compression test on the samples treated by injection method at the lowest rate also exhibited a linear relation between the mass of precipitation and unconfined compressive strength. S-wave measurement can be employed as a non-destructive test for estimation on the level of treatment and strength of the MICP-treated soils. Different mass-normalized changes in shear wave velocity of the treated samples indicate that different treatment methods and rates of precipitation influence the stiffness of the treated samples even at the same amount of precipitation. In other words, in addition to the mass of precipitation, mineral type, aggregation pattern and place of precipitation within soil (i.e. between contact points, on the surface, or in the pores) affect the mechanical properties of treated soil.

Chapter 7

CONCLUSION

7.1 Summary

Biogeotechnics, which deals with bio-mediated and bio-inspired solutions to the challenges that vex geotechnical systems, has been recently emerged as a multidisciplinary field of study in geotechnical engineering because of environmental concerns and application limitations of the conventional techniques. Within just around one decade of emerging this field, it has attracted the interest of many researchers all over the world. Industrial implementation of the biologically-based techniques into various geotechnical problems and educating the first generation of biogeotechnical engineers by 2020 have been planned in the newly established center for bio-mediated and bio-inspired geotechnics (CBBG) in USA.

Ureolysis-based microbial calcium carbonate precipitation is one of the biocementation process through which calcium carbonate precipitates by mediation of microbes as catalyzing agent. Application of this process into soil causes precipitation within pores as binding agent between grains and/or filling materials, which consequently influences mechanical properties of soil. For this purpose, treatment solution (biogrout) containing ureolytic bacteria, substrate (CaCl_2 and urea) and some nutrients and stabilizers required for bacterial activity is introduced into soil. Microbial denitrification and enzymatic

ureolysis are two other biocementation processes for calcium carbonate precipitation. Although these processes have been suggested as alternative techniques for soil treatment using microbial ureolysis process, microbial ureolysis is still the most common-used technique in the literature. Releasing ammonium by-product in the soil environment is the biggest concern in application of the ureolysis process in practice. Spatial uniform treatment, durability and cost are the other challenges of using every biological technique for soil improvement applications. These challenges mainly arise from the lack of enough control on precipitation pattern, i.e. type, time, amount and place of precipitation. As controlling the precipitation pattern requires having knowledge on how the pattern changes at different conditions, a monitoring technique for precipitation progress was developed in this study. In this regard, a hybrid method of conductometry and one precipitation mass measurement test instead of several precipitation mass measurement tests was proposed in this study. It was found to be a reliable, fast, cheap and non-expert friendly method of monitoring the precipitation progress in a treatment solution.

Monitoring the precipitation progress in treatment solution in this study revealed that the precipitation pattern follows a logistic function (designated as microbial CaCO_3 precipitation characteristics, MCPCC), which describes lag duration, precipitation rate and precipitation ratio as precipitation characteristics. It provides useful information on describing, interpreting, estimating and steering the precipitation pattern within soil. It can act as an index enabling investigation of the effect of other factors (e.g. temperature, solution ingredients, competing microorganisms, etc.) on precipitation pattern. It also facilitates designing an optimum treatment solution.

It was demonstrated in this study that initial cell concentrations, CaCl₂/urea concentrations and temperatures, as the key adjustable parameter of a treatment solution, significantly influence microbial CaCO₃ precipitation characteristics (MCPC), i.e. lag duration, precipitation rate and precipitation ratio. Effect of these parameters on the precipitation characteristics was statistically investigated and modelled. Statistical model for precipitation rate shows that it is significantly influenced by initial cell concentration, CaCl₂/urea concentration, temperature and the interaction between initial cell concentration and temperature. The only drawback of the presented model for precipitation rate is that it does not consider the condition with no precipitation caused by interaction between the lowest initial cell concentration and the highest concentration of calcium chloride and urea, due to a few number of occurrence in the set of tests conducted in this study. Therefore, it was suggested to use this model when the result obtained from the model for precipitation ratio is not zero. Precipitation ratio was observed to be a function of initial cell concentration and electrical conductivity of the treatment solution mainly caused by calcium chloride and urea. It was demonstrated that the precipitation ratio drops when the electrical conductivity of the treatment solution is above a specific value ($EC_{critical}$) corresponding to each initial cell concentration. Lag duration cannot be statistically modelled as there is a big difference between the maximum and minimum values of the response (i.e. presence of outliers). Visual examination of precipitation solution was suggested as the best way for estimation of lag duration. Excluding the tests with no precipitation which can be realized through the model for precipitation ratio, longer lag duration is expected to occur at the lowest initial cell concentration and temperature.

Effect of seawater, concentration nutrient broth and lack of air were also assessed in the present study. Seawater was chosen to see the precipitation ratio obtained from the solution with a conductivity caused by substrates except just calcium chloride and urea. There might also exist many cases of application of this technique into soil with seawater in the pores. Seawater was found to cause a reduction in precipitation ratio in the treatment solution with $EC_{critical}$ corresponding to each initial cell concentration. It was found with no influence at EC less than $EC_{critical}$ corresponding to each initial cell concentration. It suggests that the precipitation ratio is just a function of EC resulted by calcium chloride and urea not by other saline. Influence of lower concentration and lack of nutrient broth (as a general food for all kinds of microorganisms) on precipitation characteristics were chosen for investigation as lack of nutrient broth can eliminate the impact of competitor microorganisms living in soil. Lack of nutrient broth was observed to increase the rate and decrease the precipitation ratio and lag duration at the conditions with longer lag duration. It did not influence the conditions with no considerable lag duration. This behavior corresponds to the effect of nutrient broth at the conditions favoring bacterial growth. In order to evaluate the precipitation ratio at the depth of the soil, effect of lack of air was also investigated. It was perceived that precipitation happens even at the conditions with lack of air although the precipitation ratio drastically dropped at the conditions with $EC_{critical}$ corresponding to 10^7 and 10^8 cell/ml initial cell concentrations.

Potential types and morphologies of calcium carbonate precipitates within MICP treatment solution were studied at different rates of precipitation, in presence of seawater and in the absence of nutrient broth. Type and morphology of the precipitated minerals

and aging are the three important parameters which influence the mechanical properties of MICP-treated soil. Precipitation of calcite as the most stable phase of calcium carbonate is more desirable for geotechnical applications. Precipitation of non-stable phases causes change in mechanical properties as they tend to transform to more stable phases. It also influences durability of the treatment since they are more sensitive to dissolution in water and acidic environment. Although non-stable phases can get sometimes stabilized in a given condition, they may transform again by changing the biochemical conditions of soil environment. Stabilization of vaterite and aragonite was observed in this study at the presence of organic matter and Mg content of seawater. Particles precipitated within MICP process were observed to be hollow or solid, densely or loosely agglomerated, rod-shaped or spherical or irregular. That is obvious that each kind of these morphologies produces different mechanical properties. For instance, solid and densely agglomerated particles are expected to create stronger bonds between grains or increase the shear wave velocity at a higher extent; loosely agglomerated particles are more susceptible to breakage at micro level; hollow particles can retain water inside of themselves. Aging may cause change in type and/or morphology of the minerals precipitated in the pores. Vaterite was fractured into small pieces at room temperature after around one year. Monohydrocalcite was also transformed into aragonite at room temperature within a year. The ultimate mechanical properties of a MICP-treated soil is achieved when there will be no longer change in type and morphology of the precipitates within the pores. Type and morphology of the precipitated minerals can be modified to desirable ones through some curing considerations within treatment process, right after treatment, or later at the time of need.

Two treatment methods, i.e. injection method and soaking method, were evaluated. Injection method was found more efficient for precipitation of calcite at contact points between grains although only a low level of treatment can be achieved at the highest rate of precipitation using this method. Soaking method produced more amount of precipitation at both low and high precipitation rates in comparison with injection method; but, contrary to expectation, less uniform treatment resulted using soaking method. It indicates that availability and uniform distribution of the treatment solution and bacterial cells are not sufficient for obtaining uniform treatment. A linear relation between the mass of precipitation and the shear wave velocity was observed in the treated soil. Unconfined compression test on the samples treated by injection method at the lowest rate also exhibited a linear relation between the mass of precipitation and unconfined compressive strength. S-wave measurement can be employed as a non-destructive test for estimation on the level of treatment and strength of the MICP-treated soils. Different mass-normalized changes in shear wave velocity of the treated samples indicate that different treatment methods and rates of precipitation influence the stiffness of the treated samples even at the same amount of precipitation. In other words, in addition to the mass of precipitation, mineral type, aggregation pattern and place of precipitation within soil affect the mechanical properties of treated soil.

7.2 Future Research

Generally, additional collaborative interdisciplinary work by chemists, biologists, geologists, and geotechnical engineers is required to implement the biological calcium carbonate precipitation technology into geotechnical engineering applications. Going over the research studies in the literature demonstrates that the majority of the

fundamental studies has been carried out by biologists, geologists, and environmental engineers and involvement of geotechnical engineers in these efforts has been restricted. This restriction caused the lack of geotechnical insight in the studies performed by biologists, geologists, and environmental engineers and the lack of biochemical insight in the geotechnical studies. More involvement of geotechnical engineers into biological and chemical studies is an absolute necessity for development of the biological technologies for ground improvement.

Subsequent to the study presented in this dissertation, a similar fundamental study on enzymatic ureolysis process has been also initiated for comparison and better interpretation of the role of microbes in calcium carbonate precipitation at the center for biomediated and bioinspired geotechnics (CBBG), Arizona state university. Eliminating the drawbacks of the enzymatic process, i.e. controlling the precipitation rate and type of mineral, has been planned. It was consequently aimed to attain the best treatment and post treatment strategy (e.g. optimum treatment solution, injection technique, curing for obtaining calcite, etc.) through microbial and enzymatic ureolysis process.

Lastly, implementation of the ureolysis process into soil at laboratory and field scale is intended. Prior to field implementation, potential application of the technique for slope stabilization, liquefaction mitigation, dust mitigation, tunneling and bore holing, impermeable and semi-permeable crust formation is investigated through a laboratory team work on mechanical properties of treated soil.

REFERENCES

- Achal, V., Mukherjee, A., & Reddy, M. S. (2010). Biocalcification by *Sporosarcina pasteurii* using corn steep liquor as the nutrient source. *Industrial Biotechnology*, 6(3), 170-174.
- Akaike, H. (1974). A new look at the statistical model identification. *IEEE Transactions on Automatic Control*, 19(6), 716-723.
- Al Thawadi, S. (2008). *High strength in-situ biocementation of soil by calcite precipitating locally isolated ureolytic bacteria* (Doctoral dissertation, Murdoch University).
- Al Qabany, A. (2011). *Microbial carbonate precipitation in soils* (Doctoral dissertation, University of Cambridge).
- Al Qabany, A., & Soga, K. (2013). Effect of chemical treatment used in MICP on engineering properties of cemented soils. *Géotechnique*, 63(4), 331-339.
- Al Qabany, A., Soga, K., & Santamarina, C. (2011). Factors affecting efficiency of microbially induced calcite precipitation. *Journal of Geotechnical and Geoenvironmental Engineering*, 138(8), 992-1001.

Farshad, A., Lin, L., Chi, L., Huanzen, Z., & Qian, Z. (2014). A Full Contact Flexible Mold for Preparing Samples Based on Microbial-Induced Calcite Precipitation Technology. *Geotechnical Testing Journal*, 37(5), 917-921.

Anthony, J. W., Bideaux, R. A., Bladh, K. W., & Nichols, M. C. (2001). Handbook of Mineralogy (Mineralogical Society of America, Chantilly, VA).

Armstrong, R. (2009). Rachel Armstrong: Architecture that repairs itself? [Video file]. Retrieved from: http://www.ted.com/talks/rachel_armstrong_architecture_that_repairs_itself?

Bentov, S., Weil, S., Glazer, L., Sagi, A., & Berman, A. (2010). Stabilization of amorphous calcium carbonate by phosphate rich organic matrix proteins and by single phosphoamino acids. *Journal of structural biology*, 171(2), 207-215.

Blakely, R. L., & Zerner, B. (1984). Jack Bean Urease: The First Nickel Enzyme. *Journal of Molecular Catalysis*, 23, 263 – 292.

Bosak, T., & Newman, D. K. (2005). Microbial kinetic controls on calcite morphology in supersaturated solutions. *Journal of Sedimentary Research*, 75(2), 190-199.

Burbank, M. B., Weaver, T. J., Green, T. L., Williams, B. C., & Crawford, R. L. (2011). Precipitation of calcite by indigenous microorganisms to strengthen liquefiable soils. *Geomicrobiology Journal*, 28(4), 301-312.

- Burbank, M. B., Weaver, T. J., Williams, B. C., & Crawford, R. L. (2012). Urease activity of ureolytic bacteria isolated from six soils in which calcite was precipitated by indigenous bacteria. *Geomicrobiology Journal*, 29(4), 389-395.
- Burnham, K. P., & Anderson, D. R. (2004). Multimodel inference understanding AIC and BIC in model selection. *Sociological methods & research*, 33(2), 261-304.
- Castanier, S., Le Metayer-Levrel, G., & Perthuisot, J. P. (2000). Bacterial roles in the precipitation of carbonate minerals. In *Microbial Sediments*, 32-39. Springer Berlin Heidelberg.
- Chan, C. M. (2010). Bender element test in soil specimens: identifying the shear wave arrival time. *EJGE*, 15(2010), 1263-1276.
- Chave, K. E. (1954). Aspects of the biogeochemistry of magnesium 1. Calcareous marine organisms. *The Journal of geology*, 266-283.
- Cheng, L., & Cord-Ruwisch, R. (2012). In situ soil cementation with ureolytic bacteria by surface percolation. *Ecological Engineering*, 42, 64-72.
- Chu, J., Ivanov, V., Naeimi, M., Stabnikov, V., & Liu, H. L. (2014). Optimization of calcium-based bioclogging and biocementation of sand. *Acta Geotechnica*, 9(2), 277-285.

- Cobourne, G., Mountjoy, G., Rodriguez-Blanco, J. D., Benning, L. G., Hannon, A. C., & Plaisier, J. R. (2014). Neutron and X-ray diffraction and empirical potential structure refinement modelling of magnesium stabilised amorphous calcium carbonate. *Journal of Non-Crystalline Solids*, 401, 154-158.
- Dawoud, O., Chen, C. Y., & Soga, K. (2014). Microbial-Induced Calcite Precipitation (MICP) Using Surfactants. In *Geo-Congress 2014 Technical Papers@ sGeo-characterization and Modeling for Sustainability*, 1635-1643. ASCE.
- DeJong, J.T., Fritzges, M.B., Nusslein, K. (2006). Microbially Induced Cementation to Control Sand Response to Undrained Shear. *Journal of Geotechnical and Geoenvironmental Engineering*, 132(11), 1381-1392.
- De Jong, J. T., Mortensen, B. M., Martinez, B. C., & Nelson, D. C. (2010). Bio-mediated soil improvement. *Ecological Engineering*, 36(2), 197-210.
- De Jong, J. T., Soga, K. S., Kavazanjian, E., Burns, S., van Paassen, L. A., Al Qabany, A., ... & Weaver, T. (2013). Biogeochemical processes and geotechnical applications: progress, opportunities and challenges. *Geotechnique*, 63 (4), 2013.
- De Jong, J. T., Martinez, B. C., Ginn, T. R., Hunt, C., Major, D., & Tanyu, B. (2014). Development of a Scaled Repeated Five-Spot Treatment Model for Examining Microbial Induced Calcite Precipitation Feasibility in Field Applications. *Geotechnical Testing Journal*, 37(3).

Drew, G. H. (1913). On the precipitation of calcium carbonate in the sea by marine bacteria, and on the action of denitrifying bacteria in tropical and temperate seas. *Journal of the Marine Biological Association of the United Kingdom (New Series)*, 9(04), 479-524.

Ferris, F. G., Phoenix, V., Fujita, Y., & Smith, R. W. (2004). Kinetics of calcite precipitation induced by ureolytic bacteria at 10 to 20 C in artificial groundwater. *Geochimica et Cosmochimica Acta*, 68(8), 1701-1710.

Ehrlich, H.L. (2002). *Geomicrobiology*. New York, Marcel Dekker.

Fujita, Y., Taylor, J. L., Wendt, L. M., Reed, D. W., & Smith, R. W. (2010). Evaluating the potential of native ureolytic microbes to remediate a ⁹⁰Sr contaminated environment. *Environmental science & technology*, 44(19), 7652-7658.

Gat, D., Tsesarsky, M., & Shamir, D. (2011). Ureolytic calcium carbonate precipitation in the presence of non-ureolytic competing bacteria. In *Geo-Frontiers 2011@ sAdvances in Geotechnical Engineering*, 3966-3974. ASCE.

Gat, D., Tsesarsky, M., Wahanon, A., & Ronen, Z. (2014). Ureolysis and MICP with Model and Native Bacteria: Implications for Treatment Strategies. In *Geo-Congress 2014 Technical Papers@ sGeo-characterization and Modeling for Sustainability*, 1713-1720. ASCE.

- Hamdan, N. (2013). *Carbonate Mineral Precipitation for Soil Improvement through Microbial Denitrification* (Master dissertation, Arizona state university).
- Hamdan, N. (2015). *Applications of Enzyme Induced Carbonate Precipitation (EICP) for Soil Improvement* (Doctoral dissertation, Arizona state university).
- Hamdan, N., Kavazanjian Jr, E., and O'Donnell, S. (2013). Carbonate cementation via plant derived urease. In *Proc. of 18th International Conference on Soil Mechanics and Geotechnical Engineering*, Paris, 2489-2492.
- Harkes, M. P., van Paassen, L. A., Booster, J. L., Whiffin, V. S., & van Loosdrecht, M. C. (2010). Fixation and distribution of bacterial activity in sand to induce carbonate precipitation for ground reinforcement. *Ecological Engineering*, 36(2), 112-117.
- Hostomsky, J., & Jones, A. G. (1991). Calcium carbonate crystallization, agglomeration and form during continuous precipitation from solution. *Journal of Physics D: Applied Physics*, 24(2), 165.
- Hu, Y. B., Wolf-Gladrow, D. A., Dieckmann, G. S., Völker, C., & Nehrke, G. (2014). A laboratory study of ikaite ($\text{CaCO}_3 \cdot 6\text{H}_2\text{O}$) precipitation as a function of pH, salinity, temperature and phosphate concentration. *Marine Chemistry*, 162, 10-18.
- Huanc, C. K., Konn, P. F., Liniaersity, C., & York, N. (1960). Infrared study of the carbonate minerals. *Am. Mineral.*, 4(5).

- Jack, J. J. M., Roeland, J. M., Albertus, P. H. J., & Nico, A. J. M. (2000). Amorphous calcium carbonate stabilised by poly (propylene imine) dendrimers. *Chemical Communications*, (19), 1937-1938.
- Karatas, I. (2008). *Microbiological improvement of the physical properties of soils* (Doctoral dissertation, Arizona state university).
- Karol, R. H. (2003). Chemical grouting and soil stabilization, revised and expanded, Vol. 12. *CRC Press*.
- Kaur, D. N., & Mukherjee, A. (2013). Biomineralization of calcium carbonate polymorphs by the bacterial strains isolated from calcareous sites. *Journal of microbiology and biotechnology*, 23(5), 707-714.
- Kavazanjian Jr, E., & Hamdan, N. (2015). Enzyme Induced Carbonate Precipitation (EICP) Columns for Ground Improvement. In *Proc. of the ASCE Geo-Institute GeoCongress*, San Antonio, Texas, 2252-2261.
- Kavazanjian Jr, E., & Karatas, I. (2008). Microbiological improvement of the Physical Properties of Soil. In *Proc. 6th Int. Conf. on Case Histories in Geotech. Engineering*, Rolla, MO (CD-ROM).
- Kavazanjian Jr, E., O'Donnell, S., & Hamdan, N. (2015). Biogeotechnical mitigation of earthquake-induced soil liquefaction by denitrification: a two-stage process. In *Proc.*

of the 6th international conference on earthquake geotechnical engineering, New Zealand (CD-ROM).

Krumbein, W. E. (1975). Biogenic monohydrocalcite spherules in lake sediments of Lake Kivu (Africa) and the Solar Lake (Sinai). *Sedimentology*, 22(4), 631-634.

Le, C. T. (2003). *Introductory biostatistics*. John Wiley & Sons.

Li, M., Guo, H., & Cheng, X. (2011). Application of response surface methodology for carbonate precipitation production induced by a mutant strain of *ISporosarcina pasteurii*. In *Geo-Frontiers 2011@ sAdvances in Geotechnical Engineering*, 4079-4088. ASCE.

Lopez, O., Zuddas, P., & Faivre, D. (2009). The influence of temperature and seawater composition on calcite crystal growth mechanisms and kinetics: Implications for Mg incorporation in calcite lattice. *Geochimica et Cosmochimica Acta*, 73(2), 337-347.

Loste, E., Wilson, R. M., Seshadri, R., & Meldrum, F. C. (2003). The role of magnesium in stabilising amorphous calcium carbonate and controlling calcite morphologies. *Journal of Crystal Growth*, 254(1), 206-218.

Martinez, B. C., DeJong, J. T., Ginn, T. R., Montoya, B. M., Barkouki, T. H., Hunt, C., ... & Major, D. (2013). Experimental optimization of microbial-induced carbonate

- precipitation for soil improvement. *Journal of Geotechnical and Geoenvironmental Engineering*, 139(4), 587-598.
- Mitchell, J. K., & Santamarina, J. C. (2005). Biological considerations in geotechnical engineering. *Journal of geotechnical and geoenvironmental engineering*, 131(10), 1222-1233.
- Montgomery, D. C., Runger, G. C., & Hubele, N. F. (2011). *Engineering statistics*. Wiley.
- Montoya, B. M. (2012). *Bio-mediated soil improvement and the effect of cementation on the behavior, improvement, and performance of sand* (Doctoral dissertation, University of California, Davis).
- Montoya, B. M., Gerhard, R., DeJong, J. T., Wilson, D. W., Weil, M. H., Martinez, B. C., & Pederson, L. (2012). Fabrication, operation, and health monitoring of bender elements for aggressive environments. *ASTM geotechnical testing journal*, 35(5), 728-742.
- Mortensen, B. M., Haber, M. J., DeJong, J. T., Caslake, L. F., & Nelson, D. C. (2011). Effects of environmental factors on microbial induced calcium carbonate precipitation. *Journal of applied microbiology*, 111(2), 338-349.

National Research Council Opportunities for Research and Technological Innovation.

(2006). *Geological and geotechnical engineering in the new millennium: opportunities for research and technological innovation*. National Academies Press.

Neumann, M., & Epple, M. (2007). Monohydrocalcite and its relationship to hydrated amorphous calcium carbonate in biominerals. *European journal of inorganic chemistry*, 2007(14), 1953-1957.

Neupane, D., Hideaki, Y., Naoki, K., & Toshiyasu U. (2013). Applicability of Enzymatic Calcium Carbonate Precipitation as a Soil-Strengthening Technique. *Journal of Geotechnical and Geoenvironmental Engineering*, 139(12), 2201-2211.

Niedermayr, A., Köhler, S. J., & Dietzel, M. (2013). Impacts of aqueous carbonate accumulation rate, magnesium and polyaspartic acid on calcium carbonate formation (6–40 C). *Chemical Geology*, 340, 105-120.

Okwadha, G. D., & Li, J. (2010). Optimum conditions for microbial carbonate precipitation. *Chemosphere*, 81(9), 1143-1148.

Olech, Z., Zaborska, W., & Kot, M. (2014). Jack bean urease inhibition by crude juices of Allium and Brassica plants. Determination of thiosulfinates. *Food chemistry*, 145, 154-160.

- Onac, B. P. (2001). Mineralogical studies and uranium-series dating of speleothems from Scarisoara glacier cave (Bihar Mountains, Romania). *Theoretical and Applied Karstology*, 13(14).
- Parks, S. L. (2009). *Kinetics of calcite precipitation by ureolytic bacteria under aerobic and anaerobic conditions* (Doctoral dissertation, Montana State University-Bozeman, College of Engineering).
- Plummer, N. L., & Busenberg, E. (1984). The solubility of calcite, aragonite and vaterite in CO₂-H₂O solutions between 0 and 90°C, and an evaluation of the aqueous model for the system CaCO₃-CO₂-H₂O. *Geochimica et cosmochimica acta*. 46(6), 1011-1040.
- Ries, J. B., Anderson, M. A., & Hill, R. T. (2008). Seawater Mg/Ca controls polymorph mineralogy of microbial CaCO₃: A potential proxy for calcite-aragonite seas in Precambrian time. *Geobiology*, 6(2), 106-119.
- Rivadeneira, M. A., Ramos-Cormenzana, A., Delgado, G., & Delgado, R. (1996). Process of carbonate precipitation by *Deleya halophila*. *Current microbiology*, 32(6), 308-313.
- Rodriguez-Blanco, J. D., Shaw, S., Bots, P., Roncal-Herrero, T., & Benning, L. G. (2014). The role of Mg in the crystallization of monohydrocalcite. *Geochimica et Cosmochimica Acta*, 127, 204-220.

- Saikia, J., Saha, B., & Das, G. (2012). Morphosynthesis of framboidal stable vaterite using a salicylic acid-aniline dye as an additive. *RSC Advances*, 2(26), 10015-10019.
- Sanchez-Moral, S., Canaveras, J. C., Laiz, L., Sáiz-Jiménez, C., Bedoya, J., & Luque, L. (2003). Biomediated precipitation of calcium carbonate metastable phases in hypogean environments: a short review. *Geomicrobiology Journal*, 20(5), 491-500.
- Soon, N. W., Lee, L. M., Khun, T. C., & Ling, H. S. (2014). Factors Affecting Improvement in Engineering Properties of Residual Soil through Microbial-Induced Calcite Precipitation. *Journal of Geotechnical and Geoenvironmental Engineering*, 140(5).
- Stocks-Fischer, S., Galinat, J. K., & Bang, S. S. (1999). Microbiological precipitation of CaCO₃. *Soil Biology and Biochemistry*, 31(11), 1563-1571.
- Stoffers, P., & Fischbeck, R. (1974). Monohydrocalcite in the sediments of Lake Kivu (East Africa). *Sedimentology*, 21(1), 163-170.
- Stoffers, P., & Fischbeck, R. (1975). Biogenic monohydrocalcite spherules in lake sediments of Lake Kivu (Africa) and the Solar Lake (Sinai): a reply. *Sedimentology*, 22(4), 635-636.
- Sumner, J. B. (1926). The isolation and crystallization of the enzyme urease preliminary paper. *Journal of Biological Chemistry*, 69(2), 435-441.

- Swainson, I. P. (2008). The structure of monohydrocalcite and the phase composition of the beachrock deposits of Lake Butler and Lake Fellmongery, South Australia. *American Mineralogist*, 93(7), 1014-1018.
- Tai, C. Y., & Chen, F. B. (1998). Polymorphism of CaCO₃, precipitated in a constant-composition environment. *AIChE Journal*, 44(8), 1790-1798.
- Taylor, G. F. (1975). The occurrence of monohydrocalcite in two small lakes in the south-east of South Australia. *American Mineralogist*, 60, 690-697.
- Upadhyay, L. S. B. (2012). Urease inhibitors: A review. *Indian Journal of Biotechnology*, 11(4), 381-388.
- van Paassen, L. A. (2009). *Biogrout, ground improvement by microbial induced carbonate precipitation*. TU Delft, Delft University of Technology.
- van Paassen, L. A., Harkes, M. P., van Zwieten, G. A., van der Zon, W. H., van der Star, W. R. L., & van Loosdrecht, M. C. M. (2009). Scale up of BioGrout: a biological ground reinforcement method. In *Proceedings of the 17th international conference on soil mechanics and geotechnical engineering*, 2328-2333. IOS Press, Lansdale, PA.
- van Paassen, L. A. (2011). Bio-mediated ground improvement: from laboratory experiment to pilot applications. In *Geo-Frontiers 2011@ sAdvances in Geotechnical Engineering*, 4099-4108. ASCE.

van Paassen, L. A., Daza, C. M., Staal, M., Sorokin, D. Y., van der Zon, W., & van Loosdrecht, M. C. (2010a). Potential soil reinforcement by biological denitrification. *Ecological Engineering*, 36(2), 168-175.

van Paassen, L. A., Ghose, R., van der Linden, T. J., van der Star, W. R., & van Loosdrecht, M. C. (2010b). Quantifying biomediated ground improvement by ureolysis: large-scale biogrout experiment. *Journal of Geotechnical and Geoenvironmental Engineering*, 136(12), 1721-1728.

Venda Oliveira, P. J., da Costa, M. S., Costa, J. N., & Nobre, M. F. (2014). Comparison of the Ability of Two Bacteria to Improve the Behavior of Sandy Soil. *Journal of Materials in Civil Engineering*, 27(1).

Wang, Y., Moo, Y. X., Chen, C., Gunawan, P., & Xu, R. (2010). Fast precipitation of uniform CaCO₃ nanospheres and their transformation to hollow hydroxyapatite nanospheres. *Journal of colloid and interface science*, 352(2), 393-400.

Whiffin, V. S. (2004). *Microbial CaCO₃ precipitation for the production of biocement* (Doctoral dissertation, Murdoch University).

Whiffin, V. S., van Paassen, L. A., & Harkes, M. P. (2007). Microbial carbonate precipitation as a soil improvement technique. *Geomicrobiology Journal*, 24(5), 417-423.

Zuddas, P., & Mucci, A. (1994). Kinetics of calcite precipitation from seawater: I. A classical chemical kinetics description for strong electrolyte solutions. *Geochimica et Cosmochimica Acta*, 58(20), 4353-4362.

Zuddas, P., & Mucci, A. (1998). Kinetics of calcite precipitation from seawater: II. The influence of the ionic strength. *Geochimica et Cosmochimica Acta*, 62(5), 757-766.

APPENDICES

















Appendix A: Choosing the best regression line by comparing the AICc statistics of the applied models

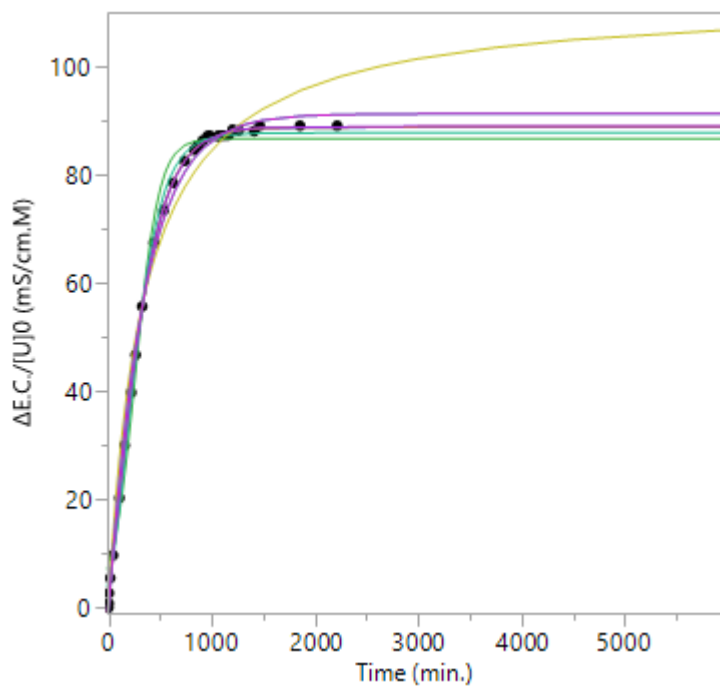
AICc value, as a measure of the goodness of fit of a model, was calculated by using the software JMP 11 to compare different models for the same data set to identify the best-fitting model. As discussed in Akaike (1974), the model with the smallest value is usually the preferred model. This information-based criterion which assesses model fit is based on a statistical technique which is called *maximum likelihood*. This technique seeks to estimate the model parameters by maximizing the likelihood function which is the product of the probability mass functions for discrete distributions evaluated at the observed data values.

$$AICc = -2\text{Log}(\text{Likelihood}) + 2k + 2k(k + 1)/(n - k - 1)$$

Where k and n are the number of estimated parameters in the model and number of observations in the data set, respectively.

As an example, the following table and figure illustrate the comparison between various models applied to one of the data sets of the present study. AICc Weight, which is a normalized representation of AIC values, is interpreted as the probability that model is the best model among the fitted models. Therefore, the model with the AICc weight closest to one is the better fit.

Model		AICc	AICc Weight		R-Square
Logistic 4P		54.529858	0.5955263		0.9997749
Gompertz 4P		56.04021	0.2798545		0.9997633
Logistic 5P		57.658224	0.1246192		0.9997751
Mechanistic Growth		124.48973	3.831e-16		0.9974468
Exponential 3P		124.48973	3.831e-16		0.9974468
Gompertz 3P		128.83886	4.354e-17		0.9970485
Logistic 3P		167.29396	1.943e-25		0.9893651
Michaelis Menten		171.67291	2.176e-26		0.9865452



Appendix B: Model statistics for precipitation rate

Different statistics were considered to check the adequacy of the model for precipitation rate. The amount and definition of each statistic were presented below:

$$\text{Precipitation rate} = 0.24 - (2.42 * 10^{-10} * \text{Initial cell conc.}) - (0.050 * \text{Urea}) - (2.68 * 10^{-3} * \text{Temperature}) + (1.16 * 10^{-11} * \text{Initial cell conc.} * \text{Temperature}) \geq 0$$

Std. Dev.	0.064	R-Squared	0.7285
Mean	0.17	Adj R-Squared	0.6813
C.V. %	38.64	Pred R-Squared	0.5649
PRESS	0.15	Adeq Precision	15.396

R-squared: A measure of the amount of variation around the mean explained by the model.

Adj R-squared: A measure of the amount of variation around the mean explained by the model, adjusted for the number of terms in the model. The adjusted R-squared decreases as the number of terms in the model increases if those additional terms don't add value to the model.

Pred R-squared: A measure of the amount of variation in new data explained by the model. The predicted R-squared and the adjusted R-squared should be within 0.20 of each other. Otherwise there may be a problem with either the data or the model. Look for outliers, consider transformations, or consider a different order polynomial.

Adequate Precision: This is a signal-to-noise ratio. It compares the range of the predicted values at the design points to the average prediction error. Ratios greater than 4 indicate adequate model discrimination.

C.V.: Coefficient of Variation, the standard deviation expressed as a percentage of the mean. Calculated by dividing the Std Dev by the Mean and multiplying by 100. Less coefficient of variation shows more closeness of the predicted values to the actual ones.

PRESS: The Predicted Residual Sum of Squares for the model. A measure of how well a particular model fits each point in the design. The coefficients for the model are calculated with one point "deleted". The new model's prediction is subtracted from the "deleted" observation to find the predicted residual. This is done for each data point. The predicted residuals are squared residuals and added together to form the PRESS.